Cranfield

College of Aeronautics Report No.9006
January 1990

AN APPROXIMATE METHOD FOR ESTIMATING THE LIFTING CHARACTERISTICS OF THIN BODIES OF NON-CIRCULAR CROSS-SECTION

P.A.T.Christopher

College of Aeronautics
Cranfield Institute of Technology
Cranfield, Bedford MK43 0AL. England

Cranfield

College of Aeronautics Report No.9006
January 1990

AN APPROXIMATE METHOD FOR ESTIMATING THE LIFTING CHARACTERISTICS OF THIN BODIES OF NON-CIRCULAR CROSS-SECTION

P.A.T.Christopher

College of Aeronautics
Cranfield Institute of Technology
Cranfield, Bedford MK43 0AL. England

ISBN 1 871564425

£10.00

Summary

In this paper a method is developed, based on that of Sacks, Ref. 12, for predicting the normal force distribution on thin bodies of non-circular cross-section. Both the indirect anddirect aerodynamic problems are addressed and the technique is shown to offer a possible means for the design of lifting bodies.

1. Introduction

The large majority of missile bodies are, essentially, axi-symmetric in form. However, the move to non-circular cross-sections is now well established, prompted by improved storage and carriage characteristics and made possible, both technically and economically, by modern manufacturing methods.

Ref. 1 provides a useful review of research on the aerodynamics of missiles having non-circular cross-sections, highlighting the aerodynamic advantages that such shapes possess when incorporated into monplanar bank-to-turn (twist and steer) configurations and describes some of the theoretical and experimental contributions to this field of study. One of the more valuable, and simple, predictive methods which has emerged is that due to Jorgensen, Ref.2. In this technique slender-body theory is used to relate the overall normal force and pitching moment chracteristics of a slender, axi-symmetric, body to those of another slender body having a constant, non-circular, cross-section geometry and the same longitudinal distribution of cross-sectional area. The method uses Bryson's approach, Ref.3, Chapter 10, to determine the section inertia coefficients and, thereby, the ratio

$$F_N = \frac{C_N \text{ (non-circular)}}{C_N \text{ (circular)}} = \frac{C_M \text{ (non-circular)}}{C_M \text{ (circular)}} \qquad (1.1)$$

of the bodies. The overall normal force coefficient on the body of non-circular section, arising from potential flow, is then taken to be

$$C_N \text{ (non-circular)} = F_N C_N \text{ (circular)}, \qquad (1.2)$$

where the latter is known, together with a similar expression for the pitching moment. This use of a slender-body factor F_N, in association with force and moment coefficients for the circular-section body which themselves are not necessarily based on slender-body theory, parallels that of Nielsen, Ref.3, Chapter 5, where wing-body interference factors based on slender-body theory are employed.

Validation of this procedure, by Jorgensen, is based on experiment on pointed bodies at supersonic speed, and, in the case of bodies of elliptic cross-section, gives good agreement. See Ref.4. Similar validation may be demonstrated at both supersonic and subsonic speeds using the data from body-alone tests reported in Ref.5. These tests were performed on two pointed bodies, one of circular section the other having a constant elliptic section of aspect ratio three and both having the same longitudinal distribution of cross-sectional area. Similar validation for non-pointed bodies does not appear to have been reported.

In Ref.6 the present author has developed a method for predicting the lifting characteristics of thin bodies having elliptic cross-sections. This has evolved from the work of Spreiter, Ref.7, which uses the theory of complex mappings of incompressible flows to generalize the earlier ideas of Munk and Jones to obtain expressions for the lifting pressure differential and load distributions on wing-body combinations. By adapting this approach to the case of an elliptic cross-section, it was shown that the longitudinal gradient, nose to tail, of normal force (see Fig.1 for notation) is given by

$$\frac{dC_z}{dx} = \frac{2\alpha\pi b}{S_R(b+c)}\left\{b\frac{dc}{dx} + (2b+c)\frac{db}{dx}\right\}, \qquad (1.3)$$

where b(x) and c(x) are the semi-major and semi-minor axes, respectively, of the elliptic cross-section, S_R the reference area, α the angle of attack and Z the force normal to the x,y plane. A similar expression may be obtained for the longtiudinal gradient of C_Y by a simple exchange of b with c and a sign reversal. These relationships may then be used to establish the factor

$$F_z(x) = \frac{\frac{dC_z}{dx}\ (\text{non-circular})}{\frac{dC_z}{dx}\ (\text{circular})} = \left(\frac{b}{b+c}\right)\left\{\frac{b\frac{dc}{dx} + (2b+c)\frac{db}{dx}}{2\,Re\frac{dR_e}{dx}}\right\}, \qquad (1.4)$$

together with a similar relation for $F_Y(x)$, where $R_e(x)$ is the radius of the 'equivalent' axi-symmetric body having the same longitudinal distribution of cross-sectional area.

The results of Ref.6 are more general than those of Jorgensen in that they deal with load distributions on bodies whose elliptic cross-sections may

not be geometrically similar, i.e. they may have a longitudinal variation of their aspect ratio b(x)/c(x). Such extra generality is valuable since it makes possible the aerodynamic analysis of more complicated body shapes such as those described in Ref.8. However, in the case when the cross-sections are geometrically similar, we have

$$\frac{b(x)}{b_M} = \frac{c(x)}{c_M} = \frac{R_e(x)}{R_M} = f(x), \tag{1.5}$$

where the subscript M refers to the position of maximum cross-sectional area. Also, on differentiation,

$$\frac{1}{b_M}\frac{db}{dx} = \frac{1}{c_M}\frac{dc}{dx} = \frac{1}{R_M}\frac{dR_e}{dx} = f'(x). \tag{1.6}$$

Substitution from 1.5 and 1.6 into 1.4 then gives

$$F = b/c$$

and, in a similar manner,

$$F_Y = c/b,$$

which are in agreement with the results of Jorgensen.

In Ref.6 particular emphasis was given to applying the method to 'thin bodies' i.e. bodies which are thin but not necessarily slender, in that they may, for example, have blunt noses. This was seen as a useful extension to the approximate 'thin body' method, presented in Ref.9, for axi-symmetric bodies with blunt noses. As a partial verification of the accuracy of the method a comparison with the exact solution for ellipsoids was then made. Having blunt noses, ellipsoids are ideal candidates for the comparison. However, being geometrically similar in cross-section, these bodies do not test the effect of variation of b/c on F_Z and F_Y. This comparison is described in Ref.10, the method for obtaining the exact results being given in Ref.11. It was found that, for a range of section aspect ratios

$$\frac{1}{4} \leq b/c \leq 4,$$

and over a range of body fineness ratios

$$5 - 20,$$

these being representative of those experienced in missile technology, the approximate method gave accurate predictions of the normal load gradient. Substantial error arose only in the two to three per cent of body length near the nose and tail. When integrated over half the length, these approximate normal force distributions produced values for C_Z, C_Y and centre of pressure position which were well within the bounds of accuracy of most 'engineering' methods.

From the foregoing it can be seen that the approximate method has been validated for pointed bodies at both subsonic and supersonic speeds and blunt bodies at low subsonic speeds, all bodies being of elliptic cross-section. This leaves plenty of scope for more extensive validation both experimentally, measuring overall pressure distributions, and theoretically, using surface singularity (panel) or field (C.F.D.) methods. One obvious way in which the study may be extended is to develop techniques suitable for bodies of cross-section other than the ellipse.

Some idea of the range of body cross-sections which are of interest can be obtained from Ref.1 and among these are bodies having corners. The latter will be subject to flow separation and vortex formation even at very low angles of attack and it is questionable whether the associated force and moment characteristics possess any portion which can be predicted by a potential flow method. Such extreme configurations tend to be confined to applications where efficient storgage is of overiding importance. This still leaves ample scope for developing approximate techniques for the design of 'lifting-body' configurations, which, by their nature, require to be aerodynamically efficient.

The proposed generalization of the approximate technique can be approached in several ways and these are briefly reviewed by Nielsen in Ref.3, Chapter 10, the application there being to the prediction of stability derivatives of wing-body combinations. Of the methods referred to the two most suitable for the present purpose is that due to Sacks, Ref.12, and that due to Bryson, Refs.13, 14, 15 and 16. These methods require the use of complex mapping procedures in order to relate the flow around the body

cross-section to that around a circle and then use residue theory to evaluate the integrals which arise. Arguing that the mapping procedure needed to be more general Skulsky, in Ref.17, developed a numerical mapping technique, based on the mapping theorem between circles and polygons, which approximates the body cross-section by means of an n-sided polygon. This technique is essentially computer oriented and in application to smooth bodies requires n to be quite large in order to smooth the resulting data. In more recent times this method has been utilized in the 'vortex cloud' method for lifting bodies, Ref.18. Further work along closely similar lines is described in Refs. 22 and 23.

In the present paper a generalization of the approximate method of Ref.6 will be described. This technique is based on that of Sacks, Ref.12, and seeks to explore the application of the method to the aerodynamic design of lifting bodies. Unlike Ref.6, which uses Spreiter's approximation for the pressure coefficient

$$C_p = - 2\phi_x / U_\infty,$$

the more accurate form appropriate to bodies of revolution (see for example Ref.19, Section 20.5) will be used. When applied to a body of elliptic cross-section this gives rise to simpler relations than 1.3, 1.4, and, in the case of such bodies having cross-sections which are geometrically similar over the whole body length, the factors F_Z and F_Y are the same as those of Jorgensen.

2. Normal Forces and Their Longitudinal Distribution

The geometry of the body and flow is illustrated in Figs.1 and 2. Fig.1 shows the body geometry and the onset flow for the case when the angle of sideslip, β, is zero, whilst Fig.2 shows the system of body axes for the moving body. We study the flow over the body by making $U_R = -U_\infty$, the body being stationary.

We are particularly interested in the distribution of the Z and Y forces along the x-axis. If p is the surface pressure on the rigid body of surface S, then the force resulting from this pressure will be

$$F = - \iint_S p \, \bar{n} \, d S, \tag{2.1}$$

where $\bar{n}$ is the unit outward normal vector to the surface and the integration symbols describe a surface integral taken over the whole of S. See for example Ref. 19, Section 10.5. Now

$$\bar{n} = n_i i + n_j j + n_k k, \tag{2.2}$$

where

$$\left.\begin{aligned} n_i &= \text{Cos } (n,x) \\ n_j &= \text{Cos } (n,y) \\ n_k &= \text{Cos } (n,z) \end{aligned}\right\}, \tag{2.3}$$

these being the direction cosines of the acute angles (n,x), (n,y) and (n,z) made between the normal and the x,y and z axes, respectively. As a result the components of F may be written

$$\left.\begin{aligned} X = F_i &= - \iint_S p n_i dS \\ Y = F_j &= - \iint_S p n_j dS \\ Z = F_k &= - \iint_S p n_k dS \end{aligned}\right\}, \tag{2.4}$$

which, in an inviscid, irrotational, flow, are all zero.

Now the integrals in 2.4 may be written in the alternative form of integrals taken over the orthogonal projections $\underline{S}$ of S. See Fig.3 and Ref.20,

Section 8.7. We have

$$\left.\begin{aligned} Y &= -\iint_{S(x,z)} p\left(\pm\frac{n_j}{\mathrm{Cos}(n,y)}\right) dz\, dx\,, \\ &\text{and} \\ Z &= -\iint_{\underline{S}(x,y)} p\left(\pm\frac{n_k}{\mathrm{Cos}(n,z)}\right) dy\, dx, \end{aligned}\right\}, \tag{2.5}$$

where the quantities in the (.) brackets are of unit magnitude and whose sign will depend on the orientation of the surface S to the directions y and z, respectively. In more detail

$$\left.\begin{aligned} Y &= -\int_{x=x_N}^{x=x_T}\left\{\int_{\underline{S}(z)} p\left(\pm\frac{n_j}{\mathrm{Cos}(n,y)}\right) dz\right\} d(-x) \\ &\text{and} \\ Z &= -\int_{x=x_N}^{x=x_T}\left\{\int_{\underline{S}(y)} p\left(\pm\frac{n_k}{\mathrm{Cos}(n,z)}\right) dy\right\} d(-x) \end{aligned}\right\}, \tag{2.6}$$

where the inner integrals are taken at a fixed value of x, over the whole face of the local sections, $\underline{S}(z)$ and $\underline{S}(y)$, of the orthogonal projections in the x,z and x,y planes, respectively, (see Fig.3) and x_N and x_T are the co-ordinates of the nose and tail, respectively. It follows that the longitudinal gradients, nose to tail, of these forces may be written as

$$\frac{dC_Y}{d(-x)} = \frac{1}{\frac{1}{2}\rho U_\infty^2 S_R}\frac{dY}{d(-x)} = -\frac{1}{S_R}\int_{\underline{S}(z)} C_p\left(\pm\frac{n_j}{\mathrm{Cos}(n,y)}\right) dz, \tag{2.7}$$

$$\frac{dC_z}{d(-x)} = \frac{1}{\frac{1}{2}\rho U_\infty^2 S_R}\frac{dZ}{d(-x)} = -\frac{1}{S_R}\int_{\underline{S}(y)} C_p\left(\pm\frac{n_k}{\mathrm{Cos}(n,z)}\right) dy, \tag{2.8}$$

where S_R is the reference area.

In order to resolve the signs of the integrals consider the geometry of the body section at a given x, Fig.4. We have

$$dy = - ds\ Cos(\pi-\chi) = ds\ Cos\chi$$

and $$dz = ds\ Sin(\pi-\chi) = ds\ Sin\chi,$$

where s has a positive orientation in an anti-clockwise sense.

But $$\chi = \frac{\pi}{2} + \lambda,$$

where λ is the angle made by the normal to the positive sense of the y-axis. Thus

$$\left.\begin{aligned} dy &= - ds\ Sin\lambda = - ds\ Cos\left(\frac{\pi}{2} - \lambda\right) \\ \text{and} \qquad dz &= ds\ Cos\lambda. \end{aligned}\right\} \tag{2.9}$$

Now the angles

$$(n,y) = \lambda \text{ and } (n,z) = \left(\frac{\pi}{2} - \lambda\right),$$

thus it follows that we must take the positive sign in 2.7 and the negative sign in 2.8. As a result we may re-write the expressions in the form of circuit integrals around the perimeter of the section, C, giving

$$\left.\begin{aligned} \frac{dC_Y}{d(-x)} &= - \frac{1}{S_R} \oint_C C_p Cos\lambda\ ds \\ \text{and} \qquad \frac{dC_z}{d(-x)} &= - \frac{1}{S_R} \oint_C C_p Sin\lambda\ ds. \end{aligned}\right\} \tag{2.10}$$

If now we combine these to produce a complex force gradient defined by

$$\frac{dC_F}{d(-x)} = \frac{dC_Y}{d(-x)} - i\,\frac{dC_z}{d(-x)}, \tag{2.11}$$

then from 2.10,

$$\frac{dC_F}{d(-x)} = - \frac{1}{S_R} \oint C_p (Cos\lambda - iSin\lambda)\ ds$$

$$= - \frac{1}{S_R} \oint C_p (dz + i\ dy)$$

$$= - \frac{i}{S_R} \oint C_p (dy - i\ dz) = - \frac{i}{S_R} \oint C_p\ d\bar{\sigma}\ . \tag{2.12}$$

where σ is the complex variable

$$\sigma = y + iz \tag{2.13}$$

and

$$\bar{\sigma} = y - iz \tag{2.14}$$

is its complex conjugate.

The pressure coefficient is given by

$$C_p = 1 - \left(\frac{|\bar{q}|}{U_\infty}\right)^2 , \tag{2.15}$$

where the total velocity vector

$$\bar{q} = \left(-U + \phi_x\right)\bar{e}_x + \left(-V + \phi_y\right)\bar{e}_y + \left(-W + \phi_z\right)\bar{e}_z , \tag{2.16}$$

U, V and W being the onset velocities, ϕ_x, ϕ_y and ϕ_z the perturbation velocities arising from the body and $\bar{e}_x$, $\bar{e}_y$, $\bar{e}_z$ unit vectors. Thus

$$U = -U_\infty \text{Cos } \sigma_i , \; V = -U_\infty \text{ Cos } \sigma_i \text{ Tan } \beta, \; W = -U_\infty \text{ Cos } \sigma_i \text{ Tan } \alpha \tag{2.17}$$

and

$$q^2 = U^2 + V^2 + W^2 - 2U\phi_x - 2V\phi_y - 2W\phi_z + \phi_x^2 + \phi_y^2 + \phi_z^2$$

$$= U_\infty^2 - 2\left(U\phi_x + V\phi_y + W\phi_z\right) + \phi_x^2 + \phi_y^2 + \phi_z^2 , \tag{2.18}$$

giving

$$C_p = \frac{2}{U_\infty^2}\left\{U\phi_x + V\phi_y + W\phi_z\right\} - \frac{1}{U_\infty^2}\left(\phi_x^2 + \phi_y^2 + \phi_z^2\right)$$

$$= 2\left\{\frac{U}{U_\infty}\frac{\phi_x}{U_\infty} + \frac{V}{U_\infty}\frac{\phi_y}{U_\infty} + \frac{W}{U_\infty}\frac{\phi_z}{U_\infty}\right\} - \frac{1}{U_\infty^2}\left(\phi_x^2 + \phi_y^2 + \phi_z^2\right). \tag{2.19}$$

We need to express C_p, and thus the normal-force gradient, in terms of the complex transverse onset velocity

$$Q = V + i\,W , \tag{2.20}$$

and the transverse complex potential

$$F = \phi + i\psi . \tag{2.21}$$

Thus

$$U_\infty^2 = U^2 + V^2 + W^2 = U^2 + (V + iW)(V - iW) = U^2 + Q\bar{Q}. \tag{2.22}$$

Now the components of the transverse fluid velocity relative to the body are (Fig. 5) defined as

$$v_r = \phi_y - V \ , \ w_r = \phi_z - W \ , \tag{2.23}$$

hence

$$v_r - iw_r = (\phi_y - i\phi_z) - (V - iW) \ .$$

But from 2.21

$$\frac{dF}{d\sigma} = \frac{\partial F}{\partial y} = \frac{\partial F}{\partial (iz)} = \phi_y - i\phi_z \ ,$$

since $\phi_y = \psi_z$ and $\phi_z = -\psi_y$. It follows that

$$v_r - iw_r = \frac{dF}{d\sigma} - \bar{Q} \ . \tag{2.24}$$

Defining q_s and q_n as the tangential and normal components of the relative transverse velocity to the body, respectively, then (Fig.5)

$$v_r + iw_r = q_s e^{i\chi} + q_n e^{i\lambda}$$

$$= q_s e^{i\chi} + q_n e^{i(\chi - \frac{\pi}{2})} = (q_s - iq_n)e^{i\chi} \ ,$$

and its complex conjugate

$$v_r - iw_r = (q_s + iq_n)e^{-i\chi} \ . \tag{2.25}$$

From 2.24 and 2.25 we obtain

$$q_s = \left(\frac{dF}{d\sigma} - \bar{Q}\right)e^{i\chi} - iq_n$$

or

$$q_s^2 = \left(\frac{dF}{d\sigma} - \bar{Q}\right)^2 e^{2i\chi} - 2iq_n\left(\frac{dF}{d\sigma} - \bar{Q}\right)e^{i\chi} - q_n^2 \ . \tag{2.26}$$

But, from Fig. 5,

$$v_r^2 + w_r^2 = q_s^2 + q_n^2;$$

which from 2.26 gives

$$v_r^2 + w_r^2 = \left(\frac{dF}{d\sigma} - \bar{Q}\right)^2 e^{2i\chi} - 2iq_n\left(\frac{dF}{d\sigma} - \bar{Q}\right)e^{i\chi} . \qquad (2.27)$$

On substitution from 2.22 and 2.33 into 2.18 we obtain

$$q^2 = (\phi_x - U)^2 + v_r^2 + w_r^2 ,$$

and on further substitution from 2.27 this becomes

$$q^2 = \left(\phi_x - U\right)^2 + \left(\frac{dF}{d\sigma} - \bar{Q}\right)^2 e^{2i\chi} - 2iq_n\left(\frac{dF}{d\sigma} - \bar{Q}\right)e^{i\chi}.$$

Thus

$$C_p = \frac{U_\infty^2 - q^2}{U_\infty^2} = \frac{1}{U_\infty^2}\left\{U^2 + Q\bar{Q} - (\phi_x - U)^2 - \left(\frac{dF}{d\sigma} - \bar{Q}\right)^2 e^{2i\chi} + 2iq_n\left(\frac{dF}{d\sigma} - \bar{Q}\right)e^{i\chi}\right\}$$

$$= \frac{1}{U_\infty^2}\left\{2U\phi_x - \phi_x^2 - \left(\frac{dF}{d\sigma} - \bar{Q}\right)^2 e^{2i\chi} + 2iq_n\left(\frac{dF}{d\sigma} - \bar{Q}\right)e^{i\chi} + Q\bar{Q}\right\} . \qquad (2.28)$$

It is customary to ignore ϕ_x^2 in comparison with $2U\phi_x$ (see Ref.19, Section 20.5), which then reduces 2.28 to

$$C_p = \frac{1}{U_\infty^2}\left\{2U\phi_x - \left(\frac{dF}{d\sigma} - \bar{Q}\right)^2 e^{2i\chi} + 2iq_n\left(\frac{dF}{d\sigma} - \bar{Q}\right)e^{i\chi} + Q\bar{Q}\right\} . \qquad (2.29)$$

Substituting for C_p into 2.12 we obtain

$$\frac{dC_F}{d(-x)} = \frac{-i}{U_\infty^2 S_R}\left\{2U\oint \phi_x d\bar{\sigma} - \oint \left(\frac{dF}{d\sigma} - \bar{Q}\right)^2 e^{2i\chi}\, d\bar{\sigma} + 2i\oint q_n\left(\frac{dF}{d\sigma} - \bar{Q}\right)e^{i\chi} d\bar{\sigma} + \oint Q\bar{Q}d\bar{\sigma}\right\} ,$$

which, on recalling, from 2.13, that

$$d\sigma = dy + idz = ds(\cos\chi + i\,\sin\chi) = ds e^{i\chi}$$

and

$$d\bar{\sigma} = dy - idz = ds(\cos\chi - i\,\sin\chi) = ds e^{-i\chi} = d\sigma e^{-2i\chi} ,$$

gives

$$\frac{dC_F}{d(-x)} = \frac{-i}{U_\infty^2 S_R}\left\{2U\oint \phi_x d\bar{\sigma} - \oint\left(\frac{dF}{d\sigma} - \bar{Q}\right)^2 d\sigma + 2i\oint q_n\left(\frac{dF}{d\sigma} - \bar{Q}\right)ds + \oint Q\bar{Q}\, d\bar{\sigma}\right\} . \qquad (2.30)$$

Now in the case of a body of revolution we express the approximate surface boundary condition in the form

$$q_n = U\frac{dR}{d(-x)} , \qquad (2.31)$$

where R is the body radius at the axial position x and $\frac{dR}{dx}$ is the surface gradient in the x-sense. See Ref.19, Section 20.2.

The corresponding result for the general slender body, with a smooth perimeter to its cross-section (see Fig.6) and a smooth variation of this perimeter with x, is

$$q_n = U\frac{d\nu}{d(-x)} \qquad (2.32)$$

where ν is the outward normal to the body, in the σ-plane, at a general station x. As a result 2.30 becomes

$$\frac{dC_F}{d(-x)} = \frac{-i}{U_\infty^2 S_R}\left\{2U\oint \phi_x d\bar{\sigma} - \oint\left(\frac{dF}{d\sigma} - \bar{Q}\right)^2 d\sigma + 2iU\oint \frac{d\nu}{d(-x)}\left(\frac{dF}{d\sigma} - \bar{Q}\right)ds + \oint Q\bar{Q}d\bar{\sigma}\right\} ,$$

which on expansion gives

$$\frac{dC_F}{d(-x)} = \frac{-i}{U_\infty^2 S_R}\left\{2U\oint \phi_x\, d\bar{\sigma} - \oint\left(\frac{dF}{d\sigma}\right)^2 d\sigma\right.$$

$$+ 2\bar{Q}\oint \frac{dF}{d\sigma}\, d\sigma - \bar{Q}^2 \oint d\sigma + 2iU \oint \frac{d\nu}{d(-x)}\,\frac{dF}{d\sigma} ds$$

$$\left. - 2iU\bar{Q}\oint \frac{d\nu}{d(-x)} ds + Q\bar{Q}\oint d\bar{\sigma}\right\}. \qquad (2.33)$$

Examining the integrals in 2.33, we see that

$$\oint d\sigma = \oint d\bar{\sigma} = 0,$$

whilst

$\oint\left(\frac{dF}{d\sigma}\right)^2 d\sigma$ is proportional to the two-dimensional normal-force predicted by the Blasius relation (see Ref.19, Section 15.6) which, because F does not, generally, contain a circulation term, is zero. Also

$$\oint \frac{d\nu}{d(-x)} ds = \frac{dS}{d(-x)}, \qquad (2.34)$$

the rate of change of cross-sectional area.

It follows that

$$\frac{dC_F}{d(-x)} = \frac{-2i}{U_\infty^2 S_R}\left\{U\oint \phi_x d\bar{\sigma} + \bar{Q}\oint \frac{dF}{d\sigma} d\sigma + iU\oint \frac{dS}{d(-x)}\,\frac{dF}{d\sigma} ds - iU\bar{Q}\,\frac{dS}{d(-x)}\right\}. \qquad (2.35)$$

Looking at the first integral in 2.35 we note that the contour of integration (the perimeter of the body cross-section) is a function of x. Thus

$$\oint \phi_x d\bar{\sigma} \neq \frac{\partial}{\partial x}\oint \phi\, d\bar{\sigma}. \qquad (2.36)$$

Now the surface of the body may be defined by either

$$\left.\begin{aligned} z &= Z_1(x,y) \\ \text{or} \\ y &= Y_1(x,z) \end{aligned}\right\}, \tag{2.37}$$

where Z_1, Y_1 are functions with appropriate smoothness and differentiability.

In Ref. 12, Appendix A, Sacks shows that

$$\oint \phi_x d\bar{\sigma} = \frac{\partial}{\partial x} \oint \phi \, d\bar{\sigma} - \int_C \phi_z \frac{\partial Z_1}{\partial x} \, dy + i \int_C \phi_y \frac{\partial Y_1}{\partial x} \, dz, \tag{2.38}$$

where the circuit integrals are taken around the cross-section at x. Now from Fig.7 we see that

$$\Delta z = \Delta\nu/\mathrm{Sin}\lambda = -\Delta\nu/\mathrm{Cos}\chi$$

and

$$\Delta y = \Delta\nu/\mathrm{Cos}\lambda = \Delta\nu/\mathrm{Sin}\chi;$$

or the slopes of the body surface are

$$\left.\begin{aligned} &\frac{\partial Z_1}{\partial x} = \frac{\Delta\nu}{\Delta x} = -\frac{\Delta\nu}{\Delta x} \,/\, \mathrm{Cos}\chi \\ &\text{and} \\ &\frac{\partial Y_1}{\partial x} = \frac{\Delta y}{\Delta x} = \frac{\Delta\nu}{\Delta x} \,/\, \mathrm{Sin}\chi \end{aligned}\right\}. \tag{2.39}$$

It follows that

$$\oint \phi_x d\bar{\sigma} = \frac{\partial}{\partial x} \oint \phi \, d\bar{\sigma} + \int_C \frac{\partial \nu}{dx} \left\{ \frac{\phi_z dy}{\mathrm{Cos}\chi} + i \frac{\phi_y dz}{\mathrm{Sin}\chi} \right\}.$$

But

$$ds\ \mathrm{Cos}\lambda = ds\ \mathrm{Sin}\chi = dz$$

and

$$-ds\ \mathrm{Sin}\lambda = ds\ \mathrm{Cos}\chi = dy;$$

hence

$$\oint \phi_x d\bar{\sigma} = \frac{\partial}{\partial x} \oint \phi \, d\bar{\sigma} + \oint \frac{d\nu}{dx} (\phi_z + i\phi_y) ds \,. \tag{2.40}$$

Using the Cauchy - Reimann relations

$$\phi_z = -\psi_y$$

and

$$\phi_z + i\phi_y = -\psi_y + i\phi_y = i(\phi_y + i\psi_y) = i\,\frac{\partial F}{\partial y} = i\,\frac{dF}{d\sigma} .$$

It follows that

$$\oint \phi_x d\bar{\sigma} = \frac{\partial}{\partial x}\oint \phi\, d\bar{\sigma} + i\oint \frac{d\nu}{dx}\,\frac{dF}{d\sigma}\, ds$$

$$= \frac{\partial}{\partial x}\oint \phi\, d\bar{\sigma} - i\oint \frac{d\nu}{d(-x)}\,\frac{dF}{d\sigma}\, ds . \qquad (2.41)$$

Substituting from 2.41 into 2.35 produces

$$\frac{dC_F}{d(-x)} = \frac{-2i}{U_\infty^2 S_R}\left\{U\,\frac{\partial}{\partial x}\oint \phi\, d\bar{\sigma} + \bar{Q}\oint \frac{dF}{d\sigma}\, d\sigma - iU\bar{Q}\,\frac{dS}{d(-x)}\right\} . \qquad (2.42)$$

From 2.21

$$\bar{F} = \phi - i\psi$$

and

$$\phi = \bar{F} + i\psi;$$

thus it follows that

$$\oint \phi\, d\bar{\sigma} = \oint \bar{F}\, d\bar{\sigma} + i\oint \psi\, d\bar{\sigma} .$$

Now on the body surface the stream function $\psi = 0$, and since the contour of integration lies on the surface then

$$\oint \psi\, d\bar{\sigma} = 0 . \qquad (2.43)$$

Thus 2.42 becomes

$$\frac{dC_F}{d(-x)} = \frac{-2i}{U_\infty^2 S_R}\left\{U\,\frac{\partial}{\partial x}\oint \bar{F}\, d\bar{\sigma} + \bar{Q}\oint \frac{dF}{d\sigma}d\sigma - iU\bar{Q}\,\frac{dS}{d(-x)}\right\} . \qquad (2.44)$$

For small angles

$$\text{Cos}\ \sigma_i \simeq 1 , \quad \text{Tan}\ \beta \simeq \beta , \quad \text{Tan}\ \alpha \simeq \alpha ;$$

thus

$$U = -U_\infty \ , \quad V = U\beta \ , \quad W = U\,\alpha$$

and

$$\bar{Q} = V - iW = U(\beta - i\alpha).$$

The cross-flow velocity normal to the x-axis is, Fig.8,

$$U_\infty \, \mathrm{Sin}\sigma_i \simeq U_\infty \sigma_i = -U\sigma_i .$$

If F_1 is the complex potential per unit of cross-flow velocity, then

$$F = -U\sigma_i F_1 . \tag{2.45}$$

Also

$$V = -U_\infty \sigma_i \mathrm{Cos}\vartheta = U\sigma_i \mathrm{Cos}\vartheta = U\beta$$

and

$$W = -U_\infty \sigma_i \mathrm{Sin}\vartheta = U\sigma_i \mathrm{Sin}\vartheta = -U\alpha;$$

implying that

$$\beta = \sigma_i \, \mathrm{Cos}\vartheta \ , \quad \alpha = -\sigma_i \mathrm{Sin}\vartheta \ ,$$

whilst

$$\bar{Q} = U\sigma_i(\mathrm{Cos}\vartheta - i\mathrm{Sin}\vartheta) = U\sigma_i e^{-i\vartheta} \ . \tag{2.46}$$

It follows that

$$\frac{dC_F}{d(-x)} = \frac{2i}{U_\infty^2 S_R}\left\{U^2\sigma_i \frac{\partial}{\partial x}\oint \bar{F}_1 \, d\bar{\sigma} + iU^2\sigma_i e^{-i\vartheta}\frac{dS}{d(-x)} + U^2\sigma_i^2 e^{-i\vartheta}\oint \frac{dF_1}{d\sigma}\, d\sigma\right\}$$

or

$$\frac{dC_F}{d(-x)} = \frac{2i\sigma_i}{S_R}\left\{\frac{\partial}{\partial x}\oint \bar{F}_1 d\bar{\sigma} - ie^{-i\vartheta}\frac{dS}{dx} + \sigma_i e^{-i\vartheta}\oint \frac{dF_1}{d\sigma} d\sigma\right\} .$$

Since we have already assumed that $\sigma_i \ll 1$, then it is appropriate to discard the non-linear term in σ_i^2, giving the linear approximation

$$\frac{dC_F}{d(-x)} = \frac{2i\sigma_i}{S_R}\left\{\frac{\partial}{\partial x}\oint \bar{F}_1 \, d\bar{\sigma} - ie^{-i\vartheta}\frac{dS}{dx}\right\} , \tag{2.47}$$

or

$$\frac{dC_F}{d(-x)} = \frac{2i\sigma_i}{S_R}\frac{\partial}{\partial x}\left\{\oint \bar{F}_1 d\bar{\sigma} - ie^{-i\vartheta}S\right\} \tag{2.48}$$

when ϑ is independent of x.

3. Bodies of Elliptic Cross-Section, Re-visited.

Before consideration of the problem of bodies of more general cross-section it is a valuable exercise to apply the new technique embodied in 2.47 to the case of an elliptic cross-section, thereby facilitating the development of the method and providing a validation of its accuracy. For this purpose we map the flow around a circular cylinder in the ζ-plane to the flow around an elliptic cylinder in the σ-plane, Fig.9. These mappings are well known andare are described in Ref.21, pp.154-156. We have in the ζ-plane a cylinder of radius

$$R = \tfrac{1}{2}(b+c), \tag{3.1}$$

where b and c are the semi-major and semi-minor axes, respectively, of the ellipse in the σ-plane. The mapping (Joukowsky)

$$\sigma = \zeta + \frac{b^2-c^2}{4\zeta} \tag{3.2}$$

maps the circular cylinder and the flow around it in the ζ-plane to an elliptic cylinder and the flow around it in the σ-plane. Conversely, the mapping

$$\zeta = \frac{1}{2}\left\{\sigma + \left(\sigma^2 - b^2 + c^2\right)^{1/2}\right\} \tag{3.3}$$

maps the elliptic cylinder and the flow around it in the σ-plane to a circular cylinder and the flow around it in the ζ-plane.

We have an onset flow $U_\infty \sigma_1$ at an angle ϑ to the positive ξ and y directions and this gives rise to a complex potential per unit of velocity

$$F_1(\zeta) = \zeta e^{-i\vartheta} + \frac{R^2}{\zeta} e^{i\vartheta}$$

$$= \zeta e^{-i\vartheta} + \frac{(b+c)^2}{4\zeta} e^{i\vartheta} . \tag{3.4}$$

Alternatively we may write

$$F_1(\zeta) = \left\{\zeta + \frac{R^2}{\zeta}\right\} \mathrm{Cos}\vartheta - i\left\{\zeta - \frac{R^2}{\zeta}\right\} \mathrm{Sin}\vartheta , \tag{3.5}$$

from which

$$\bar{F}_1(\zeta) = \left\{\zeta + \frac{R^2}{\zeta}\right\} \mathrm{Cos}\vartheta + i\left\{\zeta - \frac{R^2}{\zeta}\right\} \mathrm{Sin}\vartheta \tag{3.6}$$

and

$$\bar{F}_1(\bar{\zeta}) = \left\{\bar{\zeta} + \frac{R^2}{\bar{\zeta}}\right\} \mathrm{Cos}\vartheta + i\left\{\bar{\zeta} - \frac{R^2}{\bar{\zeta}}\right\} \mathrm{Sin}\vartheta . \tag{3.7}$$

Now we require

$$\oint_{C_\sigma} \bar{F}_1(\bar{\sigma})d\bar{\sigma} = \oint_{C_\zeta} \bar{F}_1(\bar{\zeta}) \frac{d\bar{\sigma}}{d\bar{\zeta}} d\bar{\zeta} , \tag{3.8}$$

where

$$\bar{\sigma}(\zeta) = \sigma(\zeta) = \zeta + \frac{b^2-c^2}{4\zeta} \tag{3.9}$$

and

$$\bar{\sigma}(\bar{\zeta}) = \bar{\zeta} + \frac{b^2-c^2}{4\bar{\zeta}} . \tag{3.10}$$

Hence

$$\frac{d\bar{\sigma}}{d\bar{\zeta}} = 1 - \frac{b^2-c^2}{4\bar{\zeta}^2} \tag{3.11}$$

and

$$\oint_{C_\sigma} \bar{F}_1(\bar{\sigma})d\bar{\sigma} = \oint_{C_\zeta} \bar{F}_1(\bar{\zeta}) \left(1- \frac{b^2-c^2}{4\bar{\zeta}^2}\right) d\bar{\zeta} . \tag{3.12}$$

In these expresssions C_σ is the contour in the σ-plane and C_ζ its image circle in the ζ-plane.

Now the critical points of the mapping 3.2 are given by

$$\zeta_{1,2} = \pm \frac{1}{2}\left(b^2-c^2\right)^{1/2} = \pm \frac{1}{2}\left\{(b+c)(b-c)\right\}^{1/2}, \tag{3.13}$$

whilst

$$\zeta_{1,2}/R = \pm \left(\frac{b - c}{b + c}\right)^{1/2} . \tag{3.14}$$

Since $b \geq c$ then

$$\left| \zeta_{1,2}/R \right| \leq 1,$$

and the critical points are not outside C_ζ, whilst the image points are not outside C_σ. It follows that singularities in the complex velocity, arising from the mapping, will not occur outside C_σ.

From 3.7 and 3.12 we have

$$\oint_{C_\sigma} \bar{F}_1(\bar{\sigma})d\bar{\sigma} = \oint_{C_\zeta} \left\{\left[\bar{\zeta} + \frac{R^2}{\bar{\zeta}}\right]\text{Cos}\,\vartheta + i\left[\bar{\zeta} - \frac{R^2}{\bar{\zeta}}\right]\text{Sin}\vartheta\right\}\left(1 - \frac{b^2-c^2}{4\bar{\zeta}^2}\right)d\bar{\zeta}\ . \qquad (3.15)$$

We note that the only singular points of the integrand are at $\bar{\zeta} = 0$, i.e. within C_ζ. It follows that this integral is given by

$$\oint_{C_\sigma} \bar{F}_1(\bar{\sigma})d\bar{\sigma} = \oint_{C_\infty} \left\{\left[\frac{4R^2 - (b^2-c^2)}{4\bar{\zeta}}\right]\text{Cos}\vartheta - i\left[\frac{4R^2 + (b^2-c^2)}{4\bar{\zeta}}\right]\text{Sin}\vartheta\right\} d\bar{\zeta}, \qquad (3.16)$$

where, from the theory of residues (see Ref.19, Section 14.23) the terms in $1/\bar{\zeta}$, only, have been retained and C_∞ is a circle whose radius tends to infinity. Thus

$$\oint_{C_\sigma} \bar{F}_1(\bar{\sigma})d\bar{\sigma} = \left\{\left[\frac{4R^2 - (b^2-c^2)}{4}\right]\text{Cos}\vartheta - i\left[\frac{4R^2 + (b^2-c^2)}{4}\right]\text{Sin}\vartheta\right\}\oint_{C_\infty} \frac{d\bar{\zeta}}{\bar{\zeta}}$$

$$= \left\{\frac{1}{2}(c^2 + bc)\text{Cos}\vartheta - \frac{i}{2}(b^2 + bc)\text{Sin}\vartheta\right\} \times 2\pi i$$

$$= \pi\left\{(b^2 + bc)\text{Sin}\vartheta + i(c^2 + bc)\text{Cos}\vartheta\right\} \qquad (3.17)$$

and

$$\frac{\partial}{\partial x}\oint_{C_\sigma} \bar{F}_1(\bar{\sigma})d\bar{\sigma} = \pi\left\{\left[(2b + c)\frac{db}{dx} + b\,\frac{dc}{dx}\right]\text{Sin}\vartheta\right.$$

$$\left. + i\left[(2c + b)\,\frac{dc}{dx} + c\,\frac{db}{dx}\right]\text{Cos}\vartheta\right\}\ . \qquad (3.18)$$

Now the cross-sectional area (of an ellipse) is

$$S = \pi bc \qquad (3.19)$$

and, thereby,

$$\frac{dS}{dx} = \pi\left[b\,\frac{dc}{dx} + c\,\frac{db}{dx}\right]\ , \qquad (3.20)$$

whilst

$$ie^{-i\vartheta}\frac{dS}{dx} = \pi i(\cos\vartheta - i\sin\vartheta)\left[b\frac{dc}{dx} + c\frac{db}{dx}\right]$$

$$= \pi(\sin\vartheta + i\cos\vartheta)\left[b\frac{dc}{dx} + c\frac{db}{dx}\right] . \qquad (3.21)$$

Substituting from 3.18 and 3.21 into 2.47 then gives

$$\frac{dC_F}{d(-x)} = \frac{4\pi i\sigma_i}{S_R}\left\{b\frac{db}{dx}\sin\vartheta + i\,c\frac{dc}{dx}\cos\vartheta\right\} , \qquad (3.22)$$

or

$$\frac{dC_F}{d(-x)} = -\frac{4\pi}{S_R}\left\{ib\frac{db}{dx}\alpha + c\frac{dc}{dx}\beta\right\} . \qquad (3.23)$$

Comparison with 2.11 then gives

$$\left.\begin{aligned} \frac{dC_z}{d(-x)} &= \frac{4\pi\alpha}{S_R}\,b\frac{db}{dx} \\ \text{and}\qquad \frac{dC_Y}{d(-x)} &= -\frac{4\pi\beta}{S_R}\,c\frac{dc}{dx} . \end{aligned}\right\} \qquad (3.24)$$

The corresponding results from References 6 and 10, based on Spreiter's approach, are

$$\left.\begin{aligned} \frac{dC_z}{d(-x)} &= \frac{2\pi b\alpha}{S_R(b+c)}\left\{(2b + c)\frac{db}{dx} + b\frac{dc}{dx}\right\} \\ \text{and}\qquad \frac{dC_Y}{d(-x)} &= -\frac{2\pi c\beta}{S_R(b+c)}\left\{c\frac{db}{dx} + (2c + b)\frac{dc}{dx}\right\} . \end{aligned}\right\} \qquad (3.25)$$

In general the results of our present analysis are different from those of 3.25. However, we note that when $b = c = R_e$, where $R_e(x)$ is the radius of the 'equivalent body of revolution' having the same axial distribution of cross-sectional area S(x), then both 3.24 and 3.25 become

$$\left.\begin{aligned} \frac{dC_z}{d(-x)} &= \frac{4\pi\alpha}{S_R} R_e(x) \frac{dR_e}{dx} \\ \text{and} \\ \frac{dC_Y}{d(-x)} &= -\frac{4\pi\beta}{S_R} R_e(x) \frac{dR_e}{dx} . \end{aligned}\right\} \qquad (3.26)$$

Also, in the case of a body whose elliptic cross-sections are geometrically similar, we have from 1.4, 1.5, and 1.6 that

$$F_z(x) = \frac{b_M^2}{R_M^2} .$$

But

$$S(x) = \pi\, bc(x) = \pi R_e^2(x)$$

and, in particular,

$$S_M = \pi\, b_M c_M = \pi\, R_M^2 ;$$

thus

$$F_z = \frac{b_M}{c_M} = \frac{b(x)}{c(x)} . \qquad (3.27)$$

In a closely similar manner

$$F_Y = \frac{c_M}{b_M} = \frac{c(x)}{b(x)} . \qquad (3.28)$$

The corresponding results from 3.24 and 3.26 are

$$F_z = \frac{b\,\frac{db}{dx}}{R_e \frac{dRe}{dx}} = \frac{b_M b\,(x)}{R_M R_e(x)} , \text{ from 1.6 ,}$$

$$= \frac{b_M^2}{R_M^2} = \frac{b_M}{c_M} = \frac{b(x)}{c(x)} , \text{ from 1.5}$$

and, similarly,

$$F_Y = \frac{c_M}{b_M} = \frac{c(x)}{b(x)} .$$

Thus the two methods give the same result and the comparison with the exact results for ellipsoids, described in Ref.10, are still valid.

4. Bodies of a More General Cross-Section.

Leaving aside the class of body cross-sections of polygonal shape, which may be generated from a circle by means of suitable mappings (see Refs. 17 and 18), we will concentrate on those which may be generated by means of mappings described by Laurent series. Such mappings include, as special cases, the well known Joukowski, von Mises and Karman-Trefftz mappings, used to generate aerofoil shapes, and that already used in 3.2 to generate elliptic cross-sections. See for example, Ref. 24, Chapter 7. They may be looked upon as the most obvious means of generalizing the results of Section 3.

A description of the evolution of this class of mapping, which maps from a circle to an (arbitrary!) cylinder, is given in Ref.19, Sections 15.8 - 15.10. From Fig. 10, we seek a mapping between the flow about a circular cylinder, whose centre is located at ζ_o in the ζ plane, and that about an arbitrary cylinder in the σ plane. The onset velocity is $U_\infty \sigma_i e^{-i\vartheta}$ and we may take the mapping in the form of a Laurent series about the origin

$$\sigma(\zeta) = \sum_{m=-\infty}^{\infty} G_m \zeta^m \tag{4.1}$$

and

$$\frac{d\sigma}{d\zeta} = \sum_{m=-\infty}^{\infty} mG_m \zeta^{m-1} \ . \tag{4.2}$$

Now the complex velocity in the σ plane is

$$\frac{dF}{d\sigma} = \frac{dF}{d\zeta} \Big/ \frac{d\sigma}{d\zeta} \tag{4.3}$$

and the boundary condition at infinity requires that

$$\frac{dF}{d\sigma} \to \frac{dF}{d\zeta} \to U_\infty \sigma_i e^{-i\vartheta} \text{ as } \zeta,\sigma \to \infty;$$

i.e.

$$\frac{d\sigma}{d\zeta} \to 1 \text{ as } \sigma,\zeta \to \infty \ ,$$

or

$$\zeta \to \sigma \text{ as } \sigma,\zeta \to \infty \ .$$

In order that $d\sigma/d\zeta \to 1$, in 4.2, as $\zeta \to \infty$,

$$G_o,\ G_2,\ G_3 \ldots,\ G_m$$

must be zero, and

$$G_1 = 1 \ .$$

We may, therefore, re-write 4.2 in the form

$$\frac{d\sigma}{d\zeta} = 1 - \sum_{n=1}^{\infty} nC_n/\zeta^{n+1} \tag{4.4}$$

and

$$\sigma(\zeta) = \zeta + \sum_{n=1}^{\infty} C_n/\zeta^n \ . \tag{4.5}$$

The complex potential per unit of cross-flow velocity is

$$F_1(\zeta) = (\zeta-\zeta_o)e^{-i\vartheta} + \frac{R^2}{(\zeta-\zeta_o)}\, e^{i\vartheta} \ , \tag{4.6}$$

which is an obvious generalization of 3.4, which describes the case $\zeta_o = 0$. The associated complex velocity per unit of cross-flow velocity is

$$\frac{dF_1}{d\zeta} = e^{-i\vartheta} - \frac{R^2}{(\zeta-\zeta_o)^2}\, e^{i\vartheta} \ , \tag{4.7}$$

where the cross-flow velocity is $U_\infty \sigma_i$. Alternatively, we may write

$$F_1(\zeta) = \left\{(\zeta-\zeta_o) + \frac{R^2}{(\zeta-\zeta_o)}\right\} \mathrm{Cos}\vartheta - i\left\{(\zeta-\zeta_o) - \frac{R^2}{(\zeta-\zeta_o)}\right\}\mathrm{Sin}\vartheta, \tag{4.8}$$

from which

$$\bar{F}_1(\zeta) = \left\{(\zeta-\zeta_o) + \frac{R^2}{(\zeta-\zeta_o)}\right\}\mathrm{Cos}\vartheta + i\left\{(\zeta-\zeta_o) - \frac{R^2}{(\zeta-\zeta_o)}\right\}\mathrm{Sin}\vartheta \tag{4.9}$$

and

$$\bar{F}_1(\bar{\zeta}) = \left\{(\bar{\zeta}-\zeta_o) + \frac{R^2}{(\bar{\zeta}-\zeta_o)}\right\}\text{Cos}\vartheta + i\left\{(\bar{\zeta}-\zeta_o) - \frac{R^2}{(\bar{\zeta}-\zeta_o)}\right\}\text{Sin}\vartheta \ . \tag{4.10}$$

Also,

$$\bar{\sigma} = \sigma = \zeta + \sum_{n=1}^{\infty} C_n/\zeta^n \tag{4.11}$$

and

$$\bar{\sigma}(\bar{\zeta}) = \bar{\zeta} + \sum_{n=1}^{\infty} C_n/\bar{\zeta}^n \ , \tag{4.12}$$

giving

$$\frac{d\bar{\sigma}}{d\bar{\zeta}} = 1 - \sum_{n=1}^{\infty} nC_n/\bar{\zeta}^{n+1}. \tag{4.13}$$

Now the zeros of the derivative 4.4 are the critical points of the mapping $\zeta(\sigma)$ and may be obtained by writing 4.4 in the factorized form

$$\frac{d\sigma}{d\zeta} = \left(1 - \frac{\zeta_1}{\zeta}\right)\left(1 - \frac{\zeta_2}{\zeta}\right)\left(1 - \frac{\zeta_3}{\zeta}\right) \ldots \left(1 - \frac{\zeta_k}{\zeta}\right) \ldots = \prod_{n=1}^{\infty}\left(1 - \frac{\zeta_n}{\zeta}\right) \ , \tag{4.14}$$

and solving for $\zeta = \zeta_1, \zeta_2, \ldots$ etc. Expanding the factorized polynomial gives

$$\frac{d\sigma}{d\zeta} = 1 - \left\{\sum_{n=1}^{\infty} \zeta_n\right\}/\zeta + \ldots \ , \tag{4.15}$$

and when compared with 4.4, which has no term in ζ^{-1}, shows that

$$\sum_{n=1}^{\infty} \zeta_n = 0; \tag{4.16}$$

i.e. the centroid of the critical points of the mapping 4.5 must be at the origin in the ζ-plane.

The above arguments apply equally well to mappings of finite degree, k, expressed as

$$\sigma(\zeta) = \zeta + \sum_{n=1}^{k} C_n/\zeta^n \ , \tag{4.17}$$

with

$$\frac{d\sigma}{d\zeta} = 1 - \sum_{n=1}^{k} nC_n/\zeta^{n+1} \qquad (4.18)$$

and

$$\sum_{n=1}^{k} \zeta_n = 0 \ . \qquad (4.19)$$

Additionally, if the critical points are located within the circle C_ζ then the image points will lie inside C_σ.
Thus we require that

$$\left| \frac{\zeta_n - \zeta_o}{R} \right| \leq | \ . \qquad (4.20)$$

We need to consider now the possible body cross-sections which can be generated by 4.17 and, for the purpose of substitution into 2.47, we require an expression for the cross-sectional area, S. The circle C_ζ in the ζ-plane is defined by

$$\zeta_c = \zeta_o + Re^{i\theta} \quad , \qquad (4.21)$$

where θ is measured positive anti-clockwise from the ξ axis.
The image C_σ under the mapping 4.17 is given by

$$\sigma_c = \zeta_o + Re^{i\theta} + \sum_{n=1}^{k} \frac{C_n}{(\zeta_o + Re^{i\theta})^n} \ ; \qquad (4.22)$$

i.e.

$$\sigma_c = y_c + iz_c = r_c e^{i\gamma} \qquad (4.23)$$

defines the complex co-ordinates of all points on the closed curve C_σ. The body cross-sectional area S is the area enclosed within C_σ and, in polar co-ordinates, we may express the area as

$$S = \frac{1}{2} \int_{\gamma=0}^{2\pi} r_c^2 d\gamma = \pi R_e^2 \qquad (4.24)$$

where R_e is the corresponding radius of the equivalent body of revolution.

See for example Ref.20, pp 336-339. However, from 4.23 this becomes

$$S = \frac{1}{2}\int_{\gamma=0}^{2\pi} (y_c^2 + z_c^2)d\gamma \quad = \quad \pi R_e^2 \,, \tag{4.25}$$

which is fine provided we know y_c and z_c in terms of γ.

Now

and

$$\left.\begin{aligned} y_c &= r_c(\gamma)\mathrm{Cos}\gamma \\ z_c &= r_c(\gamma)\mathrm{Sin}\gamma \end{aligned}\right\} , \tag{4.26}$$

so we may obtain S from 4.24 provided we know $r_c(\gamma)$ which, in general, we must obtain from 4.22 and 4.23.

5. Bodies Obtained When $\zeta_o = 0$, k=2; Joukowski Mapping.

Having developed a procedure for generating a wide class of body shapes and also the means for determining the normal force gradient, equation 2.47, it is rewarding to explore these shapes in a systematic manner which introduces a growing degree of complexity into their description. This parallels the procedure used to describe aerofoil sections of increasing geometric complexity. See for example Ref.24, Chapter 7.

Let us begin with the case $\zeta_o = 0$, k=2. Then from 4.14

$$\frac{d\sigma}{d\zeta} = \left(1 - \frac{\zeta_1}{\zeta}\right)\left(1 - \frac{\zeta_2}{\zeta}\right)$$

$$= 1 - \frac{(\zeta_1 + \zeta_2)}{\zeta} + \frac{\zeta_1\zeta_2}{\zeta^2}$$

$$= 1 + \frac{\zeta_1\zeta_2}{\zeta^2} \quad , \tag{5.1}$$

since, from 4.19,

$$\zeta_1 + \zeta_2 = 0 \quad . \tag{5.2}$$

It follows that

$$\sigma = \zeta - \frac{\zeta_1\zeta_2}{\zeta} = \zeta + \frac{\zeta_1^2}{\zeta} \quad , \tag{5.3}$$

where, in the general case,

$$\zeta_1 = -\zeta_2 = \xi_1 + i\eta_1, = |\zeta_1|e^{i\delta} \tag{5.4}$$

and

$$|\zeta_1| = |(\xi_1^2 + \eta_1^2)^{1/2}| \leq R. \tag{5.5}$$

Also $$\text{Tan}\delta = \eta_1/\xi_1, \text{Sin}\delta = \eta_1/|\zeta_1| \text{ and } \text{Cos}\delta = \xi_1/|\zeta_1| \quad . \tag{5.6}$$

The body shape, C_σ, generated in the σ-plane is given by

$$\sigma_c = Re^{i\theta} + R^{-1}e^{-i\theta}(\xi_1 + i\eta_1)^2$$

or

$$\frac{\sigma_c}{R} = \frac{y_c}{R} + i\,\frac{z_c}{R}$$

$$= e^{i\theta} + e^{-i\theta}\left(\frac{\xi_1 + i\eta_1}{R}\right)^2$$

$$= \mathrm{Cos}\theta + i\mathrm{Sin}\theta + \left\{\left(\frac{\xi}{R}1\right)^2 + 2i\left(\frac{\zeta}{R}1\right)\left(\frac{\eta}{R}1\right) - \left(\frac{\eta}{R}1\right)^2\right\}(\mathrm{Cos}\theta - i\mathrm{Sin}\theta)$$

or

$$\left.\begin{aligned} \frac{y}{R}c &= \left\{1 + \left(\frac{\xi}{R}1\right)^2 - \left(\frac{\eta}{R}1\right)^2\right\}\mathrm{Cos}\theta + 2\left(\frac{\xi}{R}1\right)\left(\frac{\eta}{R}1\right)\mathrm{Sin}\theta \\ \text{and} \\ \frac{z}{R}c &= 2\left(\frac{\xi}{R}1\right)\left(\frac{\eta}{R}1\right)\mathrm{Cos}\theta + \left\{1 - \left(\frac{\xi}{R}1\right)^2 + \left(\frac{\eta}{R}1\right)^2\right\}\mathrm{Sin}\theta \end{aligned}\right\} . \qquad (5.7)$$

The geometry is illustrated in Fig.11, where the two critical points, ζ_1,ζ_2 lie on a common line, defined by the axis ξ' through the origin, and which makes an angle δ to the positive direction of the ξ-axis. The image points σ_1,σ_2 of ζ_1,ζ_2, under the mapping 5.3, are given by

$$\left.\begin{aligned} \sigma_1 &= 2\zeta_1 = 2(\xi_1 + i\eta_1) = 2|\zeta_1|e^{i\delta} \\ \text{and} \\ \sigma_2 &= 2\zeta_2 = -2\zeta_1 = -2|\zeta_1|e^{i\delta} = 2|\zeta_1|e^{i(\delta+\pi)} \end{aligned}\right\} . \qquad (5.8)$$

As shown in Fig.11, they lie on a line, defined by the axis y', making an angle μ to the positive direction of the y-axis. However, from 5.8, we may conclude that

$$\left.\begin{aligned} |\sigma_1| &= 2|\zeta_1| = |\sigma_2|, \\ \text{whilst} \\ \mu &= \delta \ . \end{aligned}\right\} \qquad (5.9)$$

If now we select cartesian co-ordinates, y',z' which are rotated through the angle $\mu = \delta$ relative to the axes y,z, Fig.11, we can express the co-ordinates y'_c,z'_c of a general point P on C_σ in terms of the co-ordinates y_c,z_c. From Fig.11, lower diagram, we have

$$z'_c = (z_c - y_c \tan\delta)\cos\delta = z_c\cos\delta - y_c \sin\delta$$

$$= (z_c\xi_1 - y_c\eta_1)/|\zeta_1| \qquad (5.10)$$

and

$$y'_c = y_c \sec\delta + z'_c \tan\delta = y_c\frac{|\zeta_1|}{\xi_1} + \frac{(z_c\xi_1 - y_c\eta_1)\eta_1}{|\zeta_1|\xi_1}$$

$$= (y_c\xi_1 + z_c\eta_1)/|\zeta_1| \ . \qquad (5.11)$$

Examining the case $\theta = \delta$, then

$$\sin\theta = \eta_1/|\zeta_1| \ , \quad \cos\theta = \xi_1/|\zeta_1| \ ,$$

which on substitution into 5.7 produces

$$\left.\begin{aligned} \frac{y_c}{R} &= \left\{1 + \left(\frac{\xi}{R}_1\right)^2 - \left(\frac{\eta}{R}_1\right)^2\right\}\frac{\xi_1}{|\zeta_1|} + 2\left(\frac{\xi}{R}_1\right)\left(\frac{\eta}{R}_1\right)\frac{\eta_1}{|\zeta_1|} \\ \text{and} \\ \frac{z_c}{R} &= 2\left(\frac{\xi}{R}_1\right)\left(\frac{\eta}{R}_1\right)\frac{\xi_1}{|\zeta_1|} + \left\{1 - \left(\frac{\xi}{R}_1\right)^2 + \left(\frac{\eta}{R}_1\right)^2\right\}\frac{\eta_1}{|\zeta_1|} \end{aligned}\right\} . \qquad (5.12)$$

Further substitution from 5.12 into 5.10 and 5.11 then gives

$$z'_c(\delta) = 0, \quad y'_c(\delta)/R = 1 + \left(\frac{\xi}{R}_1\right)^2 + \left(\frac{\eta}{R}_1\right)^2, \qquad (5.13)$$

i.e. the point in the ζ-plane where C_ζ crosses the positive ξ' axis corresponds with the point in the σ-plane where C_σ crossesthe positive y' axis and the distance of this point from the origin is given by 5.13.

Examination of the case $\theta = \delta+\pi$ gives

$$\sin\theta = \sin(\delta+\pi) = -\sin\delta = -\eta_1/|\zeta_1|$$

and

$$\cos\theta = \cos(\delta+\pi) = -\cos\delta = -\xi_1/|\zeta_1| \ ;$$

from which

$$z'_c(\delta+\pi) = 0, \quad \frac{y'_c}{R}(\delta+\pi) = -\frac{y'_c}{R}(\delta) = -1 - \left(\frac{\xi}{R}_1\right)^2 - \left(\frac{\eta}{R}_1\right)^2 ; \tag{5.14}$$

i.e. the point in ζ-plane where C_ζ crosses the negative ξ' axis corresponds with the point in the σ-plane where C_σ crosses the negative y' axis, and the distance of this point from the origin is the same as that for the crossing of the positive branch of the y' axis.

Similar analysis may be made of the crossing, by $C_{\sigma'}$, of the z' axis. Thus when $\theta = \delta + \pi/2$, $\mathrm{Sin}\theta = \xi_1/|\zeta_1|$ and $\mathrm{Cos}\theta = -\eta_1/|\zeta_1|$, which yields

$$y'_c\left(\delta+\frac{\pi}{2}\right) = 0, \quad \frac{z'_c}{R}\left(\delta+\frac{\pi}{2}\right) = 1 - \left(\frac{\xi}{R}_1\right)^2 - \left(\frac{\eta}{R}_1\right)^2 . \tag{5.15}$$

Also, when $\theta = \delta + \frac{3\pi}{2}$,

$$y'_c\left(\delta+\frac{3\pi}{2}\right) = 0 , \quad \frac{z'_c}{R}\left(\delta+\frac{3\pi}{2}\right) = -\frac{z'_c}{R}\left(\delta+\frac{\pi}{2}\right) . \tag{5.16}$$

Clearly C_σ must have some regular form. That the shape is an ellipse, whose major axis lies along y' and minor axis lies along z', may be shown as follows:

Assuming the major axis is of length $y'_c(\delta)$ and the minor axis of length $z'_c\left(\delta+\frac{\pi}{2}\right)$, then from 5.11, 5.13 and 5.7

$$\frac{y'_c}{y'_c(\delta)} = \left\{\left[1 + \left(\frac{\xi}{R}_1\right)^2 - \left(\frac{\eta}{R}_1\right)^2\right] \xi_1 \mathrm{Cos}\theta + 2\left(\frac{\xi}{R}_1\right)\left(\frac{\eta}{R}_1\right)\xi_1 \mathrm{Sin}\theta \right.$$

$$\left. + 2\left(\frac{\xi}{R}_1\right)\left(\frac{\eta}{R}_1\right)\eta_1 \mathrm{Cos}\theta + \left[1 - \left(\frac{\xi}{R}_1\right)^2 + \left(\frac{\eta}{R}_1\right)^2\right]\eta_1 \mathrm{Sin}\theta \right\}$$

$$\div \left\{\left[1 + \left(\frac{\xi}{R}_1\right)^2 + \left(\frac{\eta}{R}_1\right)^2\right]|\zeta_1|\right\} .$$

$$= \frac{\left[\left(R^2+\xi_1^2-\eta_1^2\right)\xi_1 + 2\xi_1\eta_1^2\right]\mathrm{Cos}\theta + \left[2\xi_1^2\eta_1 + \left(R^2-\xi_1^2+\eta_1^2\right)\eta_1\right]\mathrm{Sin}\theta}{\left(R^2+\xi_1^2+\eta_1^2\right)|\zeta_1|}$$

$$= \left(\xi_1 \mathrm{Cos}\theta + \eta_1 \mathrm{Sin}\theta\right)/|\zeta_1| , \tag{5.17}$$

whilst

$$\frac{z'_c}{z'_c\left(\delta+\frac{\pi}{2}\right)} = (\xi_1 \mathrm{Sin}\theta - \eta_1 \mathrm{Cos}\theta)/\,|\zeta_1| \,. \tag{5.18}$$

It follows that

$$\left\{\frac{y'_c}{y'_c(\delta)}\right\}^2 + \left\{\frac{z'_c}{z'_c(\delta+\frac{\pi}{2})}\right\}^2$$

$$= \frac{(\xi_1 \mathrm{Cos}\theta + \eta_1 \mathrm{Sin}\theta)^2 + (\xi_1 \mathrm{Sin}\theta - \eta_1 \mathrm{Cos}\theta)^2}{|\zeta_1|^2}$$

$$= 1, \tag{5.19}$$

which is, of course, the equation of an ellipse. Thus C_σ is an ellipse whose

semi-major axis ....$y'_c(\delta) = R\left\{1+\left(\frac{\xi}{R}1\right)^2 + \left(\frac{\eta}{R}1\right)^2\right\}$

and

semi-minor axis ....$z'_c\left(\delta+\frac{\pi}{2}\right) = R\left\{1-\left(\frac{\xi}{R}1\right)^2 - \left(\frac{\eta}{R}1\right)^2\right\}$.

Special cases arise:

(a) when $|\zeta_1| = R$, in which case $y'_c(\delta) = 2R$, $z'_c\left(\delta+\frac{\pi}{2}\right) = 0$;

i.e. a flat plate of width 2R at angle δ to the y axis,

and

(b) when $|\zeta_1| = \xi_1 = \eta_1 = 0$, in which case $y'_c(\delta) = z'_c\left(\delta+\frac{\pi}{2}\right) = R$;

i.e. an identity mapping of the circle C_ζ.

In the general case, since we can vary the direction ϑ of the onset velolcity $U_\infty \sigma_1$ at will, no particular advantage arises from the generality of δ and it suffices to use the cases $\delta = 0$, $\eta_1 = 0$,and $\delta = \frac{\pi}{2}$, $\xi_1 = 0$, in which the major axis is aligned with the y and z directions, respectively.

It appears, then, that this case is essentially the same as that of Section 3. However, it is interesting to pursue it a little further as a pointer to procedure in more general cases. To this end we note, from 4.10, that

$$\bar{F}_1(\bar{\zeta}) = \left(\bar{\zeta} + \frac{R^2}{\bar{\zeta}}\right)\mathrm{Cos}\vartheta + i\left(\bar{\zeta} - \frac{R^2}{\bar{\zeta}}\right)\mathrm{Sin}\vartheta \tag{5.20}$$

and

$$\frac{d\bar{\sigma}}{d\bar{\zeta}} = \left(1-\frac{\zeta_1}{\zeta}\right)\left(1-\frac{\zeta_2}{\zeta}\right) = 1 - \frac{\zeta_1^2}{\bar{\zeta}^2} = 1 - \frac{\xi_1^2+\eta_1^2}{\bar{\zeta}^2}. \tag{5.21}$$

Hence

$$\oint_{C_\sigma} \bar{F}_1(\bar{\sigma})d\bar{\sigma} = \oint_{C_\zeta}\left\{\left(\bar{\zeta} + \frac{R^2}{\zeta}\right)\mathrm{Cos}\vartheta + i\left(\bar{\zeta} - \frac{R^2}{\zeta}\right)\mathrm{Sin}\vartheta\right\}\left\{1 - \frac{\xi_1^2+\eta_1^2}{\bar{\zeta}^2}\right\}d\bar{\zeta} \tag{5.22}$$

and, in a similar way to 3.15, 3.16, we have

$$\oint_{C_\sigma} \bar{F}_1(\bar{\sigma})d\bar{\sigma} = \oint_{C_\infty}\left\{\left[\frac{R^2 - (\xi_1^2+\eta_1^2)}{\bar{\zeta}}\right]\mathrm{Cos}\vartheta - i\left[\frac{R^2 + (\xi_1^2+\eta_1^2)}{\bar{\zeta}}\right]\mathrm{Sin}\vartheta\right\}d\bar{\zeta}$$

$$= \left\{\left[R^2 - (\xi_1^2+\eta_1^2)\right]\mathrm{Cos}\vartheta - i\left[R^2 + (\xi_1^2+\eta_1^2)\right]\mathrm{Sin}\vartheta\right\}\oint_{C_\infty}\frac{d\bar{\zeta}}{\bar{\zeta}}$$

$$= 2\pi i\left\{\left[R^2 - \left(\xi_1^2+\eta_1^2\right)\right]\mathrm{Cos}\vartheta - i\left[R^2 + \left(\xi_1^2+\eta_1^2\right)\right]\mathrm{Sin}\vartheta\right\}$$

$$= 2\pi R^2\left\{\left[1 + \left(\frac{\xi_1}{R}\right)^2 + \left(\frac{\eta_1}{R}\right)\right]\mathrm{Sin}\vartheta + i\left[1 - \left(\frac{\xi_1}{R}\right)^2 - \left(\frac{\eta_1}{R}\right)^2\right]\mathrm{Cos}\vartheta\right\}$$

$$= 2\pi R^2\left\{\frac{b}{R}\,\mathrm{Sin}\vartheta + i\,\frac{c}{R}\,\mathrm{Cos}\vartheta\right\}, \tag{5.23}$$

where $b \equiv y_e'(\delta)$ and $c \equiv z_c'(\delta + \pi/2)$ are the semi-major and semi-minor axes, respectively, of the ellipse C_σ

.

Differentiation then gives

$$\frac{\partial}{\partial x}\oint_{C_\sigma} \bar{F}(\bar{\sigma})\, d\bar{\sigma} = 4\pi R \frac{dR}{dx}\left\{\left(\frac{b}{R}\right) \mathrm{Sin}\vartheta + i\left(\frac{c}{R}\right) \mathrm{Cos}\vartheta\right\}$$

$$+ 2\pi R^2 \left\{\frac{d}{dx}\left(\frac{b}{R}\right) \mathrm{Sin}\vartheta + i \frac{d}{dx}\left(\frac{c}{R}\right) \mathrm{Cos}\vartheta\right\};$$

but

$$\frac{d}{dx}\left(\frac{b}{R}\right) = \frac{d}{dx}\left\{1 + \left(\frac{\xi_1}{R}\right)^2 + \left(\frac{\eta_1}{R}\right)^2\right\} = 2\left(\frac{\xi_1}{R}\right)\frac{d}{dx}\left(\frac{\xi_1}{R}\right) + 2\left(\frac{\eta_1}{R}\right)\frac{d}{dx}\left(\frac{\eta_1}{R}\right)$$

$$= -\frac{d}{dx}\left\{1 - \left(\frac{\xi_1}{R}\right)^2 - \left(\frac{\eta_1}{R}\right)^2\right\} = -\frac{d}{dx}\left(\frac{c}{R}\right), \qquad (5.24)$$

hence

$$\frac{\partial}{\partial x}\oint_{C_\sigma} \bar{F}(\bar{\sigma})\, d\bar{\sigma} = 4\pi R \frac{dR}{dx}\left\{\left(\frac{b}{R}\right) \mathrm{Sin}\,\vartheta + i\left(\frac{c}{R}\right) \mathrm{Cos}\,\vartheta\right\}$$

$$+ 2\pi R^2 \frac{d}{dx}\left(\frac{b}{R}\right)(\mathrm{Sin}\,\vartheta - i\,\mathrm{Cos}\,\vartheta). \qquad (5.25)$$

Also

$$ie^{-i\vartheta}\frac{dS}{dx} = i\frac{dS}{dx}(\mathrm{Cos}\vartheta - i\mathrm{Sin}\vartheta) = \frac{dS}{dx}(\mathrm{Sin}\vartheta + i\,\mathrm{Cos}\vartheta), \qquad (5.26)$$

where the area S of the ellipse C_σ is

$$S = \pi\, bc. \qquad (5.27)$$

In this case S is known, but in the more general case we would need to use the relation 4.25, in association with that corresponding to 5.7.

It follows from 2.47, 5.25 and 5.26, that

$$\frac{dC_F}{d(-x)} = \frac{2\sigma_i}{S_R}\left\{\left[-4\pi R \frac{dR}{dx}\left(\frac{c}{R}\right) + 2\pi R^2 \frac{d}{dx}\left(\frac{b}{R}\right) + \frac{dS}{dx}\right] \cos\vartheta \right.$$

$$\left. + i\left[4\pi R \frac{dR}{dx}\left(\frac{b}{R}\right) + 2\pi R^2 \frac{d}{dx}\left(\frac{b}{R}\right) - \frac{dS}{dx}\right] \sin\vartheta\right\} . \qquad (5.28)$$

Now

$$\frac{b}{R} = 1 + \left(\frac{\xi_1}{R}\right)^2 + \left(\frac{\eta_1}{R}\right)^2, \qquad (5.29)$$

and

$$\frac{c}{R} = 1 - \left(\frac{\xi_1}{R}\right)^2 - \left(\frac{\eta_1}{R}\right)^2. \qquad (5.30)$$

Upon adding these equations we obtain

$$b + c = 2R, \text{ or } R = (b+c)/2 \qquad (5.31)$$

and upon subtraction

$$b - c = 2R\left\{\left(\frac{\xi_1}{R}\right)^2 + \left(\frac{\eta_1}{R}\right)^2\right\} ; \qquad (5.32)$$

hence multiplication gives

$$b^2 - c^2 = 4R^2\left\{\left(\frac{\xi_1}{R}\right)^2 + \left(\frac{\eta_1}{R}\right)^2\right\} = 4\left(\xi_1^2 + \eta_1^2\right) = 4\zeta_1^2 . \qquad (5.33)$$

From (5.31)

$$\frac{b}{R} = \frac{2b}{b + c} , \frac{c}{R} = \frac{2c}{b + c} \qquad (5.34)$$

thus

$$\frac{d}{dx}\left(\frac{b}{R}\right) = \frac{\frac{db}{2dx}}{b + c} - \frac{2b}{(b + c)^2}\left(\frac{db}{dx} + \frac{dc}{dx}\right)$$

$$= 2\left(c\frac{db}{dx} - b\frac{dc}{dx}\right)/(b + c)^2 . \qquad (5.35)$$

Taking the terms in 5.28 in order we have

$$4\pi R\frac{dR}{dx}\left(\frac{c}{R}\right) = 4\pi c\frac{dR}{dx}$$

$$= 2\pi c\left(\frac{db}{dx} + \frac{dc}{dx}\right),$$

$$2\pi R^2 \frac{d}{dx}\left(\frac{b}{R}\right) = 2\pi \times \frac{1}{4}\left(b + c\right)^2 \times 2\left(c\frac{db}{dx} - b\frac{dc}{dx}\right)/(b + c)^2$$

$$= \pi\left(c\frac{db}{dx} - b\frac{dc}{dx}\right)$$

and

$$\frac{dS}{dx} = \pi\left(b\frac{dc}{dx} + c\frac{db}{dx}\right),$$

from which the [] bracketed term multiplying $Cos\vartheta$ is $-2\pi c\frac{dc}{dx}$. Obtaining the multiplier of $Sin\vartheta$ in a similar way, we find that 5.28 reduces to

$$\frac{dC_F}{d(-x)} = \frac{4\pi\sigma_i}{S_R}\left\{ib\frac{db}{dx}Sin\vartheta - c\frac{dc}{dx}Cos\vartheta\right\}. \qquad (5.36)$$

It is interesting to note that this agrees exactly with equation 3.22,which was specifically developed for the case $\delta = 0$, where the major axis is alignedwith the y direction. See Fig. 9. The implication of 5.36 isthat the form of the relation is independent of δ, but b and c, and, thereby, $\frac{db}{dx}$ and $\frac{dc}{dx}$, will change with ξ_1 and η_1.

Finally, although in this case S is known, we may verify the validity of 4.24, 4.25. We have

$$\sigma_c = y_c + iz_c = r_c e^{i\gamma} = r_c(\mathrm{Cos}\gamma + i\,\mathrm{Sin}\gamma)$$

or

$$y_c = r_c\,\mathrm{Cos}\gamma$$

and

$$z_c = r_c\,\mathrm{Sin}\gamma\ .$$

Hence

$$\frac{z_c}{y_c}(\theta) = \mathrm{Tan}\gamma$$

or

$$\frac{d}{d\theta}\left\{\frac{z_c}{y_c}(\theta)\right\} = \frac{d\gamma}{d\theta}\,\mathrm{Sec}^2\gamma,$$

giving

$$\frac{d\gamma}{d\theta} = \mathrm{Cos}^2\gamma\,\frac{d}{d\theta}\left\{\frac{z_c}{y_c}(\theta)\right\} = \left(\frac{y_c}{r_c}\right)^2\frac{d}{d\theta}\left\{\frac{z_c}{y_c}(\theta)\right\}\ . \qquad (5.37)$$

The area of the cross-section is therefore

$$S = \tfrac{1}{2}\int_o^{2\pi} r_c^2 d\gamma = \tfrac{1}{2}\int_o^{2\pi} r_c^2\,\frac{d\gamma}{d\theta}\,d\theta$$

$$= \tfrac{1}{2}\int_o^{2\pi} y_c^2\,\frac{d}{d\theta}\left\{\frac{z_c}{y_c}(\theta)\right\}d\theta;$$

but

$$\frac{d}{d\theta}\left\{\frac{z_c}{y_c}(\theta)\right\} = \left\{y_c\frac{dz_c}{d\theta} - z_c\frac{dy_c}{d\theta}\right\}/y_c^2\ ,$$

hence

$$S = \frac{1}{2}\int_0^{2\pi}\left\{y_c\frac{dz_c}{d\theta} - z_c\frac{dz_c}{d\theta} - z_c\frac{dy_c}{d\theta}\right\}d\theta \ . \qquad (5.38)$$

In the present case we may write

$$\left.\begin{aligned} y_c &= A\ \mathrm{Cos}\theta + B\ \mathrm{Sin}\theta \\ z_c &= B\ \mathrm{Cos}\theta + C\ \mathrm{Sin}\theta \end{aligned}\right\}, \qquad (5.39)$$

where

$$\left.\begin{aligned} A &= R\left\{1 + \left(\frac{\xi_1}{R}\right)^2 - \left(\frac{\eta_1}{R}\right)^2\right\} \\ B &= 2R\left(\frac{\xi_1}{R}\right)\left(\frac{\eta_1}{R}\right) \\ &\text{and} \\ C &= R\left\{1 - \left(\frac{\xi_1}{R}\right)^2 + \left(\frac{\eta_1}{R}\right)^2\right\} \end{aligned}\right\}, \qquad (5.40)$$

which yields

$$\left.\begin{aligned} \frac{dy_c}{d\theta} &= -A\ \mathrm{Sin}\theta + B\ \mathrm{Cos}\ \theta \\ &\text{and} \\ \frac{dz}{d\theta}_c &= -B\ \mathrm{Sin}\ \theta + C\ \mathrm{Cos}\ \theta. \end{aligned}\right\} \qquad (5.41)$$

Substituting from 5.39 and 5.41 gives

$$y_c\frac{dz_c}{d\theta} - z_c\frac{dy_c}{d\theta} = AC - B^2,$$

or

$$S = \frac{1}{2}(AC - B^2)\int_o^{2\pi} d\theta = \pi\ (AC - B^2), \qquad (5.42)$$

which, on further substitution from 5.40, becomes

$$S = \pi R^2 \left\{ \left[1 + \left(\frac{\xi_1}{R}\right)^2 - \left(\frac{\eta_1}{R}\right)^2 \right] \left[1 - \left(\frac{\xi_1}{R}\right)^2 + \left(\frac{\eta_1}{R}\right)^2 \right] - 4 \left(\frac{\xi_1}{R}\right)^2 \left(\frac{\eta_1}{R}\right)^2 \right\}$$

$$= \pi R^2 \left\{ 1 - \left[\left(\frac{\xi_1}{R}\right)^2 - \left(\frac{\eta_1}{R}\right) \right]^2 - 4 \left(\frac{\xi_1}{R}\right)^2 \left(\frac{\eta_1}{R}\right)^2 \right\}$$

$$= \pi R^2 \left\{ 1 - \left(\frac{\xi_1}{R}\right)^4 - \left(\frac{\eta_1}{R}\right)^4 - 2 \left(\frac{\xi_1}{R}\right)^2 \left(\frac{\eta_1}{R}\right)^2 \right\}$$

$$= \pi R^2 \left\{ \left[1 - \left(\frac{\xi_1}{R}\right)^2 - \left(\frac{\eta_1}{R}\right)^2 \right] \left[1 + \left(\frac{\xi_1}{R}\right)^2 + \left(\frac{\eta_1}{R}\right)^2 \right] \right\}$$

or

$$S = \pi \text{ bc, as required.} \qquad (5.43)$$

Having explored these elliptic cross-sections at some length, let us now proceed to the more general case $\zeta_o = 0$, $k > 2$, which is a particular sub-class of the von Mises class of mappings.

6. Von Mises Mapping; Case $\zeta_o = 0$, $k = 3$.

The elliptic cross-sections obtained in Section 5 offer a useful basis for the design of lifting bodies, particularly if the body section aspect-ratio is varied longitudinally. Such shapes formed the basis for the experimental studies described in Refs. 5 and 8. However, these shapes are uncambered with respect to their lateral axes and, in our exploration of the present technique, it would be a valuable addition if we can develop methods for generating bodies which have such a camber. A practical example of such a body is the NASA Space Shuttle.

One of the simpler examples of such a body may be obtained by taking an additional critical point, ζ_3. It is not suggested that by taking three critical points we shall be able to design cross-sections having a wide range of geometric form. However, it will serve to illustrate some of the procedure involved.

We have

$$\frac{d\sigma}{d\zeta} = \left(1 - \frac{\zeta_1}{\zeta}\right)\left(1 - \frac{\zeta_2}{\zeta}\right)\left(1 - \frac{\zeta_3}{\zeta}\right), \tag{6.1}$$

where, from 4.19,

$$\zeta_1 + \zeta_2 + \zeta_3 = 0 \tag{6.2}$$

This latter condition corresponds to requiring the centroid of the triangle, having vertices $\zeta_1, \zeta_2, \zeta_3$, to be at the origin. See Fig. 12 (a).

On expanding 6.1, using 6.2, we have

$$\frac{d\sigma}{d\zeta} = 1 + \frac{\zeta_1\zeta_2 + \zeta_2\zeta_3 + \zeta_3\zeta_1}{\zeta^2} - \frac{\zeta_1\zeta_2\zeta_3}{\zeta^3}, \tag{6.3}$$

which, upon integration, gives

$$\sigma = \zeta - \frac{\zeta_1\zeta_2 + \zeta_2\zeta_3 + \zeta_3\zeta_1}{\zeta} + \frac{\zeta_1\zeta_2\zeta_3}{2\zeta^2}, \tag{6.4}$$

the constant of integration being zero, as was assumed in the original formulation 4.5. It follows from 4.5 and 6.4 that

$$\left.\begin{aligned} C_1 &= -\zeta_1\zeta_2 - \zeta_2\zeta_3 - \zeta_3\zeta_1 \\ \text{and} \qquad C_2 &= \tfrac{1}{2}\zeta_1\zeta_2\zeta_3. \end{aligned}\right\} \tag{6.5}$$

The image C_σ of the circle $C_\zeta = Re^{i\theta}$ under the mapping 6.4 is given by

$$\sigma_c = Re^{i\theta} + \frac{C_1}{R}e^{i\theta} + \frac{C_2}{R^2}e^{-2i\theta} = y_c + iz_c \ . \tag{6.6}$$

Generally the critical points will be complex and we may write

$$\left.\begin{aligned} C_1 &= C_{11} + i\,C_{12} \\ \text{and} \qquad C_2 &= C_{21} + i\,C_{22}. \end{aligned}\right\} \tag{6.7}$$

On substitution into 6.6 we may then obtain

$$\left.\begin{aligned} \frac{y_c}{R} &= \left(1 + \frac{C_{11}}{R_2}\right)\text{Cos}\,\theta + \frac{C_{21}}{R^3}\text{Cos}\,2\theta + \frac{C_{12}}{R^2}\text{Sin}\,\theta + \frac{C_{22}}{R^3}\text{Sin}\,2\theta \\ \text{and} \qquad \frac{z_c}{R} &= \left(1 - \frac{C_{11}}{R^2}\right)\text{Sin}\,\theta - \frac{C_{21}}{R^3}\text{Sin}\,2\theta + \frac{C_{12}}{R^2}\text{Cos}\,2\theta + \frac{C_{22}}{R^3}\text{Cos}\,2\theta \end{aligned}\right\}. \tag{6.8}$$

Most bodies of interest will be symmetric with respect to the z - axis; e.g. Space Shuttle, and we seek to impose this symmetry by our choice of critical points. However, since the direction of the onset velocity $U_\infty\sigma_i$ may be chosen at will, we may relax this requirement to having symmetry with respect to the z - axis or the y - axis.

Symmetry with respect to the z - axis requires that when $\theta = \pi/2$ and $\frac{3\pi}{2}$ then $y_c/R=0$ and that

$$\left.\begin{aligned} \frac{y_c}{R}\left(\frac{\pi}{2} - \psi\right) &= -\frac{y_c}{R}\left(\frac{\pi}{2} + \psi\right) \\ \frac{z_c}{R}\left(\frac{\pi}{2} - \psi\right) &= \frac{z_c}{R}\left(\frac{\pi}{2} + \psi\right) \end{aligned}\right\}, \tag{6.9}$$

where $\psi = \theta - \pi/2$. In order to achieve these conditions it is necessary that

$$C_{12} = C_{21} = 0,$$

and 6.8 becomes

$$\left.\begin{aligned} \frac{y_c}{R} &= \left(1 + \frac{C_{11}}{R^2}\right) \text{Cos } \theta + \frac{C_{22}}{R^3} \text{ Sin } 2\theta \\ \frac{z_c}{R} &= \left(1 - \frac{C_{11}}{R^2}\right) \text{Sin } \theta + \frac{C_{22}}{R^3} \text{ Cos } 2\theta \end{aligned}\right\} \left(\begin{array}{c} \text{Symmetry} \\ \text{w.r.t.} \\ \text{z-axis} \end{array} \right) \qquad (6.10)$$

In a similar way, symmetry with respect to the y-axis requires that when $\theta = 0$ and π then $z_c/R = 0$ and that

$$\left.\begin{aligned} \frac{y_c}{R}(\theta) &= \frac{y_c}{R}(-\theta) \\ \frac{z_c}{R}(-\theta) &= -\frac{z_c}{R}(\theta) \end{aligned}\right\} \qquad (6.11)$$

This is achieved by the necessary condition that

$$C_{12} = C_{22} = 0$$

and 6.8 becomes

$$\left.\begin{aligned} \frac{y_c}{R} &= \left(1 + \frac{C_{11}}{R^2}\right) \text{Cos}\theta + \frac{C_{21}}{R^3} \text{ Cos } 2\theta \\ \frac{z_c}{R} &= \left(1 - \frac{C_{11}}{R^2}\right) \text{Sin}\theta - \frac{C_{21}}{R^3} \text{ Sin } 2\theta. \end{aligned}\right\} \left(\begin{array}{c} \text{Symmetry} \\ \text{w.r.t.} \\ \text{y-axis.} \end{array} \right) \qquad (6.12)$$

We now need to establish whether our choice of critical points can be such as to produce these conditions.

Writing

$$\zeta_n = \xi_n + i\eta_n, \qquad (6.13)$$

then, on substitution into 6.2, we have

$$\xi_1 + \xi_2 + \xi_3 + i(\eta_1 + \eta_2 + \eta_3) = 0$$

or

and

$$\left.\begin{aligned} \xi_3 &= -\xi_1 - \xi_2 \\ \eta_3 &= -\eta_1 - \eta_2 \end{aligned}\right\} . \qquad (6.14)$$

From 6.5 and 6.13 we obtain

$$\begin{aligned} -C_1 &= \left[\left(\xi_1\xi_2 - \eta_1\eta_2\right) + \left(\xi_2\xi_3 - \eta_2\eta_3\right) + \left(\xi_1\xi_3 - \eta_1\eta_3\right)\right] \\ &+ i\left[\left(\xi_1\eta_2 + \xi_2\eta_1\right) + \left(\xi_2\eta_3 + \xi_3\eta_2\right) + \left(\xi_1\eta_3 + \xi_3\eta_1\right)\right] \end{aligned} \tag{6.15}$$

and

$$\begin{aligned} 2C_2 &= \left[\xi_3\left(\xi_1\xi_2 - \eta_1\eta_2\right) - \eta_3\left(\xi_1\eta_2 + \xi_2\eta_1\right)\right] \\ &+ i\left[\xi_3\left(\xi_1\eta_2 + \xi_2\eta_1\right) + \eta_3\left(\xi_1\xi_2 - \eta_1\eta_2\right)\right]. \end{aligned} \tag{6.16}$$

Hence, using 6.14,

$$\left.\begin{aligned} -C_{11} &= \xi_1\xi_2 - \eta_1\eta_2 - \xi_3^2 + \eta_3^2, \\ -C_{12} &= \xi_1\eta_2 + \xi_2\eta_1 - 2\xi_3\eta_3 , \\ 2C_{21} &= \xi_3\left(\xi_1\xi_2 - \eta_1\eta_2\right) - \eta_3\left(\xi_1\eta_2 + \xi_3\eta_1\right) \\ \text{and} \\ 2C_{22} &= \xi_3\left(\xi_1\eta_2 + \xi_2\eta_1\right) + \eta_3\left(\xi_1\xi_2 - \eta_1\eta_2\right) . \end{aligned}\right\} \tag{6.17}$$

Choosing $\xi_3 = 0$, or $\xi_1 = -\xi_2$, then

$$-C_{12} = \xi_1\eta_2 + \xi_2\eta_1 = \xi_1\left(\eta_2 - \eta_1\right) ,$$

which is zero if $\eta_1 = \eta_2$. Also

$$2C_{21} = -\eta_3\xi_1\left(\eta_2 - \eta_1\right) = 0.$$

Thus for this choice of critical points, which are symmetrically disposed with respect to the η-axis, as in Fig.12(b), σ_c will, from 6.10, be symmetric with respect to the z-axis. In addition we shall have

$$\left.\begin{aligned} \zeta_1 &= \xi_1 + i\eta_1 \\ \zeta_2 &= -\xi_1 + i\eta_1 \\ \zeta_3 &= -2i\eta_1 \ , \end{aligned}\right\} , \tag{6.18}$$

whilst

$$-C_{11} = -\xi_1^2 - \eta_1^2 + 4\eta_1^2 = -\xi_1^2 + 3\eta_1^2$$

and

$$C_{22} = \eta_1\left(\xi_1^2 + \eta_1^2\right),$$

or

$$\left.\begin{aligned} \frac{C_{11}}{R^2} &= \left(\frac{\xi_1}{R}\right)^2 - 3\left(\frac{\eta_1}{R}\right)^2 \\ \text{and} \qquad \frac{C_{22}}{R^3} &= \left(\frac{\eta_1}{R}\right)\left\{\left(\frac{\xi_1}{R}\right)^2 + \left(\frac{\eta_2}{R}\right)^2\right\} . \end{aligned}\right\} \tag{6.19}$$

Alternatively, by choosing $\eta_3 = 0$ or $\eta_1 = -\eta_2$, then

$$-C_{12} = \xi_1\eta_2 + \xi_2\eta_1 = \eta_1(\xi_2 - \xi_1),$$

which is zero if $\xi_1 = \xi_2$. Also

$$2C_{22} = \xi_3(\xi_1\eta_2 + \xi_2\eta_1) = \xi_3\eta_1(\xi_2 - \xi_1) = 0 .$$

Thus for this second choice of critical points, which are symmetrically disposed with respect to the ξ-axis, as in Fig.12(c), σ_c will, from 6.12, by symmetric with respect to the y-axis. Also we shall have

$$\left.\begin{aligned} \zeta_1 &= \xi_1 + i\eta_1 \\ \zeta_2 &= \xi_1 - i\eta_1 \\ \zeta_3 &= -2\xi_1 \ , \end{aligned}\right\} \tag{6.20}$$

whilst

$$-C_{11} = \eta_1^2 - 3\xi_1^2$$

and

$$C_{21} = -\xi_1\left(\xi_1^2 + \eta_1^2\right),$$

or

$$\left.\begin{aligned} \frac{C_{11}}{R^2} &= 3\left(\frac{\xi_1}{R}\right)^2 - \left(\frac{\eta_1}{R}\right)^2 \\ \text{and} \\ \frac{C_{21}}{R^3} &= -\left(\frac{\xi_1}{R}\right)\left\{\left(\frac{\xi_1}{R}\right)^2 + \left(\frac{\eta_1}{R}\right)^2\right\}. \end{aligned}\right\} \qquad (6.21)$$

By taking values of ξ_1/R and η_1/R such that the values of ζ_1,ζ_1,ζ_3 lie inside $C_{\zeta,}$ as in Fig. 12 (c), we may readily generate families of cambered shapes. Some examples of these are shown in Fig. 13. The degenerate case is obtained when $\xi_1/R = 0$, hence $\zeta_3 = 0$ and C_σ becomes an ellipse. As we make ξ_1/R more negative, η_1/R being fixed, so the extent of the camber produced increases. The reverse camber is obtained by a change of sign in ξ_1/R.

The shapes generated in this exercise all have symmetry with respect to the y-axis. We may generate the same set of shapes, but now having symmetry with respect to the z-axis, by simply interchanging ξ_1 with η_1 and writing the expressions for y_c, z_c interchanging ξ_1 with η_1 and writing the expressions for y_c, z_c in terms of $\psi = \frac{\pi}{2} - \theta$, where ψ is the angle measured from the vertical axis of symmetry. We may demonstrate this by first taking $C_{12} = 0$ in 6.8 and then substituting from either 6.19 or 6.21. In the case of

z - symmetry ($C_{21} = 0$)

$$\left.\begin{aligned} \frac{y_c}{R} &= \left\{1 + \left(\frac{\xi_1}{R}\right)^2 - 3\left(\frac{\eta_1}{R}\right)^2\right\}\text{Cos }\theta + \left(\frac{\eta_1}{R}\right)\left\{\left(\frac{\xi_1}{R}\right)^2 + \left(\frac{\eta_1}{R}\right)^2\right\}\text{Sin }2\theta \\ \text{and} \\ \frac{z_c}{R} &= \left\{1 - \left(\frac{\xi_1}{R}\right)^2 + 3\left(\frac{\eta_1}{R}\right)^2\right\}\text{Sin }\theta + \left(\frac{\eta_1}{R}\right)\left\{\left(\frac{\xi_1}{R}\right)^2 + \left(\frac{\eta_1}{R}\right)^2\right\}\text{Cos }2\theta, \end{aligned}\right\}, \qquad (6.22)$$

whilst in the case of

y - symmetry ($C_{22} = 0$)

$$\left.\begin{aligned} \frac{y_c}{R} &= \left\{1 - \left(\frac{\eta_1}{R}\right)^2 + 3\left(\frac{\xi_1}{R}\right)^2\right\}\text{Cos}\theta - \left(\frac{\xi_1}{R}\right)\left\{\left(\frac{\xi_1}{R}\right)^2 + \left(\frac{\eta_1}{R}\right)^2\right\}\text{Cos } 2\theta \\ \text{and} \\ \frac{z_c}{R} &= \left\{1 + \left(\frac{\eta_1}{R}\right)^2 - 3\left(\frac{\xi_1}{R}\right)^2\right\}\text{Sin}\theta + \left(\frac{\xi_1}{R}\right)\left\{\left(\frac{\xi_1}{R}\right)^2 + \left(\frac{\eta_1}{R}\right)^2\right\}\text{Sin } 2\theta \end{aligned}\right\} . \qquad (6.23)$$

If now we re-write 6.22 in terms of ψ, and interchange ξ_1 and η_1, we obtain

$$\left.\begin{aligned} &\left\{1 + \left(\frac{\eta_1}{R}\right)^2 - 3\left(\frac{\xi_1}{R}\right)^2\right\}\text{Sin}\psi + \left(\frac{\xi_1}{R}\right)\left\{\left(\frac{\xi_1}{R}\right)^2 + \left(\frac{\eta_1}{R}\right)^2\right\}\text{Sin } 2\psi = \text{(i)} \\ &\text{and} \\ &\left\{1 - \left(\frac{\eta_1}{R}\right)^2 + 3\left(\frac{\xi_1}{R}\right)^2\right\}\text{Cos}\psi - \left(\frac{\xi_1}{R}\right)\left\{\left(\frac{\xi_1}{R}\right)^2 + \left(\frac{\eta_1}{R}\right)^2\right\}\text{Cos } 2\psi = \text{(ii)}. \end{aligned}\right\} \qquad (6.24)$$

Thus 6.24(i) has the same form as the z_c/R equation in 6.23 and 6.24(ii) has the same form as the y_c/R equation in 6.23. By taking θ and ψ over the same range of values we see that 6.24 generates the same shape σ_c, with respect to the y-axis, as 6.23. This confirms that 6.22 defines the same family of shapes as 6.23, but rotated through a right-angle.

From this exercise we see that considerable variety of body cross-section is possible, even with the restrictions that we have placed on the location of critical points. An even greater variation of shape will, presumably, be possible by taking a larger number of critical points.

Having examined the cambering produced by the presence of the third critical point ζ_3, let us now turn to obtaining the related expression for the gradient of the normal force. We have, from 5.20, the relation for $\bar{F}_1(\bar{\zeta})$, whilst from 6.3 and 6.5

$$\frac{d\bar{\sigma}}{d\bar{\zeta}} = \frac{d\sigma}{d\zeta}(\bar{\zeta}) = 1 - \frac{C_{11}}{\bar{\zeta}^2} - 2\frac{C_{21}}{\bar{\zeta}^3} \cdot \qquad (6.25)$$

It follows that

$$\oint_{C_\sigma} \bar{F}_1(\bar{\sigma})d\bar{\sigma} = \oint_{C_\zeta} \bar{F}_1\ (\bar{\zeta})\frac{d\sigma}{d\bar{\zeta}}\ d\bar{\zeta}$$

$$= \oint_{C_\zeta} \left\{\left(\bar{\zeta} + \frac{R}{\bar{\zeta}}\right)\mathrm{Cos}\vartheta + i\left(\bar{\zeta} - \frac{R^2}{\bar{\zeta}}\right)\mathrm{Sin}\vartheta\right\}\left\{1 - \frac{C_{11}}{\bar{\zeta}^2}\right\}d\bar{\zeta}\ , \qquad (6.26)$$

since the term containing C_{21} will not contribute to the residue. Thus

$$\oint_{C_\sigma} \bar{F}_1(\bar{\sigma})d\bar{\sigma} = \oint_{C_\infty} \left\{\left[\frac{R^2 - C_{11}}{\bar{\zeta}}\right]\mathrm{Cos}\vartheta - i\left[\frac{R^2 + C_{11}}{\bar{\zeta}}\right]\mathrm{Sin}\vartheta\right\}d\bar{\zeta}$$

$$= \left\{\left(R^2 - C_{11}\right)\mathrm{Cos}\vartheta - i\left(R^2 + C_{11}\right)\mathrm{Sin}\vartheta\right\}\oint_{C_\infty} \frac{d\bar{\zeta}}{\bar{\zeta}}$$

$$= 2\pi i\left\{\left(R^2 - C_{11}\right)\mathrm{Cos}\vartheta - i\left(R^2 + C_{11}\right)\mathrm{Sin}\vartheta\right\}$$

$$= 2\pi R^2\left\{\left[1 + \left(\frac{C_{11}}{R^2}\right)\right]\mathrm{Sin}\vartheta + i\left[1 - \left(\frac{C_{11}}{R^2}\right)\mathrm{Cos}\vartheta\right\}\right. . \qquad (6.27)$$

We may obtain the cross-sectional area from 5.38 and 6.8, where we confine ourselves to the class of symmetric body previously discussed and illustrated in Fig.13. Since $C_{12} = 0$ in both these cases of body symmetry we may substitute this into 6.8. Thus we have

$$\frac{1}{R}\frac{dy_c}{d\theta} = -\left(1 + \frac{C_{11}}{R^2}\right)\mathrm{Sin}\theta - 2\frac{C_{21}}{R^3}\mathrm{Sin}2\theta + \frac{C_{22}}{R^3}\mathrm{Cos}2\theta,$$

and

$$\frac{1}{R}\frac{dz_c}{d\theta} = \left(1 - \frac{C_{11}}{R^2}\right)\mathrm{Cos}\theta - 2\frac{C_{21}}{R^3}\mathrm{Cos}2\theta - 2\frac{C_{22}}{R^3}\mathrm{Sin}2\theta,$$

from which

$$\frac{1}{R^2}\left\{ y_c \frac{dz_c}{d\theta} - z_c \frac{dy_c}{d\theta} \right\}$$

$$= \left[\left(1+ \frac{C_{11}}{R^2}\right)\mathrm{Cos}\theta + \frac{C_{21}}{R^2}\mathrm{Cos}2\theta + \frac{C_{22}}{R^3}\mathrm{Sin}2\theta\right]\left[\left(1- \frac{C_{11}}{R^2}\right)\mathrm{Cos}\theta - 2\frac{C_{21}}{R^3}\mathrm{Cos}2\theta - 2\frac{C_{22}}{R^3}\mathrm{Sin}2\theta\right]$$

$$+ \left[\left(1- \frac{C_{11}}{R^2}\right)\mathrm{Sin}\theta - \frac{C_{21}}{R^3}\mathrm{Sin}2\theta - \frac{C_{22}}{R^3}\mathrm{Cos}2\theta\right]\left[\left(1+ \frac{C_{11}}{R^2}\right)\mathrm{Sin}\theta + 2\frac{C_{21}}{R^3}\mathrm{Sin}2\theta - 2\frac{C_{22}}{R^3}\mathrm{Cos}2\theta\right]$$

$$= 1 - \left(\frac{C_{11}}{R^2}\right)^2 - 2\left(\frac{C_{21}}{R^3}\right)^2 - 2\left(\frac{C_{22}}{R^3}\right)^2 + \text{terms in } \mathrm{Sin}\theta\ \mathrm{Sin}2\theta,\ \mathrm{Cos}\theta\mathrm{Cos}2\theta, \text{ etc.}$$

It follows that

$$S = \frac{1}{2}\int_o^{2\pi}\left\{ y_c \frac{dz_c}{d\theta} - z_c \frac{dy_c}{d\theta} \right\} d\theta$$

$$= \frac{1}{2} R^2\left\{1 - \left(\frac{C_{11}}{R^2}\right)^2 - 2\left(\frac{C_{21}}{R^3}\right)^2 - 2\left(\frac{C_{22}}{R^3}\right)^2\right\}\int_o^{2\pi} d\theta$$

or

$$S = \pi R^2\left\{1- \left(\frac{C_{11}}{R^2}\right)^2 - 2\left(\frac{C_{21}}{R^3}\right)^2 - 2\left(\frac{C_{22}}{R^3}\right)^2\right\}, \qquad (6.28)$$

since

$$\int_o^{2\pi} \mathrm{Sin}\theta\ \mathrm{Sin}2\theta\ d\theta = \int_o^{2\pi} \mathrm{Sin}\theta\ \mathrm{Cos}2\theta\ d\theta \ \ldots \text{ etc. are zero.}$$

In 6.28, C_{21} will be zero when the body is symmetric about the z-axis and C_{22} will be zero when the body is symmetric about the y-axis.

From 6.27, 6.28 and 2.48 we then obtain

$$\frac{dC_F}{d(-x)} = \frac{2_i\sigma_i}{S_R}\frac{\partial}{\partial_x}\left\{2\pi R^2\left[1 + \left(\frac{C_{11}}{R^2}\right)\right]\text{Sin}\,\vartheta + i\left[1 - \left(\frac{C_{11}}{R^2}\right)\text{Cos}\,\vartheta\right]\right.$$

$$\left. - i\,e^{-i\vartheta}\pi R^2\left[1 - \left(\frac{C_{11}}{R^2}\right)^2 - 2\left(\frac{C_{21}}{R^3}\right)^2 - 2\left(\frac{C_{22}}{R^3}\right)^2\right]\right\}$$

$$= \frac{2\pi\sigma_i}{S_R}\frac{\partial}{\partial x}\left\{R^2\left[2i\left[1 + \left(\frac{C_{11}}{R^2}\right)\right]\text{Sin}\vartheta - 2\left[1 - \left(\frac{C_{11}}{R^2}\right)\right]\text{Cos}\vartheta\right.\right.$$

$$\left.\left. + \left(\text{Cos}\vartheta - i\text{Sin}\vartheta\right)\left[1 - \left(\frac{C_{11}}{R^2}\right)^2 - 2\left(\frac{C_{21}}{R^3}\right)^2 - 2\left(\frac{C_{22}}{R^3}\right)^2\right]\right]\right\}$$

$$= \frac{2\pi\sigma_i}{S_R}\frac{\partial}{\partial x}\left\{R^2\left[\left[1 + 2\left(\frac{C_{11}}{R^2}\right) + \left(\frac{C_{11}}{R^3}\right)^2 + 2\left(\frac{C_{21}}{R^3}\right)^2 + 2\left(\frac{C_{22}}{R^3}\right)^2\right] i\,\text{Sin}\vartheta\right.\right.$$

$$\left.\left. - \left[1 - 2\left(\frac{C_{11}}{R^2}\right) + \left(\frac{C_{11}}{R^2}\right)^2 + 2\left(\frac{C_{21}}{R^3}\right)^2 + 2\left(\frac{C_{22}}{R^3}\right)^2\right]\text{Cos}\vartheta\right]\right\}$$

$$= -\frac{2\pi}{S_R}\frac{\partial}{\partial x}\left\{R^2\left[i\alpha\left[1 + 2\left(\frac{C_{11}}{R^2}\right) + \left(\frac{C_{11}}{R^2}\right)^2 + 2\left(\frac{C_{21}}{R^3}\right)^2 + 2\left(\frac{C_{22}}{R^3}\right)^2\right]\right.\right.$$

$$\left.\left. + \beta\left[1 - 2\left(\frac{C_{11}}{R^2}\right) + \left(\frac{C_{11}}{R^2}\right)^2 + 2\left(\frac{C_{21}}{R^3}\right)^2 + 2\left(\frac{C_{22}}{r^3}\right)^2\right]\right]\right\}. \quad (6.29)$$

Hence, from 2.11,

$$\frac{dC_z}{d(-x)} = \frac{d\pi\alpha}{S_R}\frac{\partial}{\partial x}\left\{N_z R^2\right\} = \frac{2\pi\alpha}{S_R}\left\{N_z\frac{dR^2}{dx} + R^2\frac{dN_z}{dx}\right\} \quad (6.30)$$

and

$$\frac{dC_Y}{d(-x)} = -\frac{2\pi\beta}{S_R}\left\{N_Y\frac{dR^2}{dx} + R^2\frac{dN_Y}{dx}\right\}, \quad (6.31)$$

where, we define,

$$\left.\begin{aligned} N_Z &= 1 + 2\left(\frac{C_{11}}{R^2}\right) + \left(\frac{C_{11}}{R^2}\right)^2 + 2\left(\frac{C_{21}}{R^3}\right) + 2\left(\frac{C_{22}}{R^3}\right)^2 \\ \text{and} \\ N_Y &= 1 - 2\left(\frac{C_{11}}{R^2}\right) + \left(\frac{C_{11}}{R^2}\right)^2 + 2\left(\frac{C_{21}}{R^3}\right)^2 + 2\left(\frac{C_{22}}{R^3}\right)^2. \end{aligned}\right\} \quad (6.32)$$

In these expressions we have, in the case of bodies with

z-symmetry,

$$C_{11},\ C_{22} \text{ given by 6.19, and } C_{21} = 0:$$

whilst in the case of bodies with

y-symmmetry,

$$C_{11},\ C_{21} \text{ given by 6.21, and } C_{22} = 0.$$

In addition we may obtain the relative loading factors F_z and F_Y, where

$$F_z = \frac{dC_z}{d(-x)} \text{ (non-circular)} \div \frac{dC_z}{d(-x)} \text{ (circular)}$$

$$= \frac{2\pi\alpha}{S_R} \frac{d}{dx} \left\{N_z R^2\right\} \div \frac{2\alpha}{S_R} \frac{d}{dx} (S),$$

since $N_Z = N_Y = 1$ for the circular section. Now

$$S = \pi R_e^2$$

is defined by (6.28), where R_e is the radius of the body of revolution having the same longitudinal distribution of cross-sectional area. If we write

$$k_R^2 = \left(\frac{R_e}{R}\right)^2 = 1 - \left(\frac{C_{11}}{R^2}\right)^2 - 2\left(\frac{C_{21}}{R^3}\right)^2 - 2\left(\frac{C_{22}}{R^3}\right)^2, \qquad (6.33)$$

then

$$F_z = \frac{d}{dx} \left\{N_z R^2\right\} \div \frac{d}{dx} \left\{k_R^2 R^2\right\} \qquad (6.34)$$

whilst

$$F_Y = \frac{d}{dx} \left\{N_Y R^2\right\} \div \frac{d}{dx} \left\{k_R^2 R^2\right\}. \qquad (6.35)$$

In the special case where the cross-section is geometrically similar at all stations x, then

$$\frac{dN_z}{dx} = \frac{dN_Y}{dx} = \frac{dk_R^2}{dx} = 0$$

and

$$\left.\begin{aligned} F_z &= \frac{N_z}{k_R^2} \\ F_Y &= \frac{N_Y}{k_R^2} \end{aligned}\right\} \qquad (6.36)$$

Having demonstrated how cambered cross-sections may be generated by using three critical points, let us move on to consider the extra generality provided by four singular points.

7. Von Mises Mapping - Case $\zeta_o = 0$, $k = 4$.

The procedure follows closely that of Section 6. We have

$$\frac{d\sigma}{d\zeta} = \left(1 - \frac{\zeta_1}{\zeta}\right)\left(1 - \frac{\zeta_2}{\zeta}\right)\left(1 - \frac{\zeta_3}{\zeta}\right)\left(1 - \frac{\zeta_4}{\zeta}\right), \tag{7.1}$$

where

$$\zeta_1 + \zeta_2 + \zeta_3 + \zeta_4 = 0. \tag{7.2}$$

This last condition requiring the centroid of the quadrilatral, having vertices ζ_1, ζ_2, ζ_3, ζ_4, to be at the origin, Fig.14(a).

Expanding 7.1 we obtain

$$\frac{d\sigma}{d\zeta} = \left\{1 - \frac{(\zeta_1 + \zeta_2)}{\zeta} + \frac{\zeta_1\zeta_2}{\zeta^2}\right\}\left\{1 - \frac{(\zeta_3 + \zeta_4)}{\zeta} + \frac{\zeta_3\zeta_4)}{\zeta^2}\right\}.$$

But, from 7.2, $\zeta_1 + \zeta_2 = -\zeta_3 - \zeta_4$, hence

$$\frac{d\sigma}{d\zeta} = \left\{1 - \frac{(\zeta_1 + \zeta_2)}{\zeta} + \frac{\zeta_1\zeta_2}{\zeta^2}\right\}\left\{1 + \frac{(\zeta_1 + \zeta_2)}{\zeta} + \frac{\zeta_3\zeta_4}{\zeta^2}\right\}$$

$$= 1 - \frac{(\zeta_1 + \zeta_2)^2 - \zeta_1\zeta_2 - \zeta_3\zeta_4}{\zeta^2} - \frac{(\zeta_1 + \zeta_2)(\zeta_3\zeta_4 - \zeta_1\zeta_2)}{\zeta^3}$$

$$+ \frac{\zeta_1\zeta_2\zeta_3\zeta_4}{\zeta^4}$$

$$= 1 - \frac{C_1}{\zeta^2} - \frac{2C_2}{\zeta^3} - \frac{3C_3}{\zeta^4}, \tag{7.3}$$

where

$$\left.\begin{aligned} C_1 &= (\zeta_1 + \zeta_2)^2 - \zeta_1\zeta_2 - \zeta_3\zeta_4 \\ C_2 &= \tfrac{1}{2}(\zeta_1 + \zeta_2)(\zeta_3\zeta_4 - \zeta_1\zeta_2) \end{aligned}\right\} \tag{7.4}$$

and

$$C_3 = -\frac{1}{3}\zeta_1\zeta_2\zeta_3\zeta_4 .$$

On integration

$$\sigma = \zeta + \frac{C_1}{\zeta} + \frac{C_2}{\zeta^2} + \frac{C_3}{\zeta^3} \quad , \tag{7.5}$$

and the image of the generating circle $Re^{i\theta}$ under this mapping is

$$\sigma_c = Re^{i\theta} + \frac{C_1}{R} e^{-i\theta} + \frac{C_2}{R^2} e^{-2i\theta} + \frac{C_3}{R^3} e^{-3i\theta} = y_c + iz_c \quad . \tag{7.6}$$

Writing

$$C_n = C_{n1} + iC_{n2} \tag{7.7}$$

and substituting into 7.6, we may obtain

$$\frac{y_c}{R} = (1 + \frac{C_{11}}{R^2})\text{Cos}\theta + \frac{C_{12}}{R^2}\text{Sin}\theta + \frac{C_{21}}{R^3}\text{Cos}2\theta + \frac{C_{22}}{R^3}\text{Sin}2\theta$$

$$+ \frac{C_{31}}{R^4}\text{Cos}3\theta + \frac{C_{32}}{R^4}\text{Sin}3\theta \quad , \tag{7.8}$$

and

$$\frac{z_c}{R} = (1 - \frac{C_{11}}{R^2})\text{Sin}\theta + \frac{C_{12}}{R^2}\text{Cos}\theta - \frac{C_{21}}{R^3}\text{Sin}2\theta + \frac{C_{22}}{R^3}\text{Cos}2\theta$$

$$- \frac{C_{31}}{R^4}\text{Sin}3\theta + \frac{C_{32}}{R^4}\text{Cos}3\theta \quad . \tag{7.9}$$

We will concentrate on a class of bodies having symmetry with respect to the z-axis. For this we require:

(i) $\frac{y_c}{R} = 0$ when $\theta = \frac{\pi}{2}$ and $\frac{3\pi}{2}$

and

(ii) $\frac{y_c}{R}\left(\frac{\pi}{2} + \psi\right) = -\frac{y_c}{R}\left(\frac{\pi}{2} - \psi\right)$

$$\frac{z_c}{R}\left(\frac{\pi}{2} + \psi\right) = \frac{z_c}{R}\left(\frac{\pi}{2} - \psi\right) ,$$

where

$$\psi = \frac{\pi}{2} - \theta .$$

Now

$$\frac{y_c}{R}\left(\frac{\pi}{2}\right) = \frac{C_{12}}{R^2} - \frac{C_{21}}{R^3} - \frac{C_{32}}{R^4}$$

and

$$\frac{y_c}{R}\left(\frac{3\pi}{2}\right) = -\frac{C_{12}}{R^2} - \frac{C_{21}}{R^3} + \frac{C_{32}}{R^4} ,$$

so in order to meet condition (i)

$$C_{12} = C_{21} = C_{32} = 0. \qquad (7.10)$$

Inserting these values into (7.8) then allows us to write

$$\frac{y_c}{R}\left(\frac{\pi}{2} + \psi\right) = -\left(1 + \frac{C_{11}}{R^2}\right)\text{Sin } \psi - \frac{C_{22}}{R^3}\text{ Sin } 2\psi + \frac{C_{31}}{R^4}\text{ Sin } 3\ \psi$$

and

$$\frac{y_c}{R}\left(\frac{\pi}{2} - \psi\right) = \left(1 + \frac{C_{11}}{R^2}\right)\text{ Sin } \psi + \frac{C_{22}}{R^3}\text{ Sin } 2\ \psi - \frac{C_{31}}{R^4}\text{ Sin } 3\ \psi$$

or $$\frac{y_c}{R}\left(\frac{\pi}{2} + \psi\right) = -\frac{y_c}{R}\left(\frac{\pi}{2} - \psi\right) .$$

Also

$$\frac{z_c}{R}\left(\frac{\pi}{2}+\psi\right) = \left(1-\frac{C_{11}}{R^2}\right)\text{Cos }\psi - \frac{C_{22}}{R^3}\text{Cos }2\psi + \frac{C_{31}}{R^4}\text{Cos }3\psi$$

$$= \frac{z_c}{R}\left(\frac{\pi}{2}-\psi\right).$$

Thus both conditions (i) and (ii) are met if (7.10) is imposed.
The equations defining σ_c become

$$\left.\begin{aligned}\frac{y_c}{R} &= \left(1+\frac{C_{11}}{R^2}\right)\text{Cos }\theta + \frac{C_{22}}{R^3}\text{Sin }2\theta + \frac{C_{31}}{R^4}\text{Cos }3\theta \\ \frac{z_c}{R} &= \left(1-\frac{C_{11}}{R^2}\right)\text{Sin }\theta + \frac{C_{22}}{R^3}\text{Cos }2\theta - \frac{C_{31}}{R^4}\text{Sin }3\theta\end{aligned}\right\}\ \text{(z - symmetry)} \qquad (7.11)$$

We need now to choose the position of the critical points in order to meet the z-symmetry condition (7.10). For this purpose we will follow the procedure of Section 6, where we chose the critical points to have symmetry with respect to the η-axis in order to produce a body cross-section having symmetry with respect to the z-axis. As will be seen , this choice is a sufficient one to produce the required symmetry, but it may not be a necessary one. This issue we will leave open (perhaps indefinitely!)

Fig 14(b) illustrates the geometry of our choice. We have, from (7.2)

$$\sum_{n=1}^{4}\xi_n = 0\ , \qquad \sum_{n=1}^{4}\eta_2 = 0\ , \qquad (7.12)$$

and, from Fig.14(b), we have chosen

$$\left.\begin{aligned}\xi_1+\xi_2 &= 0\ , \qquad \xi_3+\xi_4 = 0 \\ \eta_1 &= \eta_2, \qquad \eta_3 = \eta_4.\end{aligned}\right\} \qquad (7.13)$$

Hence

$$\sum_{n=1}^{4}\xi_n = 0\ , \qquad \text{is satisfied,}$$

whilst

$$\sum_{n=1}^{4} \eta_n = 2\,(\eta_1 + \eta_3) = 0$$

gives

$$\eta_1 = \eta_2 = -\eta_3 = -\eta_4 . \tag{7.14}$$

Substituting into (7.4) then produces

$$\left.\begin{aligned} C_{11} &= \xi_1^2 - 2\eta_1^2 + \xi_3^2 , \qquad C_{12} = 0 \\ C_{12} &= 0 , \qquad C_{22} = \eta_1 \left(\xi_1^2 + \xi_3^2\right) \\ C_{31} &= -\frac{1}{3}\left(\xi_1^2 + \eta_1^2\right)\left(\xi_3^2 + \eta_1^2\right), \; C_{32} = 0 . \end{aligned}\right\} \tag{7.15}$$

By way of an afterthought on the choice of critical points, we can see that the choice

$$\zeta_2 = -\zeta_1 , \; \eta_1 = \eta_2 = 0 \qquad \text{(Real points)}$$

$$\eta_4 = -\eta_3 , \; \zeta_3 = \zeta_4 = 0 \qquad \text{(Imaginary points)}$$

is another possible one. If then we substitute into equation (7.4) we obtain

$$C_1 = C_{11} = \zeta_1^2 - \eta_3^2 , \; C_{12} = 0$$

$$C_2 = 0 , \; C_{21} = C_{22} = 0$$

$$C_3 = \frac{1}{3}\,\zeta_1^2\,\eta_3^2 = C_{31} , \; C_{32} = 0$$

Such an arrangement means that the body generated has symmetry with respect to the z-axis ($C_{12} = C_{21} = 0$)and, in addition, symmetry with respect to the y-axis($C_{12} = C_{22} = 0$).

This double symmetry can be a useful property, particularly when dealing with winged configurations (see Ref.26), it will not be pursued further here.

Before examining the range of body shapes generated by (7.11), (7.15), let us obtain the expressions for the gradient of normal force. From (7.3)

$$\frac{d\bar{\sigma}}{d\bar{\zeta}} = \frac{d\sigma}{d\zeta}(\bar{\zeta}) = 1 - \frac{C_{11}}{\bar{\zeta}^2} - 2\frac{C_{21}}{\bar{\zeta}^3} - 3\frac{C_{31}}{\bar{\zeta}^4}, \tag{7.16}$$

hence the expression for

$$\oint_{C_\sigma} \bar{F}_1(\bar{\sigma})\, d\,\bar{\sigma} = \oint_{C_\zeta} \bar{F}_1(\bar{\zeta})\, \frac{d\bar{\sigma}}{d\bar{\zeta}}\, d\bar{\zeta}$$

remains the same as (6.26) and (6.27) the terms containing C_{21} and C_{31} not contributing to the residue. Also on using (7.11)and (5.38) we find that

$$S = \pi R^2 \left\{1 - \left(\frac{C_{11}}{R^2}\right)^2 - 2\left(\frac{C_{22}}{R^3}\right)^2 - 3\left(\frac{C_{31}}{R^4}\right)^2 \right\} . \tag{7.17}$$

It follows from (2.48) that

$$\frac{dC_F}{d(-x)} = \frac{2i\sigma_i}{S_R}\frac{d}{dx}\left\{2\pi R^2 \left[\left[1 + \left(\frac{C_{11}}{R^2}\right)\right] \text{Sin}\,\vartheta + i\left[1 - \left(\frac{C_{11}}{R^2}\right)\right] \text{Cos}\,\vartheta\right]\right.$$

$$\left. - i\, e^{-i\vartheta}\, \pi R^2 \left[1 - \left(\frac{C_{11}}{R^2}\right)^2 - 2\left(\frac{C_{22}}{R^3}\right)^2 - 3\left(\frac{C_{31}}{R^4}\right)^2\right]\right\}$$

or

$$\frac{dC_F}{d(-x)} = -\frac{2\pi}{S_R}\frac{d}{dx}\left\{R^2\left[i\alpha\left[1+2\left(\frac{C_{11}}{R^2}\right) + \left(\frac{C_{11}}{R^2}\right)^2 + 2\left(\frac{C_{22}}{R^3}\right)^2 + 3\left(\frac{C_{31}}{R^4}\right)^2\right]\right.\right.$$

$$+\beta\left[1-2\left(\frac{C_{11}}{R^2}\right)+\left(\frac{C_{11}}{R^2}\right)^2+2\left(\frac{C_{22}}{R^2}\right)^2+3\left(\frac{C_{31}}{R^4}\right)^2\right]\Bigg\}. \tag{7.18}$$

Hence

$$\left.\begin{aligned}\frac{dC_z}{d(-x)} &= \frac{2\pi\alpha}{S_R}\frac{d}{dx}\left\{N_z R^2\right\}\\ \text{and}\\ \frac{dC_Y}{d(-x)} &= -\frac{2\pi\beta}{S_R}\frac{d}{dx}\left\{N_Y R^2\right\}\end{aligned}\right\}, \tag{7.19}$$

where

$$\left.\begin{aligned}N_z \quad & 1+2\left(\frac{C_{11}}{R^2}\right)+\left(\frac{C_{11}}{R^2}\right)^2+2\left(\frac{C_{22}}{R^3}\right)^2+3\left(\frac{C_{31}}{R^4}\right)^2\\ \text{and}\\ N_Y &= 1-2\left(\frac{C_{11}}{R^2}\right)+\left(\frac{C_{11}}{R^2}\right)^2+2\left(\frac{C_{22}}{R^3}\right)^2+3\left(\frac{C_{31}}{R^4}\right)^2 = N_z-4\left(\frac{C_{11}}{R^2}\right).\end{aligned}\right\} \tag{7.20}$$

Let us return now to the range of body shapes which may be generated by the geometric equations (7.11) and (7.15). Some idea of what is possible is shown in Fig.15. For example Fig.15(a) shows the case $\xi_1/_R=0.6$, $\eta_1/_R=0$, which is a family of body cross-sections symmetric with respect to both the z and the y-axes. Starting with $\xi_3/_R=0$, which gives an ellipse, the increase of $\xi_3/_R$ produces a flattening and widening of the shape, until at $\xi_{3/R}=0.6$ the depth is nearly constant over 60 per cent of the width. Relative to this basic case, the effect of making η_1/R negative is to cause the body depth to become greater, the width to become smaller, whilst simultaneously producing a convex upward camber. This is illustrated in Fig.15(b). These effects are progressive with further decrease in η_1/R as shown in Fig.15(c). As mentioned in Section 1, bodies with corners are unlikely to have their aerodynamic characteristics accurately predicted by the present technique. Thus a body having a cross-section defined by $\xi_1/R=0.6$, $\xi_3/R=0.6$, $\eta_1/R=-0.4$, Fig.15(c), is not a serious candidate. However, it does serve to illustrate the wide variety of cross-section which can be generated by this relatively simple mapping. Variants on this theme can be obtained, thus decreases of ξ_1/R will cause the bodies to be narrower and increases, wider; whilst making η_1/R positive will produce bodies with concave upward camber. Let us now leave these specific low-order mappings and consider the more general case.

8. Von Mises Mapping; Case $\zeta_\cdot = o,k.$

Having demonstrated the useful range of body cross-sections which can be generated by the use of three and four critical points, we turn to the more general case, where k is any positive integer. In application we anticipate that $k \leq 10$. Such generality should permit a very wide range of body shapes and, perhaps, provide a basis for a 'direct ' method in which the body shape is known and the critical points, or coefficients C_{n1}, C_{n2}, are to be determined.

Re-capitulating, we have

$$\frac{d\sigma}{d\zeta} = 1 - \sum_{n=1}^{k} nC_n / \zeta^{n+1}, \tag{8.1}$$

$$\sigma(\zeta) = \zeta + \sum_{n=1}^{k} C_n / \zeta^n , \tag{8.2}$$

with

$$\sum_{n=1}^{k} \zeta_n = 0 . \tag{8.3}$$

This last condition corresponds to requiring the centroid of the polygon, having vertices $\zeta_1, \zeta_2, \ldots, \zeta_k$, to be at the origin.

The image C_σ of the circle $C_\zeta = Re^{i\theta}$ under the mapping (8.2) is given by

$$\frac{\sigma_c}{R} = e^{i\theta} + \frac{1}{R} \sum_{n=1}^{k} \left\{ C_n e^{-in\theta} R^{-n} \right\} = \frac{y_c}{R} + i\frac{z_c}{R}$$

or, upon substitution from (7.7)

$$\frac{\sigma_c}{R} = \text{Cos}\theta + i\ \text{Sin}\theta + \sum_{n=1}^{k} \left\{ \left(C_{n1} + iC_{n2} \right) \left(\text{Cos}n\theta - i\text{Sin}n\theta \right) R^{-(n+1)} \right\}$$

$$= \text{Cos}\theta + i\ \text{Sin}\theta + \sum_{n=1}^{k} \left\{ \left[\left[C_{n1}\text{Cos}n\theta + C_{n2}\text{Sin}n\theta \right] . \right. \right.$$

$$\left. \left. + i \left[- C_{n1}\text{Sin}n\theta + C_{n2}\text{Cos}n\theta \right] \right] R^{-(n+1)} \right\} . \tag{8.4}$$

Thus

$$\frac{y_c}{R} = \text{Cos}\theta + \sum_{n=1}^{k} \left\{ \left[C_{n1}\text{Cos}n\theta + C_{n2}\text{Sin}n\theta \right] R^{-(n+1)} \right\} \tag{8.5}$$

and

$$\frac{z_c}{R} = \text{Sin}\ \theta + \sum_{n=1}^{k} \left\{ \left[-C_{n1}\text{Sin}n\theta + C_{n2}\text{Cos}n\theta \right] R^{-(n+1)} \right\} . \tag{8.6}$$

We wish to impose the same conditions of symmetry, with respect to the z-axis, as used in Section 7. Thus

$$\frac{y_c}{R}\left(\frac{\pi}{2}\right) = \sum_{n=1}^{k} \left\{ \left[C_{n1}\text{Cos}\frac{n\pi}{2} + C_{n2}\text{Sin}\frac{n\pi}{2} \right] R^{-(n+1)} \right\}$$

$$= \frac{C_{12}}{R^2} - \frac{C_{21}}{R^3} - \frac{C_{32}}{R^4} + \frac{C_{41}}{R^5} + \frac{C_{52}}{R^6} - \frac{C_{61}}{R^7} - \cdots\cdots$$

$$= (-1)^{m+1} \sum_{m=1}^{k/2} \left\{ C_{(2m-1)2} R^{-2m} - C_{2m1} R^{-(2m+1)} \right\} . \tag{8.7}$$

In a similar manner

$$\frac{y_c}{R}\left(\frac{3\pi}{2}\right) = \sum_{n=1}^{k} \left\{ \left[C_{n1}\text{Cos}\frac{3n\pi}{2} + C_{n2}\text{Sin}\frac{3n\pi}{2} \right] R^{-(n+1)} \right\}$$

$$= \sum_{n=1}^{k} \left\{ \left[C_{n1}\text{Cos}\frac{n\pi}{2} - C_{n2}\text{Sin}\frac{n\pi}{2} \right] R^{-(n+1)} \right\}$$

$$= (-1)^{m} \sum_{m=1}^{k/2} \left\{ C_{(2m-1)2} R^{-2m} + C_{2m1} R^{-(2m+1)} \right\} . \tag{8.8}$$

It follows that

$$\frac{y_c}{R}\left(\frac{\pi}{2}\right) = \frac{y_c}{R}\left(\frac{3\pi}{2}\right) = 0$$

when

$C_{(2m-1)2}$ and C_{2m1}

are all zero for $1 \le m \le k/2$. (8.9)

Writing (8.5) in terms of $\psi = \frac{\pi}{2} - \theta$ we obtain

$$\frac{y_c}{R}(\theta) = \text{Cos}\left(\frac{\pi}{2} - \psi\right) + \sum_{n=1}^{k}\left\{\left[C_{n1}\text{Cosn}\left(\frac{\pi}{2} - \psi\right) + C_{n2}\text{Sinn}\left(\frac{\pi}{2} - \psi\right)\right]R^{-(n+1)}\right\}$$

$$= \text{Sin}\psi + \sum_{n=1}^{k}\left\{\left[C_{n1}\left(\text{Cos}\frac{n\pi}{2}\ \text{Cosn}\psi + \text{Sin}\frac{n\pi}{2}\ \text{Sinn}\psi\right)\right.\right.$$

$$\left.\left. + C_{n2}\left(\text{Sin}\frac{n\pi}{2}\ \text{Cosn}\psi - \text{Cos}\ \frac{n\pi}{2}\ \text{Sinn}\psi\right)\right]R^{-(n+1)}\right\} .$$

On using (8.9) this becomes

$$\frac{y_c}{R}(\theta) = \frac{y_c}{R}\left(\frac{\pi}{2} - \psi\right)$$

$$= (1 + \frac{C_{11}}{R^2})\ \text{Sin}\psi + \frac{C_{22}}{R^3}\ \text{Sin}\psi - \frac{C_{31}}{R^4}\ \text{Sin}\psi - \frac{C_{42}}{R^5}\ \text{Sin}4\psi$$

$$+ \frac{C_{51}}{R^6}\ \text{Sin}5\psi + \frac{C_{62}}{R^7}\ \text{Sin}6\psi . \qquad (8.10)$$

Similarly

$$\frac{y_c}{R}\left(\frac{\pi}{2} + \psi\right) = (1 + \frac{C_{11}}{R^2})\ \text{Sin}(-\psi) + \frac{C_{22}}{R^3}\ \text{Sin}2(-\psi) - \frac{C_{31}}{R^4}\ \text{Sin}3(-\psi) \ .....$$

$$= -(1 + \frac{C_{11}}{R^2})\ \text{Sin}\psi - \frac{C_{22}}{R^4}\ \text{Sin}2\psi + \frac{C_{31}}{R^4}\ \text{Sin}3\psi \ .....$$

$$= -\frac{y}{c}\left(\frac{\pi}{2} - \psi\right) .$$

Also

$$\frac{z_c}{R}\left(\frac{\pi}{2} - \psi\right) = \text{Sin}\left(\frac{\pi}{2} - \psi\right) + \sum_{n=1}^{k}\{[-C_{n1}\text{Sin}\ n\left(\frac{\pi}{2} - \psi\right) + C_{n2}\ \text{Cos}\ n\left(\frac{\pi}{2} - \psi\right)]R^{-(n+1)}\}$$

$$= \text{Cos}\psi + \sum_{n=1}^{k} \{[-C_{n1}(\text{Sin}\,\frac{n\pi}{2}\ \text{Cos}\ n\psi - \text{Cos}\,\frac{n\pi}{2}\ \text{Sin}\ n\psi)$$

$$+ C_{n2}(\text{Cos}\,\frac{n\pi}{2}\ \text{Cos}\ n\psi + \text{Sin}\,\frac{n\pi}{2}\ \text{Sin}\ n\psi)]R^{-(n+1)}\}$$

$$= (1-\frac{C_{11}}{R^2})\text{Cos}\psi - \frac{C_{22}}{R^3}\ \text{Cos}2\psi + \frac{C_{31}}{R^4}\ \text{Cos}3\psi + \frac{C_{42}}{R^5}\ \text{Cos}4\psi - \frac{C_{51}}{R^6}\ \text{Cos}5\psi \qquad (8.11)$$

whilst

$$\frac{z_c}{R}(\frac{\pi}{2} + \psi) = (1 - \frac{C_{11}}{R^2})\text{Cos}(-\psi) - \frac{C_{22}}{R^3}\ \text{Cos}2(-\psi) + \frac{C_{31}}{R^4}\ \text{Cos}3(-\psi)$$

$$+ \frac{C_{42}}{R^5}\ \text{Cos}4(-\psi) - \ldots\ldots$$

$$= \frac{z_c}{R}(\frac{\pi}{2} - \psi).$$

It follows that the symmetry conditions are met if (8.9) is imposed.

The more general result for the cross-sectional area may also be obtained.

From (8.5)

$$\frac{1}{R}\frac{dy_c}{d\theta} = -\text{Sin}\theta - \sum_{n=1}^{k} \{n[C_{n1}\text{Sin}\theta - C_{n2}\text{Cosn}\theta]R^{-(n+1)}\}\ ,$$

and from (8.6)

$$\frac{1}{R}\frac{dz_c}{d\theta} = \text{Cos}\theta - \sum_{n=1}^{k} \{n[C_{n1}\text{Cosn}\theta + C_{n2}\ \text{Sinn}\theta]R^{-(n+1)}\}\ .$$

Hence

$$\frac{1}{R^2}\{y_c\frac{dz_c}{d\theta} - z_c\frac{dy_c}{d\theta}\}$$

$$= \{[\mathrm{Cos}\theta + \sum_{n=1}^{k} \{[C_{n1}\mathrm{Cos}n\theta + C_{n2}\ \mathrm{Sin}n\theta]\ R^{-(n+1)}\}]$$

$$x[\mathrm{Cos}\theta - \sum_{n=1}^{k} \{n[C_{n1}\mathrm{Cos}n\theta + C_{n2}\ \mathrm{Sin}n\theta]R^{-(n+1)}\}]\}$$

$$+ \{[\mathrm{Sin}\theta + \sum_{n=1}^{k} \{[-C_{n1}\mathrm{Sin}n\theta + C_{n2}\mathrm{Cos}n\theta]R^{-(n+1)}\}]$$

$$x[\mathrm{Sin}\theta + \sum_{n=1}^{k} \{n[C_{n1}\mathrm{Sin}n\theta - C_{n2}\mathrm{Cos}n\theta]R^{-(n+1)}\}]\} \ .$$

On expanding these products and substituting into (5.38)

we obtain, after neglecting the integrals which are zero;

i.e. $\int_0^{2\pi} \mathrm{Sin}\ n\theta\ \mathrm{Sin}\ m\theta\ d\theta$,.....etc,

$$S = \frac{1}{2}\ R^2 \int_0^{2\pi} \{\mathrm{Cos}^2\theta - \sum_{n=1}^{k} [n[(\frac{C_{n1}}{R^{(n+1)}})^2\ \mathrm{Cos}^2 n\theta + (\frac{C_{n2}}{R^{(n+1)}})^2 \mathrm{Sin}^2 n\theta]]$$

$$+ \mathrm{Sin}^2\theta - \sum_{n=1}^{k} [n[(\frac{C_{n1}}{R^{(n+1)}})^2 \mathrm{Sin}^2 n\theta + (\frac{C_{n2}}{R^{(n+1)}})^2 \mathrm{Cos}^2 n\theta]]\}\ d\theta$$

$$= \frac{1}{2}\ R^2\{1 - \sum_{n=1}^{k} [n[(\frac{C_{n1}}{R^{(n+1)}})^2 + (\frac{C_{n2}}{R^{(n+1)}})^2]]\} \int_0^{2\pi} d\theta$$

or

$$S = \pi R^2\{1 - \sum_{n=1}^{k} [n[(\frac{C_{n1}}{R^{(n+1)}})^2 + (\frac{C_{n2}}{R^{(n+1)}})^2]]\}. \qquad (8.12)$$

In this expression the coefficients defined by (8.9) will be zero, and the leading terms will be given by

$$S = \pi R^2\{1-(\frac{C_{11}^2}{R^2}) - 2(\frac{C_{22}^2}{R^3}) - 3(\frac{C_{31}^2}{R^4}) - 4(\frac{C_{42}^2}{R^5})$$

$$- 5(\frac{C_{51}^2}{R^6}) - 6(\frac{C_{62}^2}{R^7}) -.....\} . \qquad (8.13)$$

Because terms in C_{21}, C_{22}, C_{31}, etc. do not contribute to the residue then equation (6.27) will apply to this general case. Substituting into (2.48) then gives

$$\frac{dC_F}{d(-x)} = \frac{2\pi\sigma_i}{S_R}\frac{d}{dx}\{R^2[2i[1+(\frac{C_{11}}{R^2})]Sin\vartheta - 2[1-(\frac{C_{11}}{R^2})]\,Cos\,\vartheta$$

$$+(Cos\vartheta - i\,Sin\vartheta)\left(\frac{S}{\pi R^2}\right)]\}$$

$$= \frac{2\pi\sigma_i}{S_R}\frac{d}{dx}\{R^2[[2+2(\frac{C_{11}}{R^2})-\left(\frac{S}{\pi R^2}\right)]i\,Sin\,\vartheta$$

$$-[2-2(\frac{C_{11}}{R^2}) - \left(\frac{S}{\pi R^2}\right)]Cos\,\vartheta]\}$$

$$= -\frac{2\pi}{S_R}\frac{d}{dx}\{R^2[i\alpha\,[2 + 2\,(\frac{C_{11}}{R^2}) - \left(\frac{S}{\pi R^2}\right)]$$

$$+ \beta\,[\,2-2(\frac{C_{11}}{R^2}) - \left(\frac{S}{\pi R^2}\right)]]\} . \qquad (8.14)$$

Thus

$$\left.\begin{aligned} \frac{dC_z}{d(-x)} &= \frac{2\pi\alpha}{S_R}\frac{d}{dx}\{N_z R^2\} \\ \text{and} \\ \frac{dC_Y}{d(-x)} &= -\frac{2\pi\beta}{S_R}\frac{d}{dx}\{N_Y R^2\}, \end{aligned}\right\} \qquad (8.15)$$

where

$$N_z = 2 + 2\left(\frac{C_{11}}{R^2}\right) - \left(\frac{S}{\pi R^2}\right)$$

$$= 1 + 2\left(\frac{C_{11}}{R^2}\right) + \left(\frac{C_{11}}{R^2}\right)^2 + 2\left(\frac{C_{22}}{R^3}\right)^2 + 3\left(\frac{C_{31}}{R^4}\right)^2 + 4\left(\frac{C_{42}}{R^5}\right)^2 + \ldots\ldots \qquad (8.16)$$

and

$$N_Y = N_z - 4\left(\frac{C_{11}}{R^2}\right)$$

$$= 1 - 2\left(\frac{C_{11}}{R^2}\right) + \left(\frac{C_{11}}{R^2}\right)^2 + 2\left(\frac{C_{22}}{R^3}\right)^2 + 3\left(\frac{C_{31}}{R^4}\right)^2 + 4\left(\frac{C_{42}}{R^5}\right)^2 + \ldots\ldots \qquad (8.17)$$

9. Some Ideas on a Possible Direct Method.

Having discussed the indirect method of body generation at some length let us turn to the 'direct' problem of determining the mapping which generates a given shape. The shape σ_c is fully specified and it is assumed that it is such that the generalized Von Mises mapping, described in Section 8, is capable of defining it. The situation is illustrated in Fig.16, where we map from acircle $\zeta_c = Re^{i\theta}$ to a closed contour $\sigma_c = r_c e^{i\gamma}$ which is symmetric with respect to the z-axis. It follows thay y_c and z_c are defined by equations (8.10) and (8.11), respectively, which we re-write as

$$\left.\begin{aligned} \frac{y_c}{R} &= \frac{r_c}{R}\,\mathrm{Sin}\,\mu = \left(1+\frac{C_{11}}{R^2}\right)\mathrm{Sin}\psi + \frac{C_{22}}{R^3}\,\mathrm{Sin}2\psi - \frac{C_{31}}{R^4}\,\mathrm{Sin}3\psi\ldots\ldots \\ \text{and} \\ \frac{z_c}{R} &= \frac{r_c}{R}\,\mathrm{Cos}\mu = \left(1-\frac{C_{11}}{R^2}\right)\mathrm{Cos}\psi - \frac{C_{22}}{R^3}\,\mathrm{Cos}2\psi + \frac{C_{31}}{R^4}\,\mathrm{Cos}3\psi\ldots\ldots \end{aligned}\right\} \quad (9.1)$$

We wish to establish a technique, which will necessarily be iterative in character, to determine the coefficients C_{11}/R^2, etc. For this purpose re-write (9.1) in the form:-

$$\left.\begin{aligned} \Delta y &= \frac{y_c}{R} - \mathrm{Sin}\psi = c_{11}\,\mathrm{Sin}\psi + c_{22}\,\mathrm{Sin}2\psi - c_{31}\,\mathrm{Sin}3\psi - \ldots \\ \text{and} \\ \Delta z &= \frac{z_c}{R} - \mathrm{Cos}\psi = -c_{11}\,\mathrm{Cos}\psi - c_{22}\,\mathrm{Cos}2\psi + c_{31}\,\mathrm{Cos}3\psi + \ldots \end{aligned}\right\} \quad (9.2)$$

where

$$c_{11} = \frac{C_{11}}{R^2}\ ,\ c_{22} = \frac{C_{22}}{R^3}\ ,\ c_{31} = \frac{C_{31}}{R^4}\ ,\ c_{42} = \frac{C_{42}}{R^5}\ ,\ldots\ldots$$

$$c_{n1} = \frac{C_{n1}}{R^{n+1}}\ ,c_{n2} = \frac{C_{n2}}{R^{n+1}}\ \ldots\text{etc}\,,\ \ldots\ldots \qquad n\neq m\,; \tag{9.3}$$

and Δy, Δz may be viewed as a measure of distortion between ζ_c and σ_c, which would be identical if c_{11}, c_{22},....etc were all zero.

In the above expression for Δy the coefficients c_{n1},c_{m2} are those of "half-range" Fourier sine series, Δy being an "odd" function. As a result the coefficients may be expressed in the form

$$c_{11} = \frac{2}{\pi}\int_0^{\pi} \Delta y\ (\psi)\ \text{Sin}\psi\ d\psi$$

$$c_{22} = \frac{2}{\pi}\int_0^{\pi} \Delta y\ (\psi)\ \text{Sin}2\psi\ d\psi$$

$$c_{31} = -\frac{2}{\pi}\int_0^{\pi} \Delta y\ (\psi)\ \text{Sin}3\psi\ d\psi$$

.....

$$c_{n1} = \pm\ \frac{2}{\pi}\int_0^{\pi} \Delta y(\psi)\ \text{Sin}\ n\psi\ d\psi$$

$$c_{m2} = \pm\ \frac{2}{\pi}\int_0^{\pi} \Delta y(\psi)\ \text{Sin}\ m\psi\ d\psi$$

.....etc. (9.4)

The signs of the coefficients alternate in pairs in accordance with the signs in equation (9.2) or (8.10). See for example Ref.20, pp. 393-6.

Unfortunately, although we know σ_c in terms of y_c v z_c, or γ v r_c, we do not know y_c or z_c as a function of ψ, and as a result we are not able to obtain

$\Delta_y(\psi)$ and hence the coefficients c_{11}, c_{22},....etc. In fact $\Delta y(\psi)$ depends, through (9.2), on a knowledge of these coefficients. This is, of course, a classical situation for the establishment of an iterative procedure to solve the equations of (9.2), simultaneously.

Let us start the iteration by choosing N equal angular divisions in ψ between the points A(ψ = o, μ = o) and B(ψ = π, μ = π), Fig. 16, and assume that, initially, the corresponding angular divisions in μ are the same as those in ψ. We already know, of course, that the form of (9.2) ensures that the mapping carries A in the ζ plane into A in the σ plane and similarly with B. The scheme is shown in Fig. 17. It follows that at a point on ζ_c defined by ψ_n and R, there is a corresponding point on σ_c defined by $(r_c)_n$ and μ_n or $(y_c, z_c)_n$, where

$$\left(\frac{z_c}{y_c}\right)_n = \cot \mu_n = \operatorname{Tan} \gamma_n \qquad (9.5)$$

and in the zeroeth iteration we have chosen $\mu_{no} = \psi_n$. Thus the initial values $(y_c)_{no}$ and $(z_c)_{no}$ are readily available from (9.5) and the fact that

$$(r_c)_n^2 = (y_c)_n^2 + (z_c)_n^2 . \qquad (9.6)$$

We may use this information in (9.2) to write

$$(\Delta y)_{no} = \left(\frac{y_c}{R}\right)_{no} - \operatorname{Sin}\psi_n = (c_{11})_{yo} \operatorname{Sin}\psi_n + (c_{22})_{yo} \operatorname{Sin}2\psi_n - \text{.....etc .,} \qquad (9.7)$$

where the subscript $(\ )_{yo}$ refers to values of the coefficients obtained by Fourier-fitting $(\Delta y)_{no}$ and where $1 \leq n \leq N$.

The coefficients in (9.7) may be obtained from the finite-difference form of (9.4), which may be written as

$$(c_{11})_{yo} = \frac{2}{\pi} \sum_{n=1}^{N} (\Delta y)_{no} \operatorname{Sin}\psi_n \frac{\pi}{N} = \frac{2}{N} \sum_{n=1}^{N} (\Delta y)_{no} \operatorname{Sin}\psi_n$$

$$(c_{22})_{yo} = \frac{2}{N} \sum_{n=1}^{N} (\Delta y)_{no} \operatorname{Sin}2\psi_n$$

$$(c_{31})_{yo} = -\frac{2}{N} \sum_{n=1}^{N} (\Delta y)_{no} \operatorname{Sin}3\psi_n , \qquad (9.8)$$

and so on.

If now we substitute these values of the coefficients into the Δz equation of (9.2) we obtain

$$(\Delta z)_{n1} = -(c_{11})_{yo}\cos\psi_n - (c_{22})_{yo}\cos 2\psi_n + (c_{31})_{yo}\cos 3\psi_n + \ldots, \qquad (9.9)$$

$$1 \leq n \leq N;$$

from which

$$\left(\frac{z_c}{R}\right)_{n1} = (\Delta z)_{n1} + \cos\psi_n \,. \qquad (9.10)$$

In a closely similar manner to the foregoing, we may use the known value of $(z_c)_{no}$ in the Δz equation of (9.2) to obtain

$$(c_{11})_{zo} = -\frac{2}{N}\sum_{n=1}^{N}(\Delta z)_{no}\cos\psi_n$$

$$(c_{22})_{zo} = -\frac{2}{N}\sum_{n=1}^{N}(\Delta z)_{no}\cos 2\psi_n \qquad (9.11)$$

and so on. Substituting these values into the Δy equation of (9.2) then gives

$$(\Delta y)_{n1} = (c_{11})_{zo}\sin\psi_n + (c_{22})_{zo}\sin 2\psi_n - (c_{31})_{zo}\sin 3\psi_n - \ldots \qquad (9.12)$$

$$1 \leq n \leq N;$$

from which

$$\left(\frac{y_c}{R}\right)_{n1} = (\Delta y)_{n1} + \sin\psi_n \,. \qquad (9.13)$$

In general the point $\left(\frac{y_c}{R}, \frac{z_c}{R}\right)_{n1}$ will not lie on σ_c, Fig. 18, and it will be necessary to iterate further. Thus we may repeat the previous process to give

$$(\Delta y)_{n2} = (c_{11})_{z1}\,\mathrm{Sin}\psi_n + (c_{22})_{z1}\mathrm{Sin}2\psi_n - (c_{31})_{z1}\mathrm{Sin}3\psi_n - \ldots.$$

and

$$(\Delta z)_{n2} = -(c_{11})_{y1}\mathrm{Cos}\psi_n - (c_{22})_{y1}\mathrm{Cos}2\psi_n + (c_{31})_{y1}\mathrm{Cos}3\psi_n + \ldots.,$$

(9.14)

where the coefficients have been obtained from the Fourier fitting process defined by

$$(c_{11})_{z1} = -\frac{2}{N}\sum_{n=1}^{N}(\Delta z)_{n1}\mathrm{Cos}\psi_n \ldots\ldots\text{etc}.$$

and

$$(c_{11})_{y1} = \frac{2}{N}\sum_{n=1}^{N}(\Delta y)_{n1}\mathrm{Sin}\psi_n \ldots\ldots\text{etc}.$$

(9.15)

Again the point $\left(\frac{y_c}{R}, \frac{z_c}{R}\right)_{nz}$ may not lie on σ_c, Fig 18, and the iteration must continue. Thus the jth iteration gives

$$(\Delta y)_{nj} = (c_{11})_{z(j-1)}\,\mathrm{Sin}\psi_n + (c_{22})_{z(j-1)}\mathrm{Sin}2\psi_n - (c_{31})_{z(j-1)}\mathrm{Sin}3\psi_n - \ldots$$

and

$$(\Delta z)_{nj} = -(c_{11})_{y(j-1)}\mathrm{Cos}\psi_n - (c_{22})_{y(j-1)}\mathrm{Cos}2\psi_n + (c_{31})_{y(j-1)}\mathrm{Cos}3\psi_n + \ldots$$

(9.16)

where

$$(c_{11})_{z(j-1)} = -\frac{2}{N}\sum_{n=1}^{N}(\Delta z)_{n(j-1)}\cos\psi_n$$

...etc;

and

$$(c_{11})_{y(j-1)} = \frac{2}{N}\sum_{n=1}^{N}(\Delta y)_{n(j-1)}\sin\psi_n \qquad (9.17)$$

...etc.

When

$$\left.\begin{aligned}(\Delta y)_{nj} - (\Delta y)_{n(j-1)} &= (\varepsilon_y)_n\\ \text{and}\\ (\Delta z)_{nj} - (\Delta z)_{n(j-1)} &= (\varepsilon_z)_n\end{aligned}\right\} \qquad (9.18)$$

are sufficiently small the process may be deemed to have converged. However, depending on the value of N, the point $\left(\frac{y_c}{R}, \frac{z_c}{R}\right)_{nj}$ may not lie very accurately on σ_c and coefficients $(c..)_{yj}$ and $(c..)_{zj}$ may differ appreciably. Nevertheless this is the best approximation for the value of N chosen.

In order to obtain a satisfactory value of N we may substitute the values of the coefficients $(c..)_{yj}$ or $(c..)_{zj}$ into (8.12) or (8.13), the expression for the cross-sectional area S and compare this with the known value. If this is not accurate the value of N may be increased until satisfactory accuracy is obtained. Under converged conditions, presumably, the coefficients $(c..)_{yj}$ and $(c..)_{zj}$ will also be the same.

At this stage the method has not been explored numerically, further work will be reported on at a later date.

Having obtained the coefficients to a satisfactory degree of accuracy the normal load gradients may be calculated from (8.15). Thus

$$\frac{dC_z}{d(-x)} = \frac{2\pi\alpha}{S_R}\frac{d}{dx}\{N_z R^2\}$$

$$= \frac{2\pi\alpha}{S_R}\frac{d}{dx}\{2(1+c_{11})R^2 - \frac{S}{\pi}\}$$

$$= \frac{2\pi\alpha}{S_R}\{4(1+c_{11})R\frac{dR}{dx} + 2R^2\frac{dc_{11}}{dx} - \frac{1}{\pi}\frac{dS}{dx}\} \qquad (9.19)$$

and

$$\frac{dC_Y}{d(-x)} = -\frac{2\pi\beta}{S_R}\{4(1-c_{11})R\frac{dR}{dx} - 2R^2\frac{dc_{11}}{dx} - \frac{1}{\pi}\frac{dS}{dx}\}. \qquad (9.20)$$

It will be noted that in the indirect method we choose R,i.e. ζ_c, and the co-ordinates y_c, z_c of points on σ_c come out as they will. In the direct method σ_c is already specified and we are required to choose an appropriate R. One way of doing this is to choose ζ_c such that σ_c lies inside $\zeta_{c_{Max}}$, i.e. $R > r_c$

This will, from our previous analysis, ensure that implicit critical points of the desired mapping can be located within ζ_c. It will be a sufficient, but not necessary, condition. However, we do not know $r_{c_{Max}}$ since we do not know the location of the origin y=o, z=o. Since we have assumed that the Van Mises mapping is capable of defining σ_c, then presumably we may choose both the origin of the y,z axes and, hence, $r_{c_{Max}}$. As a result the mapping defined by (9.1) will not be unique and the choice of origin in the σ-plane and R may influence the convergence of the numerical scheme.

Another feature of this process is that the choice of origin in the σ-plane and the ratio of $r_{c_{Max.}}(x)/R(x)$ needs to be an invariant procedure with axial position x. This is not difficult with bodies having symmetry with respect to both the z and y axes, but in cases where there is axial camber a clear definition is required.

In all the previous analysis it has been assumed, implicitly, that points on the body axis where

$$\frac{d}{dx}\left\{N_F R^2\right\} = 0 \qquad \left(N_F \equiv N_z \text{ or } N_y\right) \qquad (9.21)$$

are isolated points. When we are considering a body which has an axial segment Δx for which the cross-section is geometrically similar over Δx, then $\frac{dN_z}{dx} = o$ over Δx. If, in addition, $R^2(x)$, hence $S(x)$, are constant over Δx, then (9.21) applies over the whole of Δx, which means that

$$\frac{dC_F}{d(-x)} = 0 \text{ over } \Delta x.$$

Since $R_e(x)$ will also be constant over Δx then we can see that

$$F_z(x) = \frac{\frac{dC_z}{d(-x)} \text{ (non-circular)}}{\frac{dC_z}{d(-x)} \text{ (circular)}} = \frac{0}{0} \text{ (??)}, \qquad (9.22)$$

over Δx and similarly for F_Y. For an isolated point, corresponding to $\Delta x \to 0$, this poses no problem, since we can approach the point as close as we wish. When $\Delta x > 0$, a finite segment, then it raises the question of how to determine $F_z(x)$ and $F_Y(x)$.

Clearly there are interesting matters which remain to be explored.

10. Conclusions .

It has been shown that the method of Sacks, Ref. 12, in its linear form, provides a useful, and relatively easy, method for predicting the normal force distribution on thin bodies of non-circular cross-section. From this we are able to calculate the ratio, F_N, between the normal force gradient on the body of non-circular cross section and that of circular cross-section, the cross-sectional area distribution, in the axial sense, being the same for both bodies.

From a known, accurate, distribution on a body of revolution we may then calculate the distribution on related families of bodies of non-circular cross-section simply by multiplying by $F_N(x)$. The accurate distribution on the body of revolution may come from any convenient source including experiment. One way is to generate the lifting body by means of axial distributions of doublets using either the approximate technique of Ref.9 or the numerical method of Ref.25.

In the case of bodies of elliptic cross-section this technique has been shown to give good agreement with exact theoretical results. See Refs. 10 and 11. Experimental verification of the method, on pointed bodies of elliptic cross-section tested at both supersonic and subsonic speeds, is provided, in terms of overall normal force and moment characteristics, by the results of Refs. 4 and 5. Further extensive validation, both theoretically and experimentally, is desirable.

In this paper both the indirect and direct aerodynamic problems have been addressed, and in the case of the latter a sketch of a possible numerical scheme, to obtain the appropriate mapping function, has been developed. This requires further work.

Finally, and obviously, the technique, when fully developed, should provide a useful and economical means for the design of lifting bodies at modest angle of attack.

References .

1. Jackson, C.M. (Jr) and Sawyer, W.C. 'Bodies with non-circular cross-sections and bank-to-turn missiles' 'Tactical Missile Aerodynamics' Progress in Astronautics and Aeronautics, Vol.104,pp 168-197 Published by AIAA (1986)

2. Jorgensen, L.H. 'Prediction of static aerodynamic characteristics for space-shuttle-like and other bodies at angles-of-attack from zero to one-hundred and eighty degrees' NASA TN.D-6996 (1973)

3. Nielsen, J.N. 'Missile Aerodynamics' McGraw-Hill (1960)

4. Jorgensen, L.H. 'Inclined bodies of various cross-sections at supersonic speeds. NASA MEMO 10-3-58A (1958)

5. Graves, E.B. 'Aerodynamic characteristics of a mono-planar missile concept with bodies of circular and elliptical cross-sections' NASA TM 74079 (1977)

6. Christopher, P.A.T. 'The lifting characteristics of slender and thin bodies with elliptic cross-sections' College of Aeronautics, CIT, Cranfield Report No 8813 (1988)

7. Spreiter, J.R. 'The aerodynamic forces on slender plane- and cruciform-wing and body combinations' NACA Report 962 (1950)

8. Graves, E.B. and Fournier, R.H. 'Effect of nose bluntness and afterbody shape on aerodynamic characteristics of a monoplanar missile concept with bodies of circular and elliptical cross-sections at Mach number of 2.50'
NASA TM 80055 (1979)

9. Christopher, P.A.T 'Aerodynamic characteristics of thin bodies in incompressible flow'
College of Aeronautics,
CIT, Cranfield.
Report No 8803 (1988)

10. Christopher, P.A.T 'An approximate technique for estimating the longitudinal gradient of normal force on thin bodies of elliptic cross-section'
College of Aeronautics, CIT, Cranfield
Report No 8904 (1989)

11. Christopher, P.A.T 'The aerodynamic characteristics of ellipsoids in inviscid flow'
College of Aeronautics,
CIT, Cranfield Report No 8902 (1989)

12. Sacks, A.H. 'Aerodynamic forces, moments, and stability derivatives for slender bodies of general cross-section'
NACA TN 3283 (1954)

13 Bryson, A.E.(Jr) 'Stability derivatives for a slender missile with application to a wing-body-vertical-tail configuration'.
J Aero Sciences, Vol 20 No 5
pp. 297-308 (1953)

14 Summers, R.G. 'On determining the additional apparent mass of a wing-body-vertical-tail cross section'
J.Aero Sci, Vol 20, No 12,pp.856-857. (1953)

15 Bryson, A.E.(Jr) 'Comment on the stability derivatives of a wing-body-vertical-tail configuration' J.Aero Sci,Vol 21, No 1, p.59 (1954)

16 Bryson, A.E.(Jr) 'Evaluation of the inertia coefficients of the cross-section of a slender body' J.Aero Sci, Vol 21, No 6,pp 424-427 (1954)

17 Skulsky, R.S. 'A conformal mapping method to predict low-speed aerodynamic characteristics of arbitrary slender re-entry shapes' J. Spacecraft, Vol 3 No 2, pp 247-253 (1966)

18 Mendenhall,M.R. and Allen, J.M. 'Prediction of vortex shedding from non-circular bodies at high angles of attack in supersonic flow' AGARD-CP-336 'Missile Aerodynamics' Item 17 (1983)

19 Karamcheti, K 'Principles of Ideal-Fluid Aerodynamics' John Wiley (1966)

20 Kreyszig, E 'Advanced Engineering Mathematics' Third Edition, Wiley (1972)

21 Milne-Thompson,L.M. 'Theoretical Hydrodynamics' Macmillan (1938)

22 Sigal, A. and Lapidot, E. 'Aerodynamic characteristics of configurations having bodies with square, rectangular, and circular cross-sections' J. Spacecraft, Vol 26 No 2, pp 85-89 (1989)

23 Lapidot, E. and Sigal, A. 'An interactive software for preliminary aerodynamic design of slender bodies having arbitrary cross-section' 29th Israel Conference on Aviation and Astronautics, Technion, Haifa, Israel, pp. 99-108 (1987)

24 Milne-Thompson, L.M. 'Theoretical Aerodynamics' Macmillan (1948)

25 Hamwi, S 'Approximate methods for predicting the lifting characteristics of wing-body combinations' College of Aeronautics, CIT, Cranfield Ph.D. Thesis (1990)

26 Christopher, P.A.T 'An approximate technique for estimating the lifting characteristics of thin wing-body combinations College of Aeronautics, CIT, Cranfield Report No (to appear)

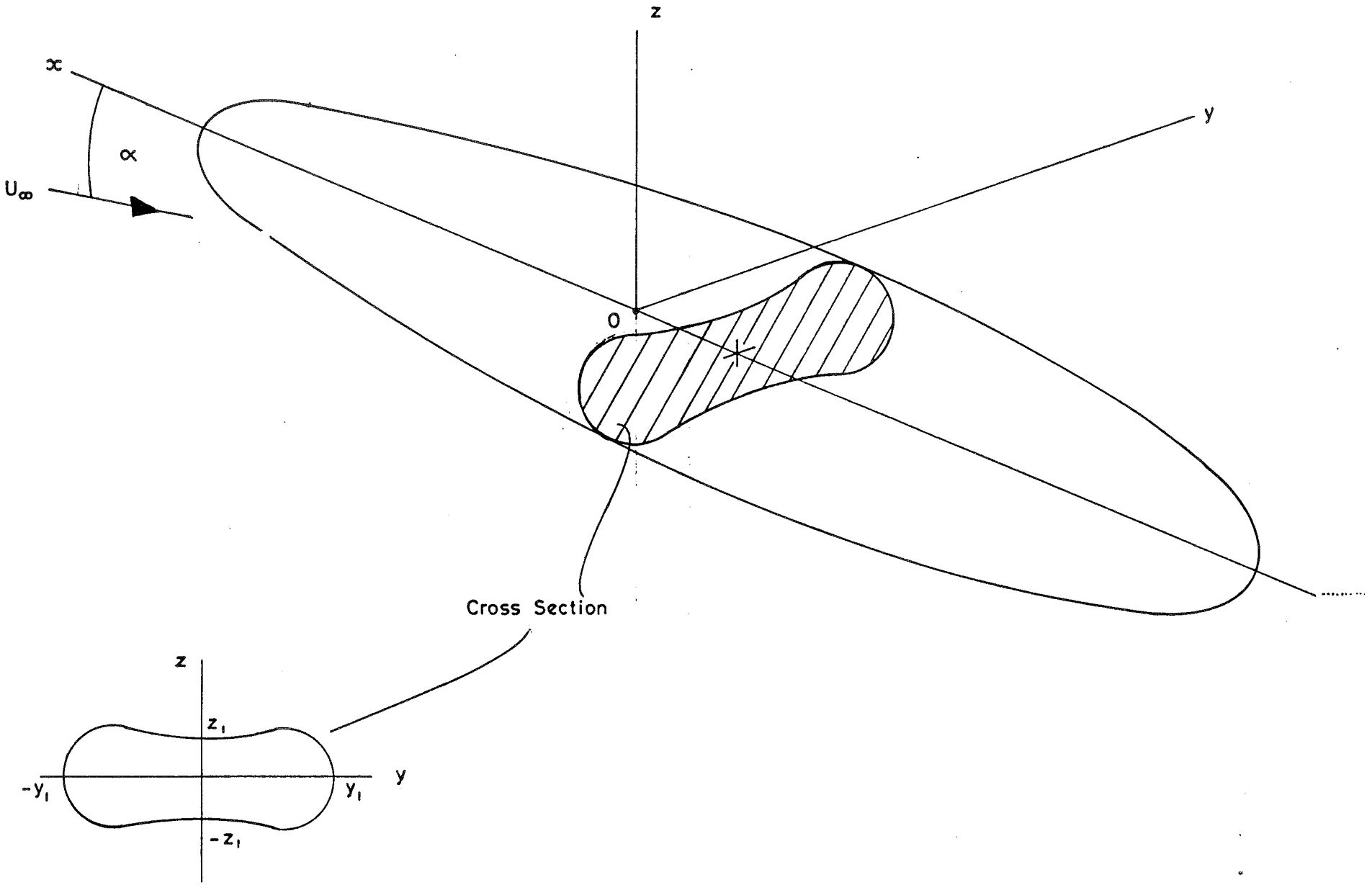

Fig.1. Geometry of Body and Flow.

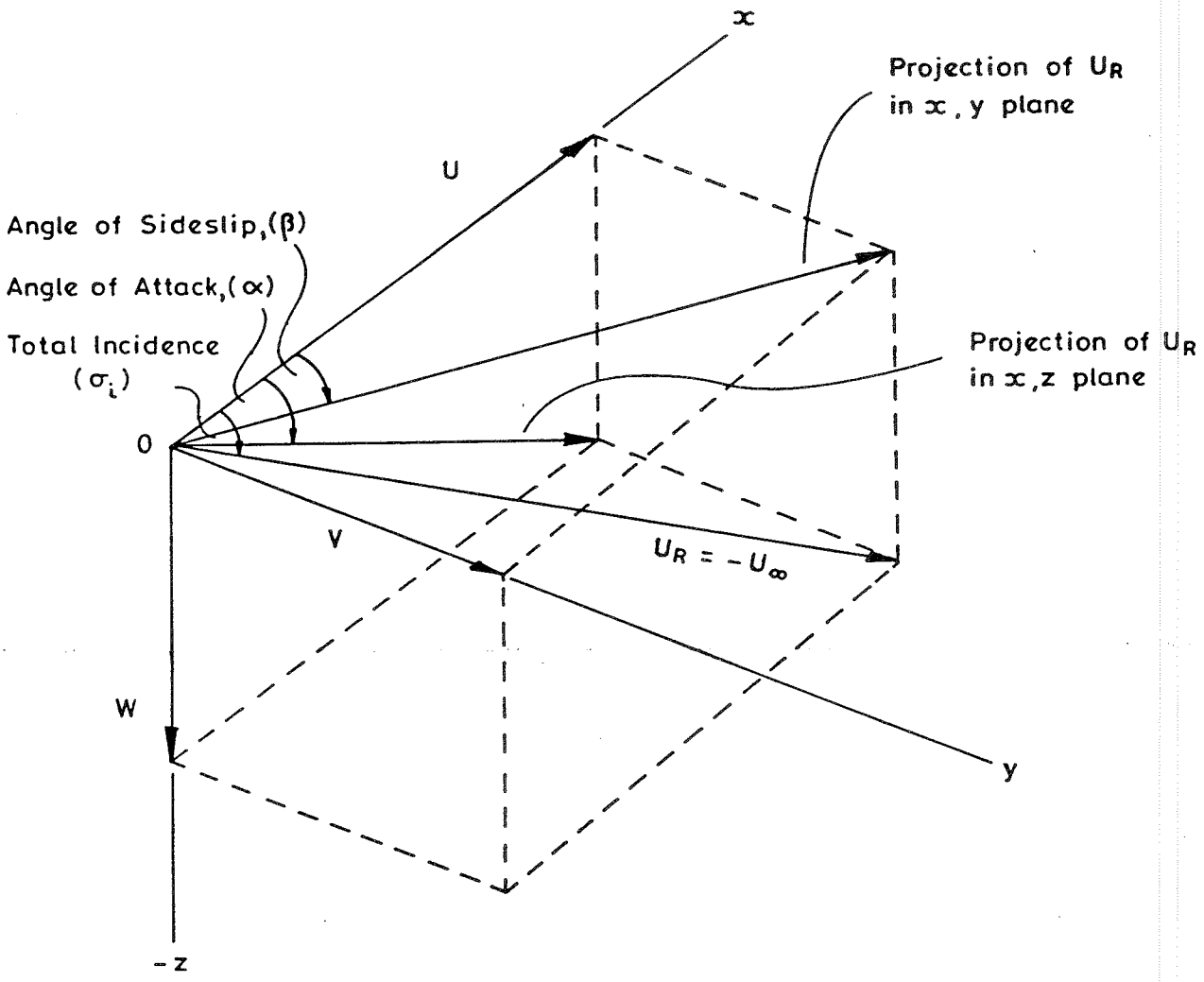

$$\text{Tan } \alpha = W/U \ , \ \text{Tan } \beta = V/U \ , \ \text{Cos } \sigma_i = U/U_R = -U/U_\infty$$

$$\text{Tan}^2 \sigma_i = \text{Tan}^2 \alpha + \text{Tan}^2 \beta$$

Fig. 2 System of Body Axis

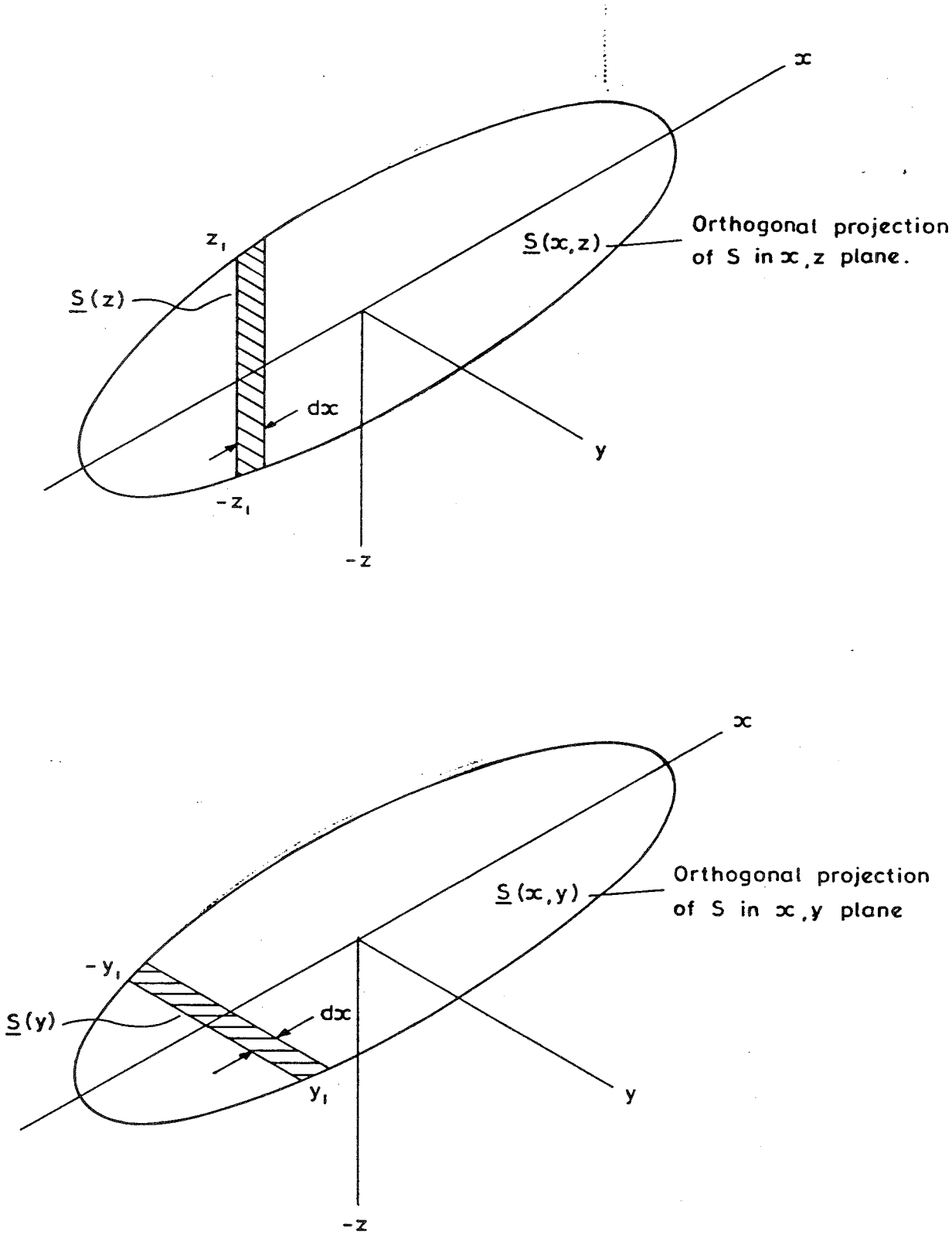

Fig.3. Orthogonal Projections and Elementary Areas of Integration.

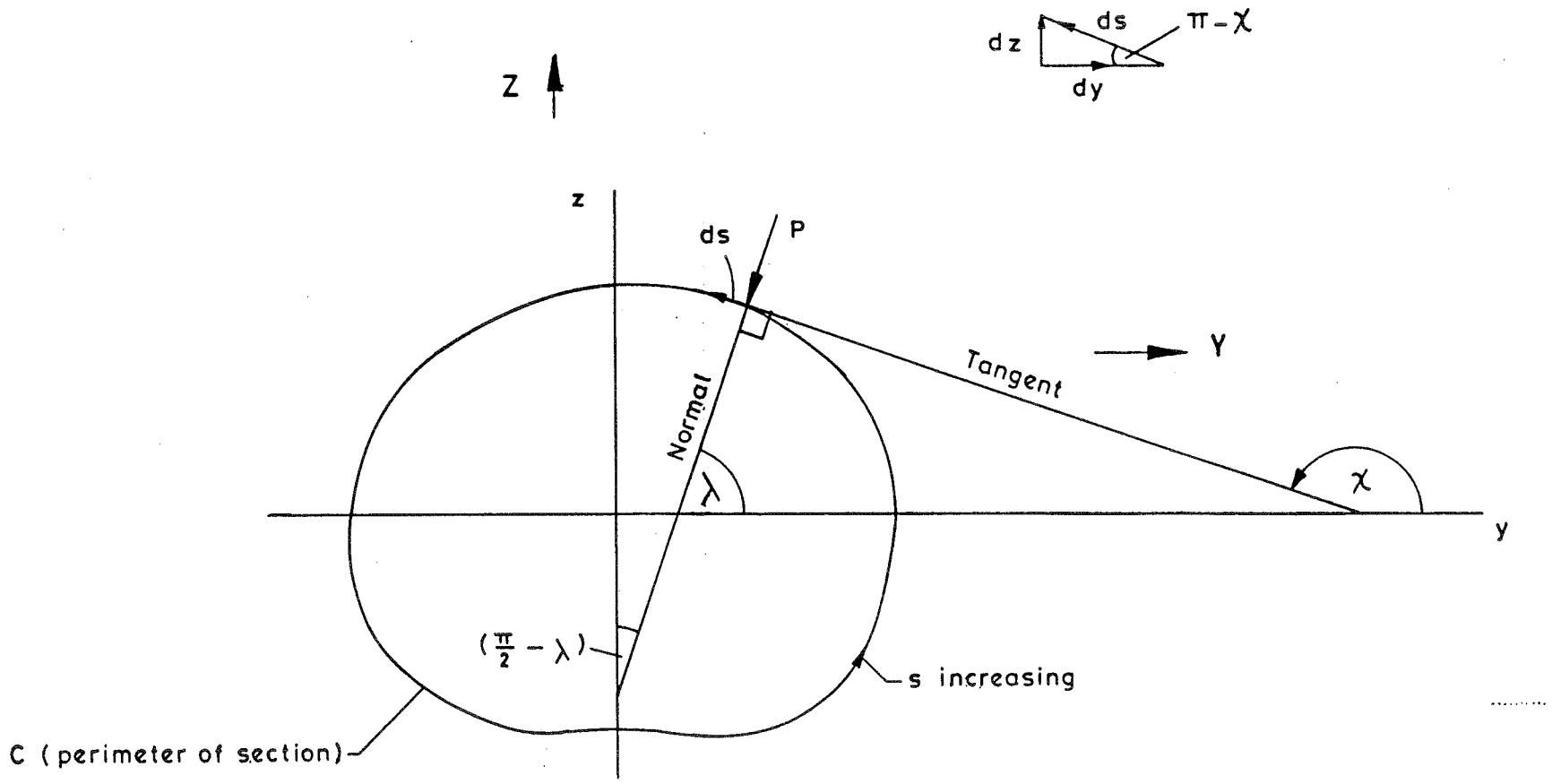

Fig. 4. Geometry of Body Section and Orientation of Circuit Integral.

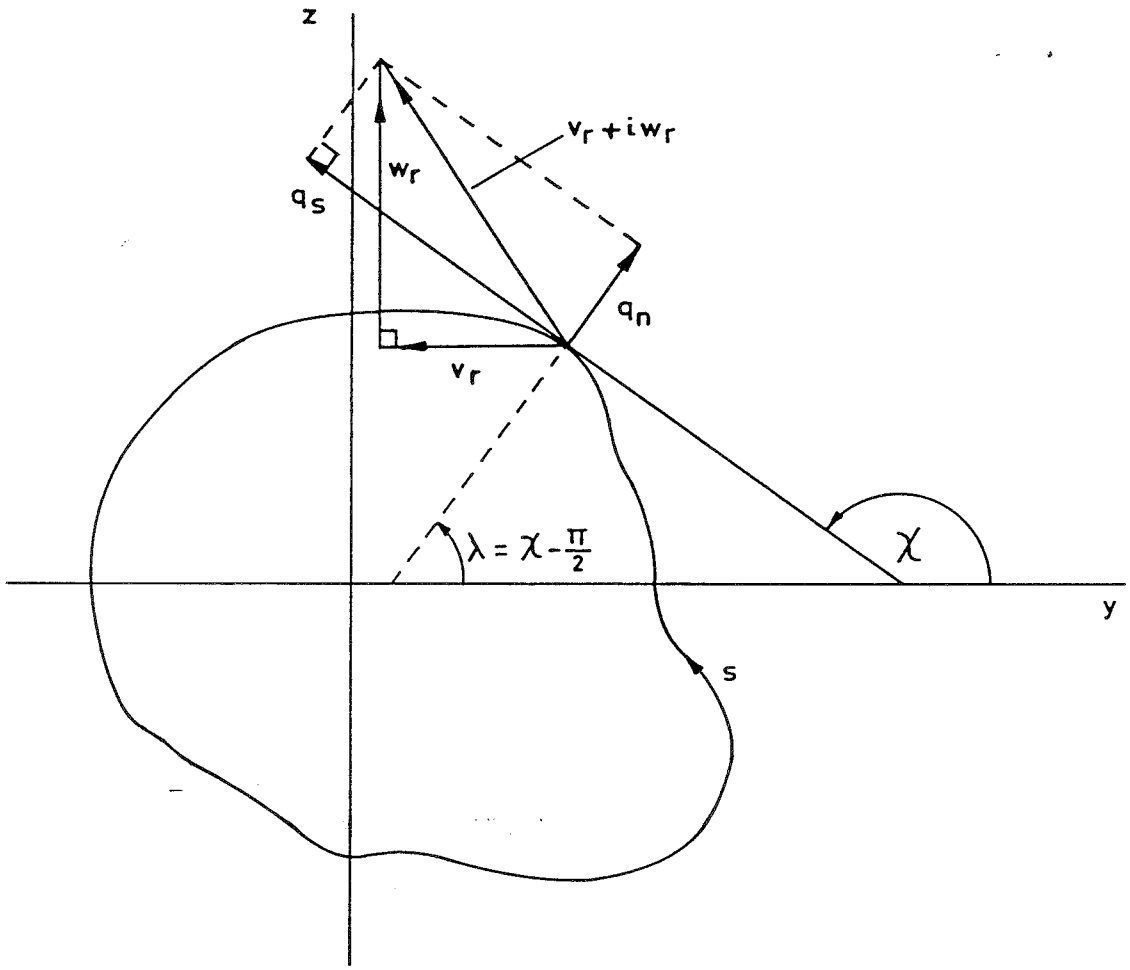

$$v_r + iw_r = q_s e^{i\chi} + q_n e^{i\lambda} = q_s e^{i\chi} + q_n e^{i(\chi - \frac{\pi}{2})} = (q_s - iq_n) e^{i\chi}$$

$v_r - iw_r =$ complex conjugate of $(v_r + iw_r)$

$$= (q_s + iq_n) e^{-i\chi}$$

Fig.5. Velocities on the Body Surface.

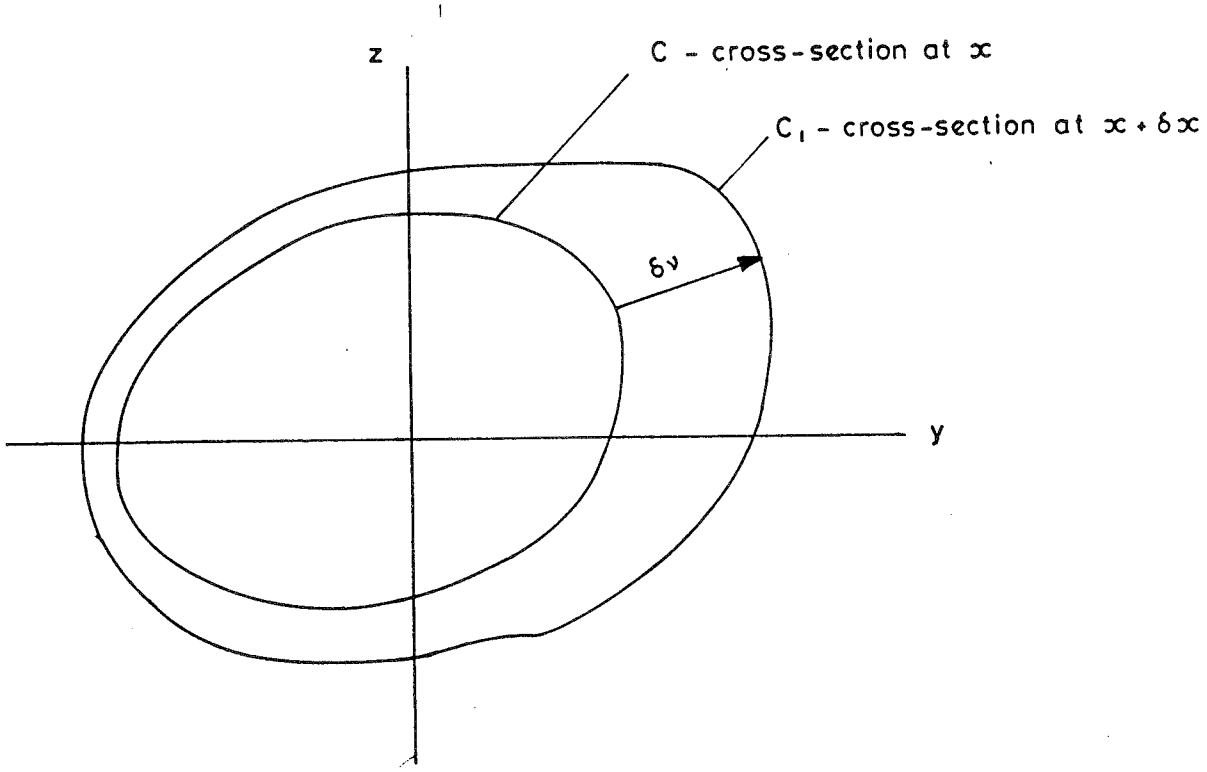

Fig.6. Variation of Cross-Section Along x-Axis

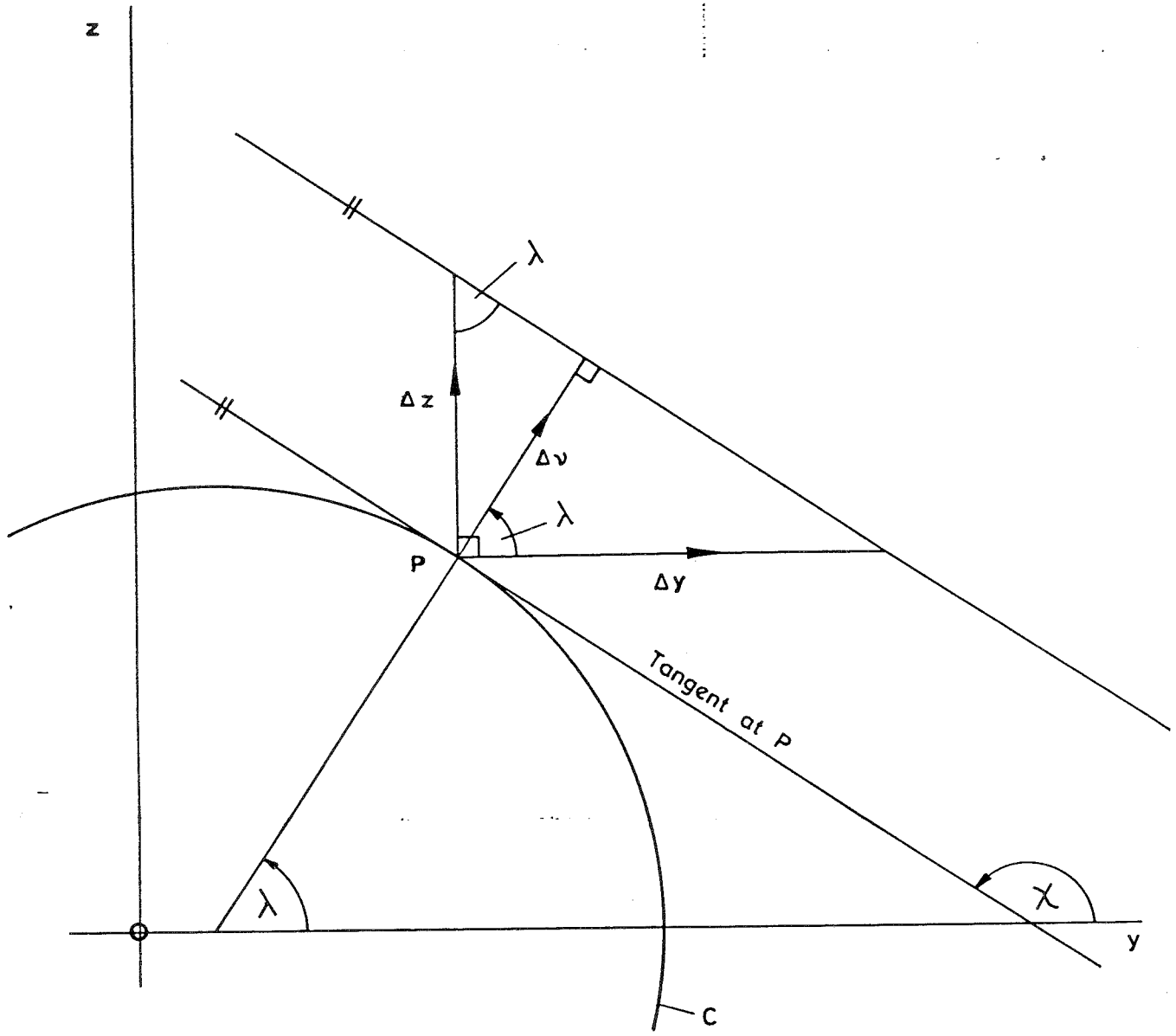

Fig.7. Determination of the Slopes of the Body Surface - Components of the Increment in Outward Normal Δν.

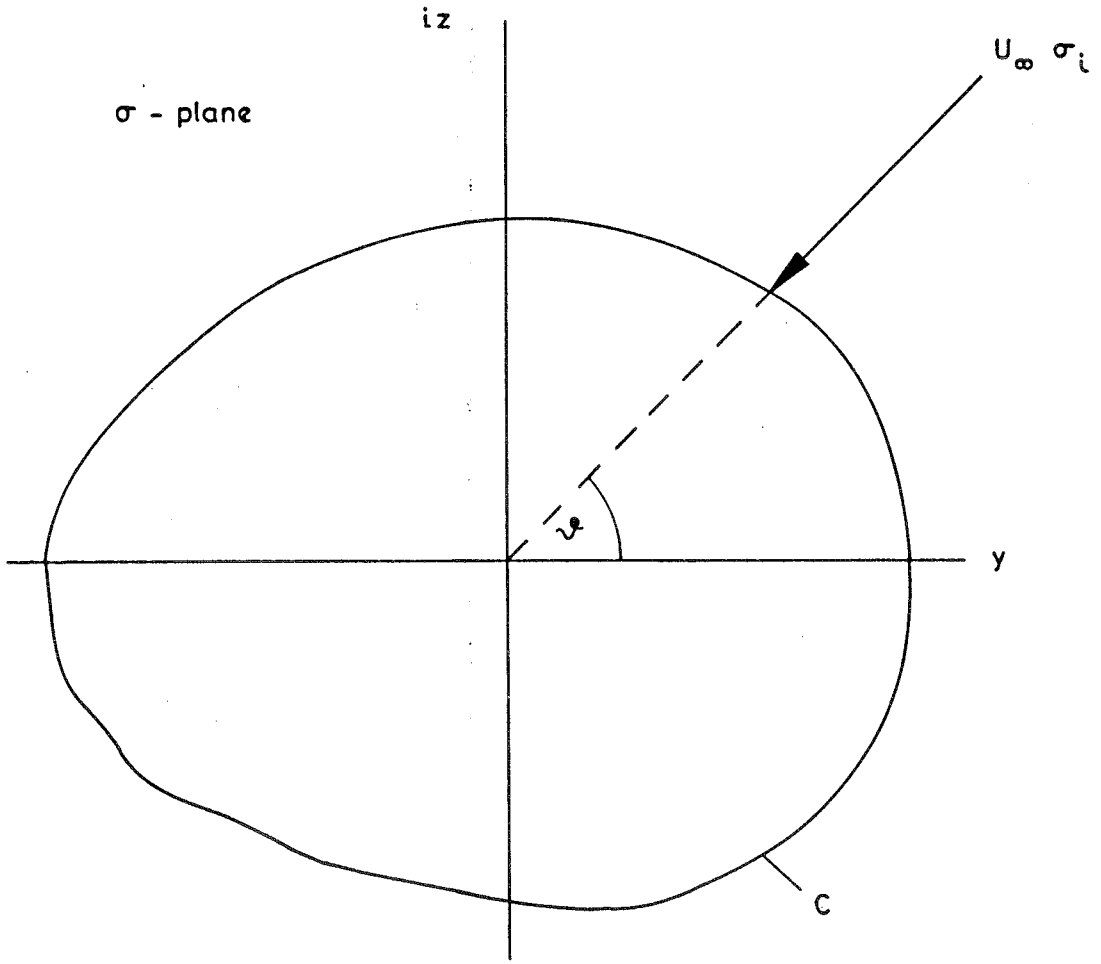

Fig.8. Definition of the Complex Transverse Velocity

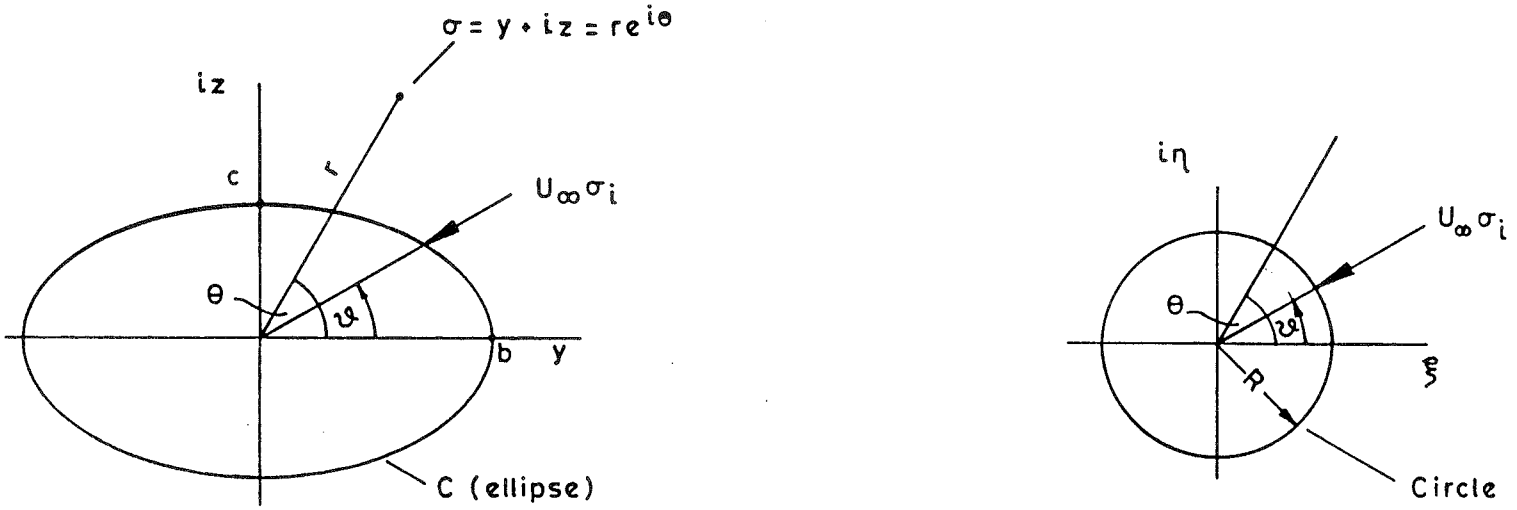

Fig.9. Geometry of Mapping.

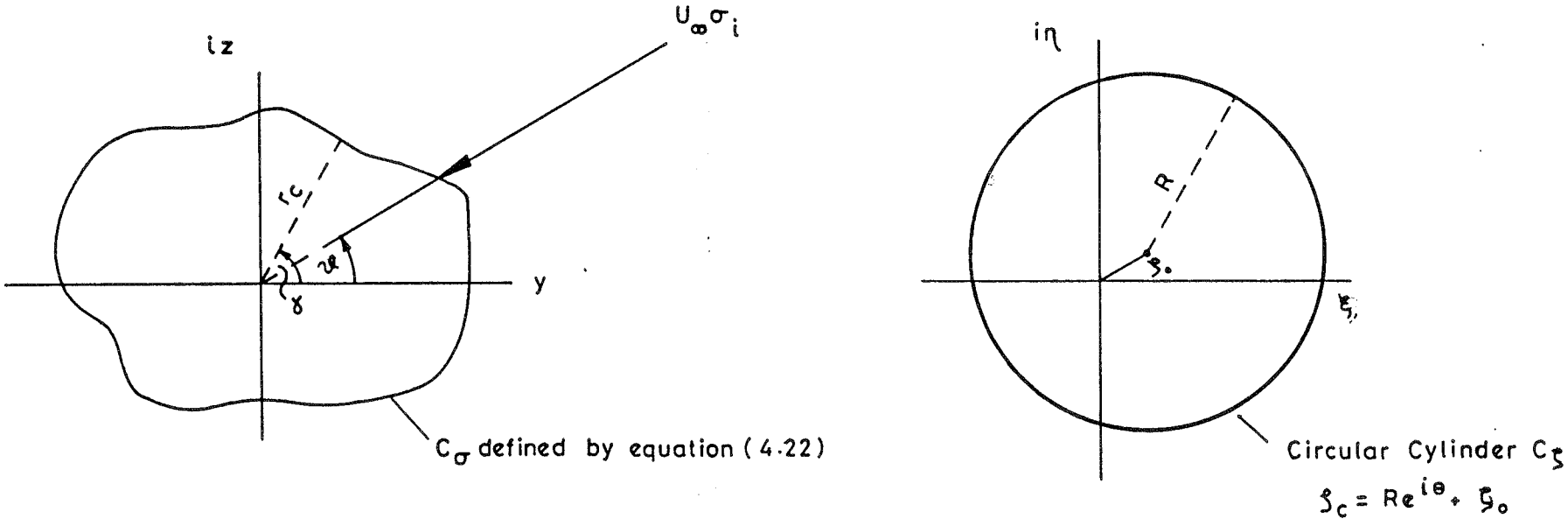

Fig.10. Geometry of Mapping - General Case

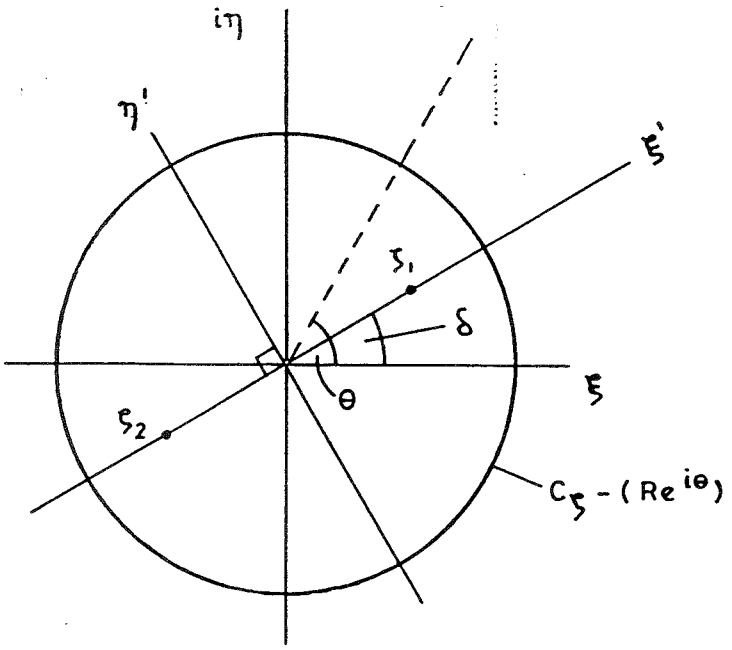

ζ - plane

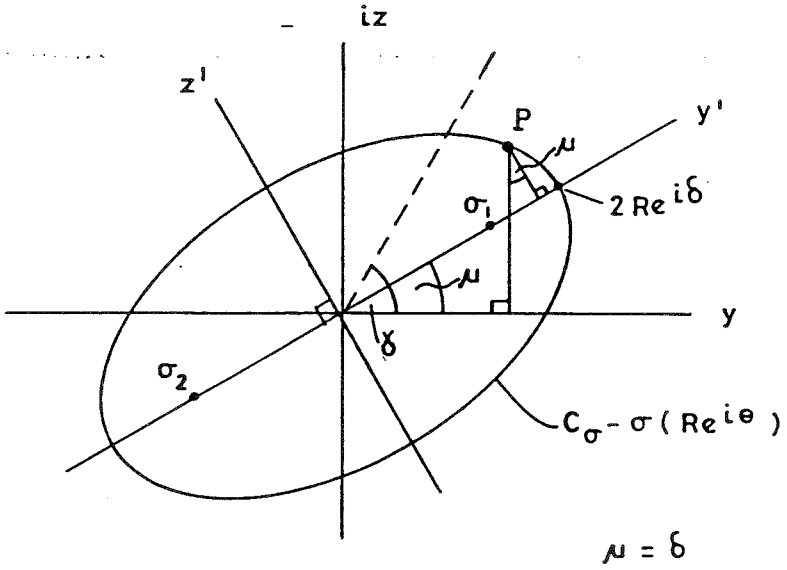

σ - plane

Fig. 11. Geometry of the Mapping - $\zeta_0 = 0$, $k = 2$.

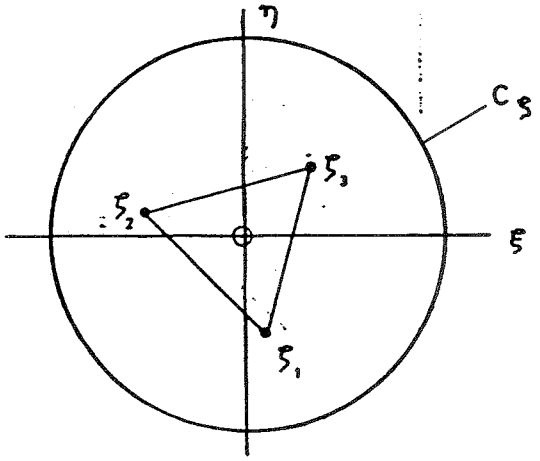

(a) General Case

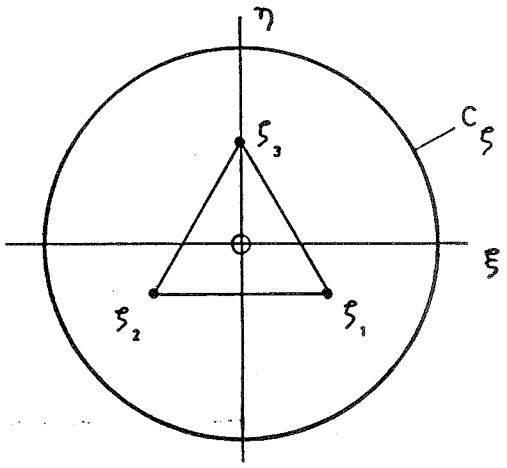

(b) Symmetry with respect to η and z-axes

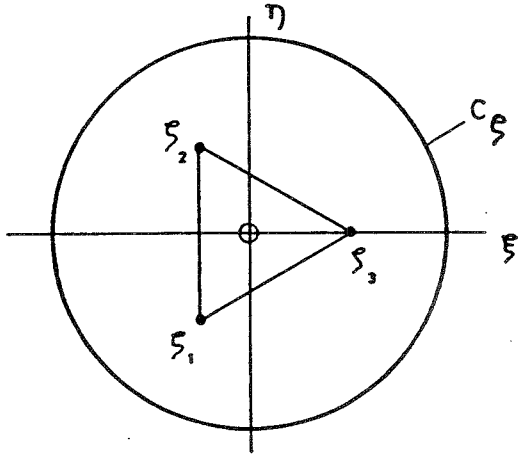

(c) Symmetry with respect to ξ and y-axes

Fig .12. Location of Critical Points $\zeta_o = 0$, $k = 3$.

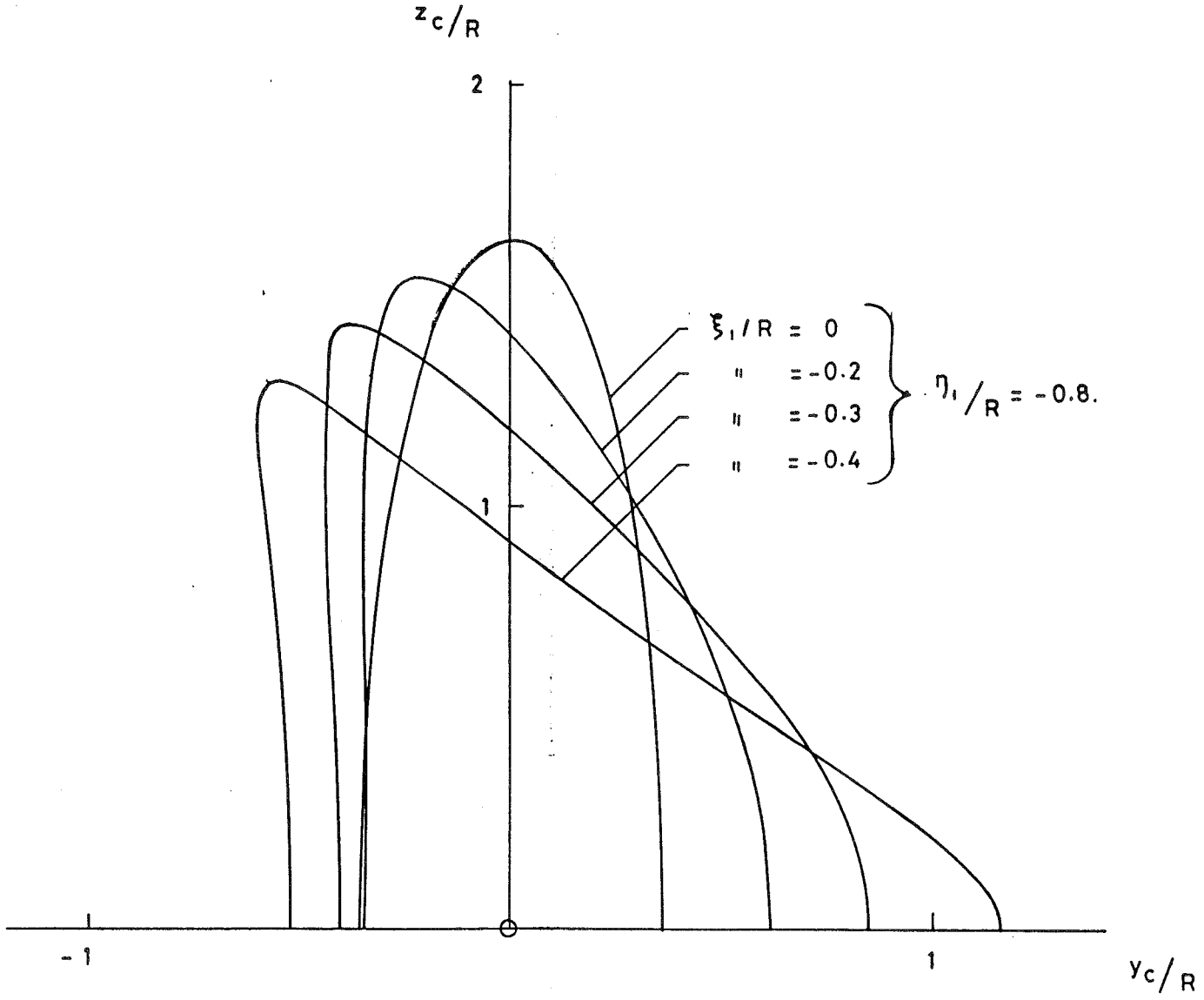

Fig. 13. Generation of Camber. Case $\zeta_0 = 0$, $k = 3$.

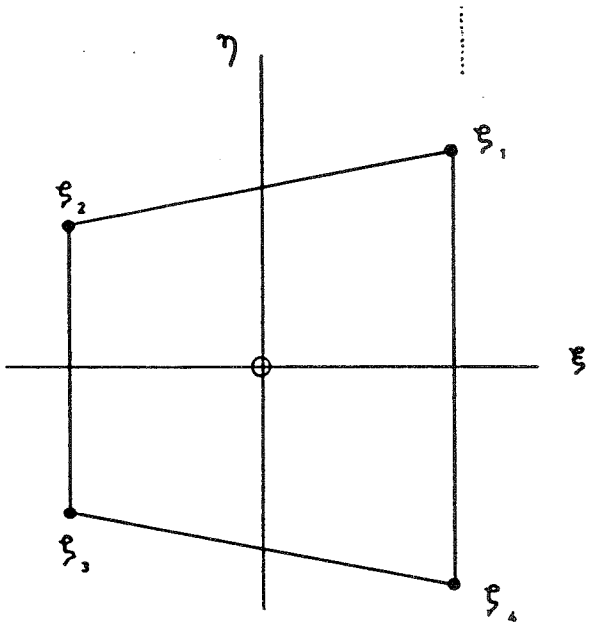

(a) General Case

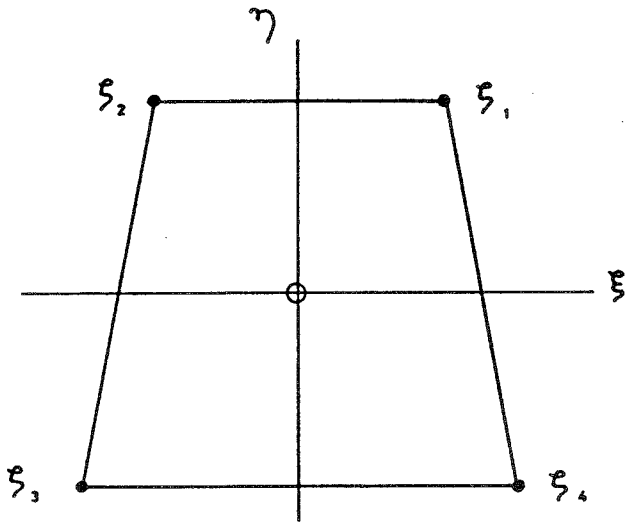

(b) Symmetry with respect to η and z-axes

Fig.14. Location of Critical Points $\zeta_0 = 0$, $k = 4$

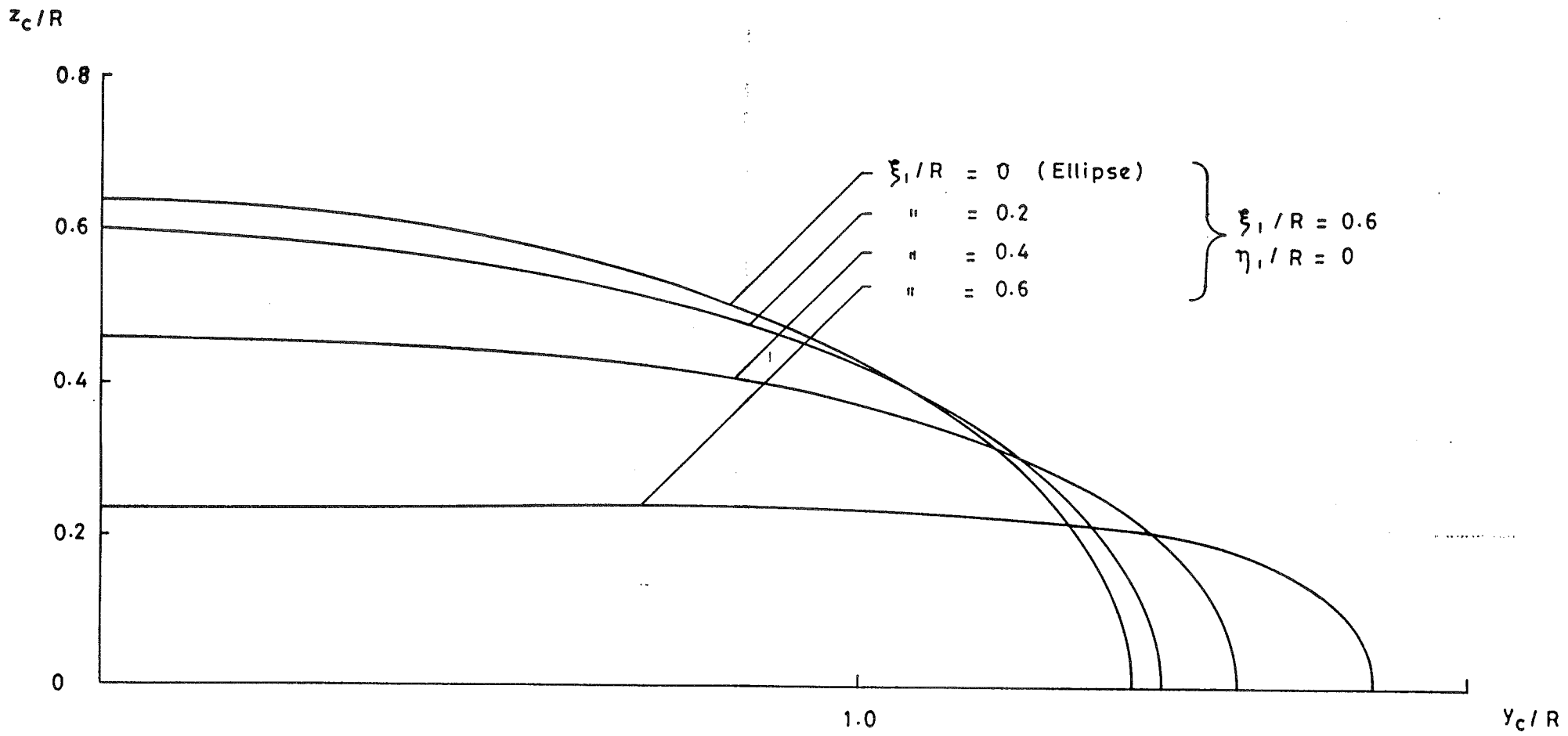

Fig. 15 (a). Body Cross-Section, Case $f_o = 0$, $k = 4$.

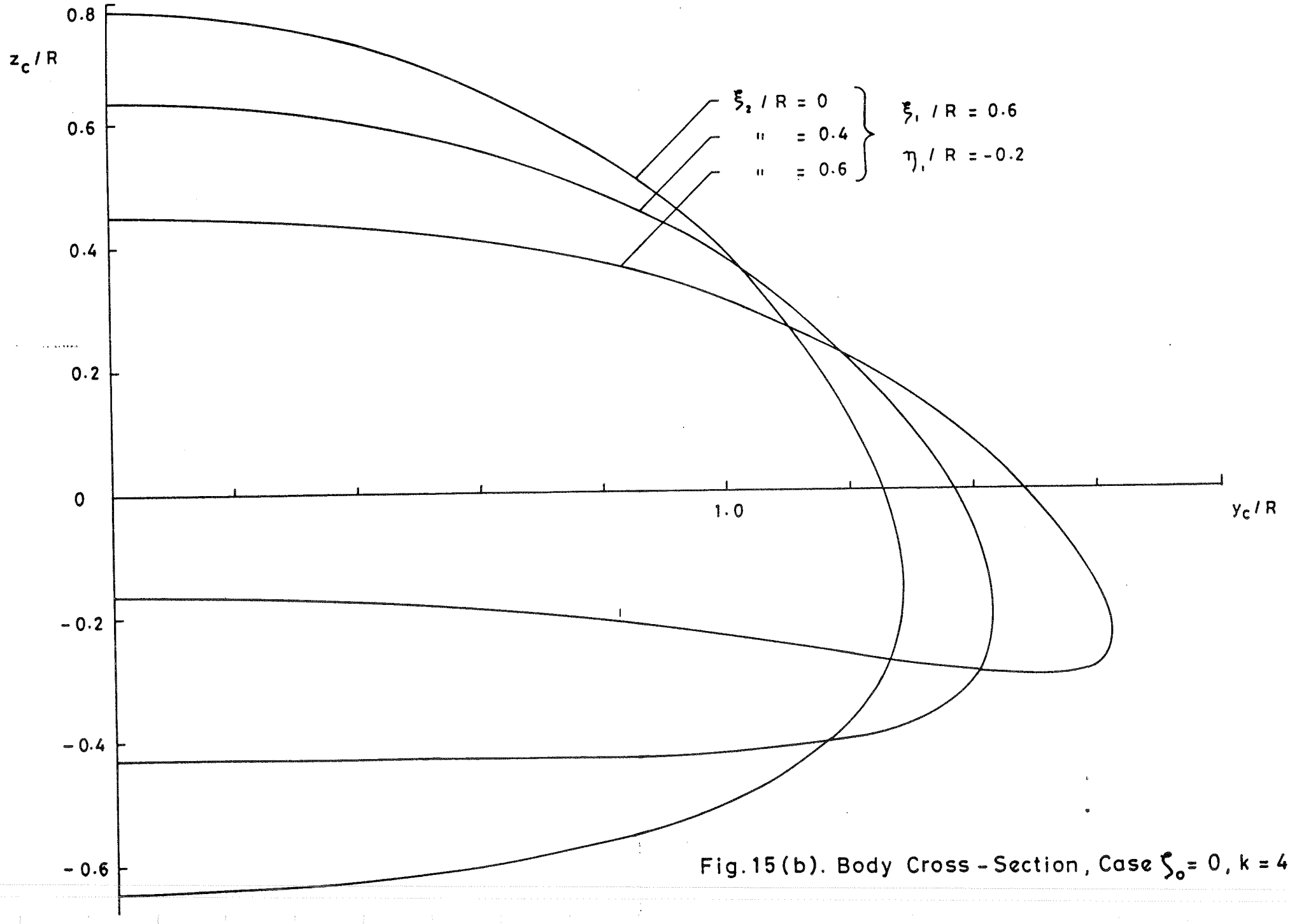

Fig. 15 (b). Body Cross - Section, Case $\zeta_0 = 0$, $k = 4$.

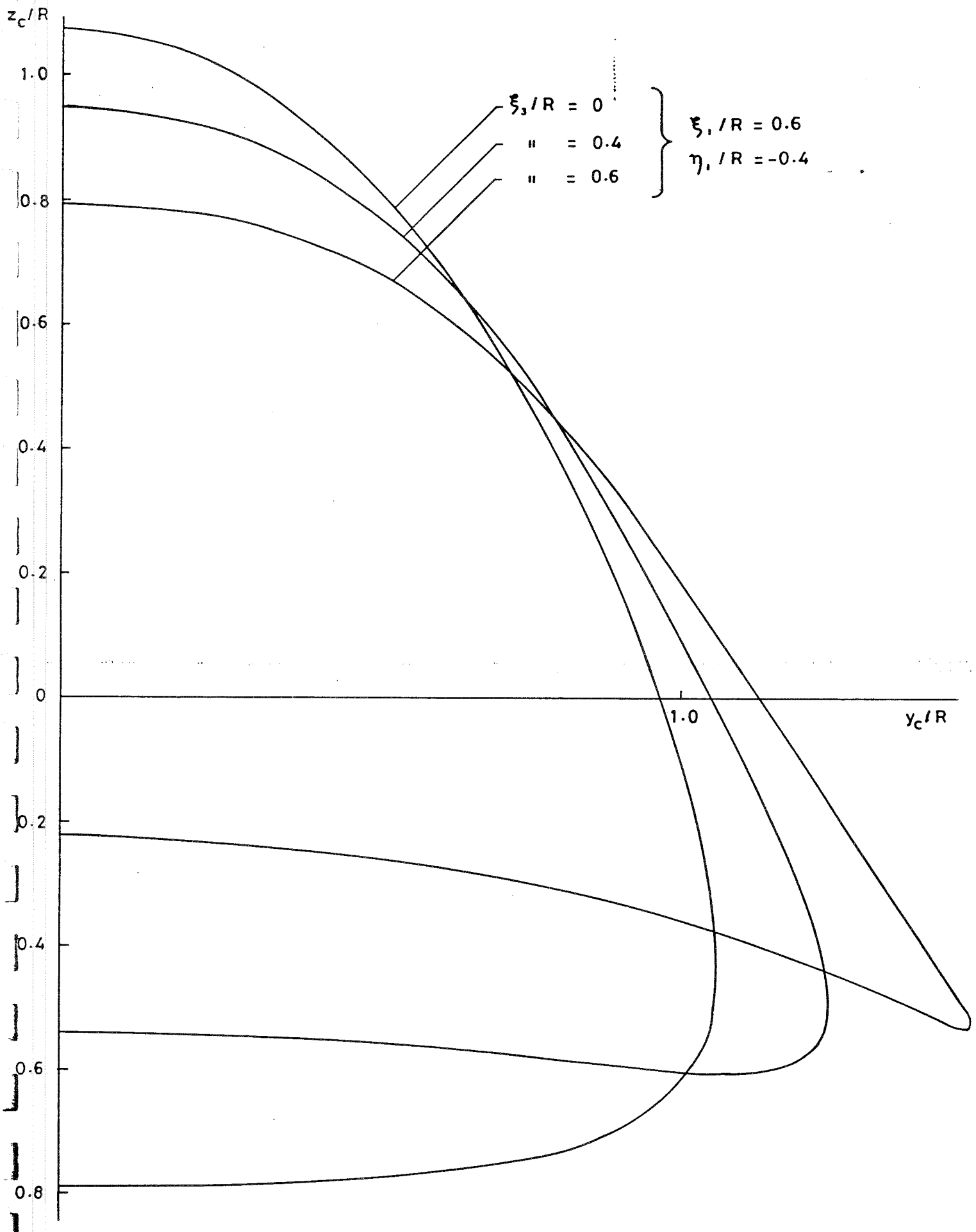

Fig. 15 (c). Body Cross-Section. Case $\Gamma_0 = 0$, $k = 4$.

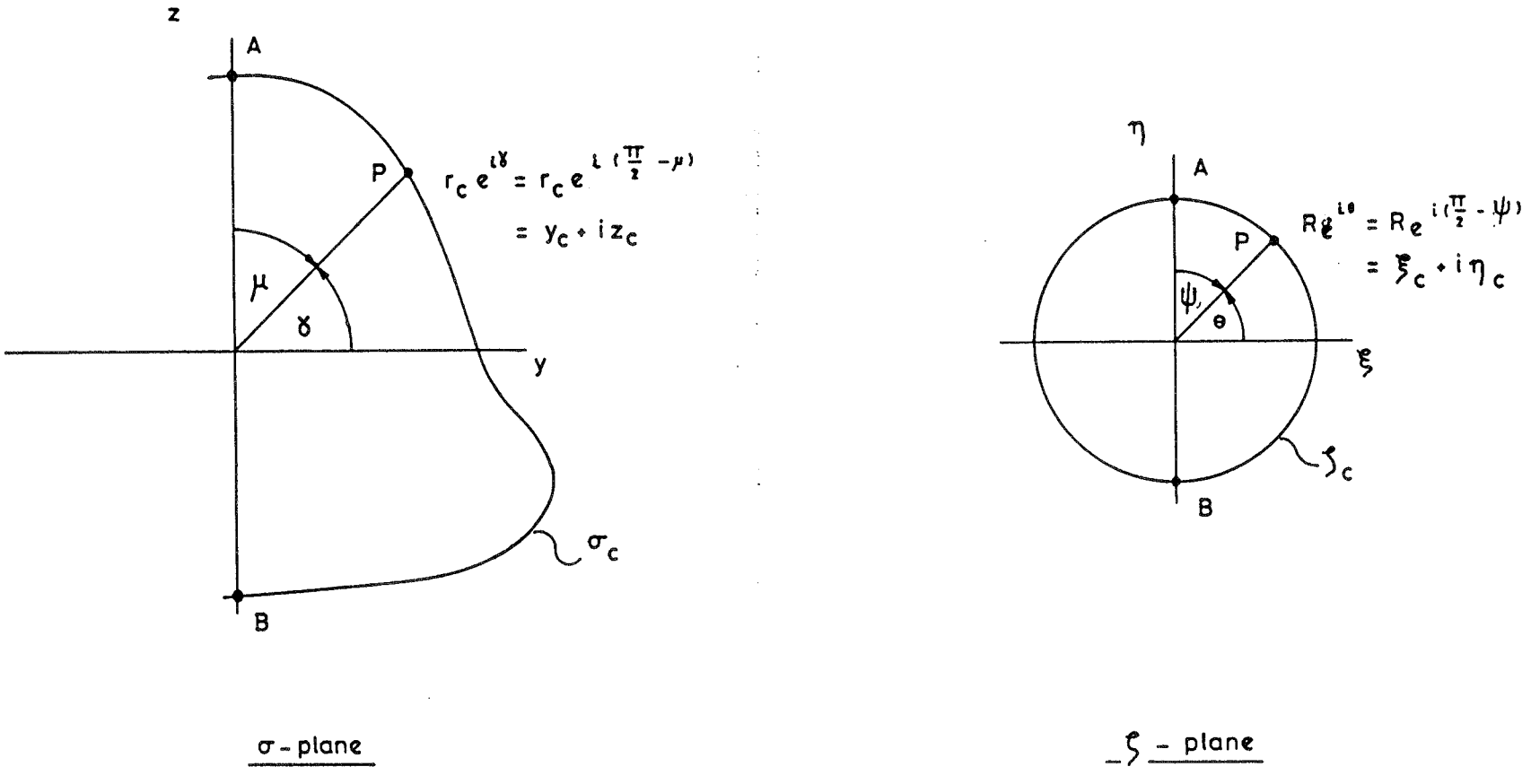

Fig. 16 Geometry Associated with the 'Direct' Method.

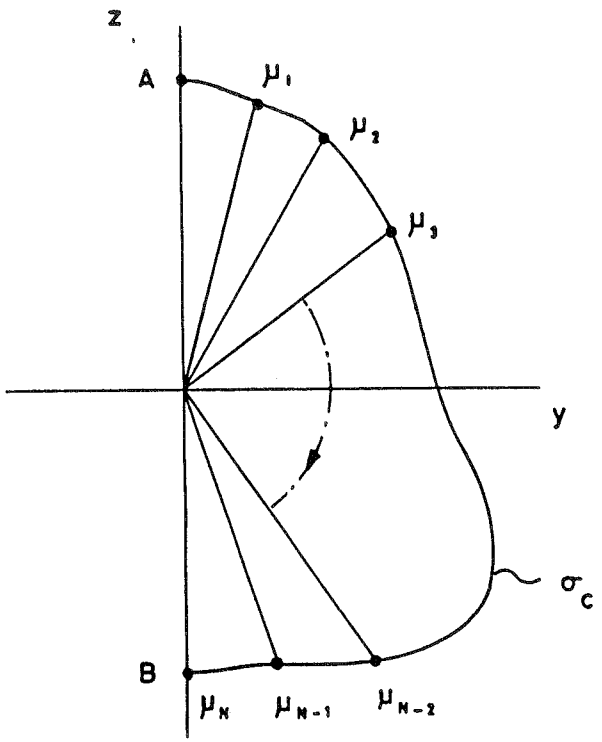

σ - plane

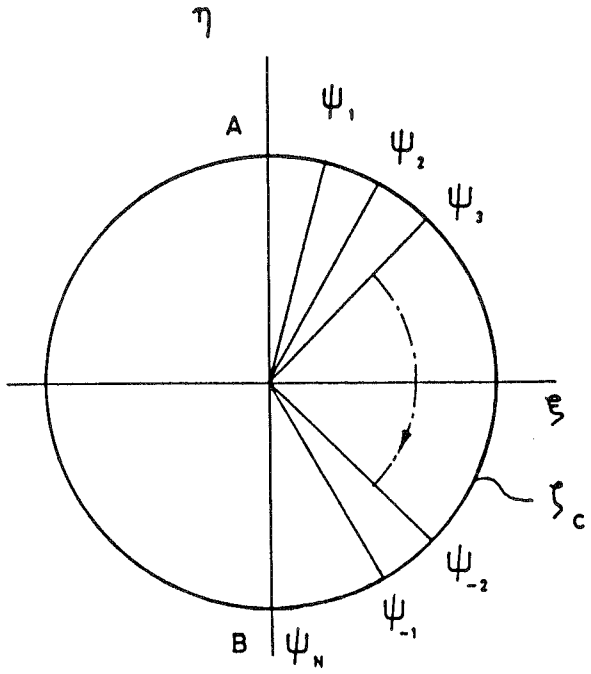

ζ - plane

Fig.17 The Geometry of the Scheme for Fourier-Fitting ζ_c to σ_c.

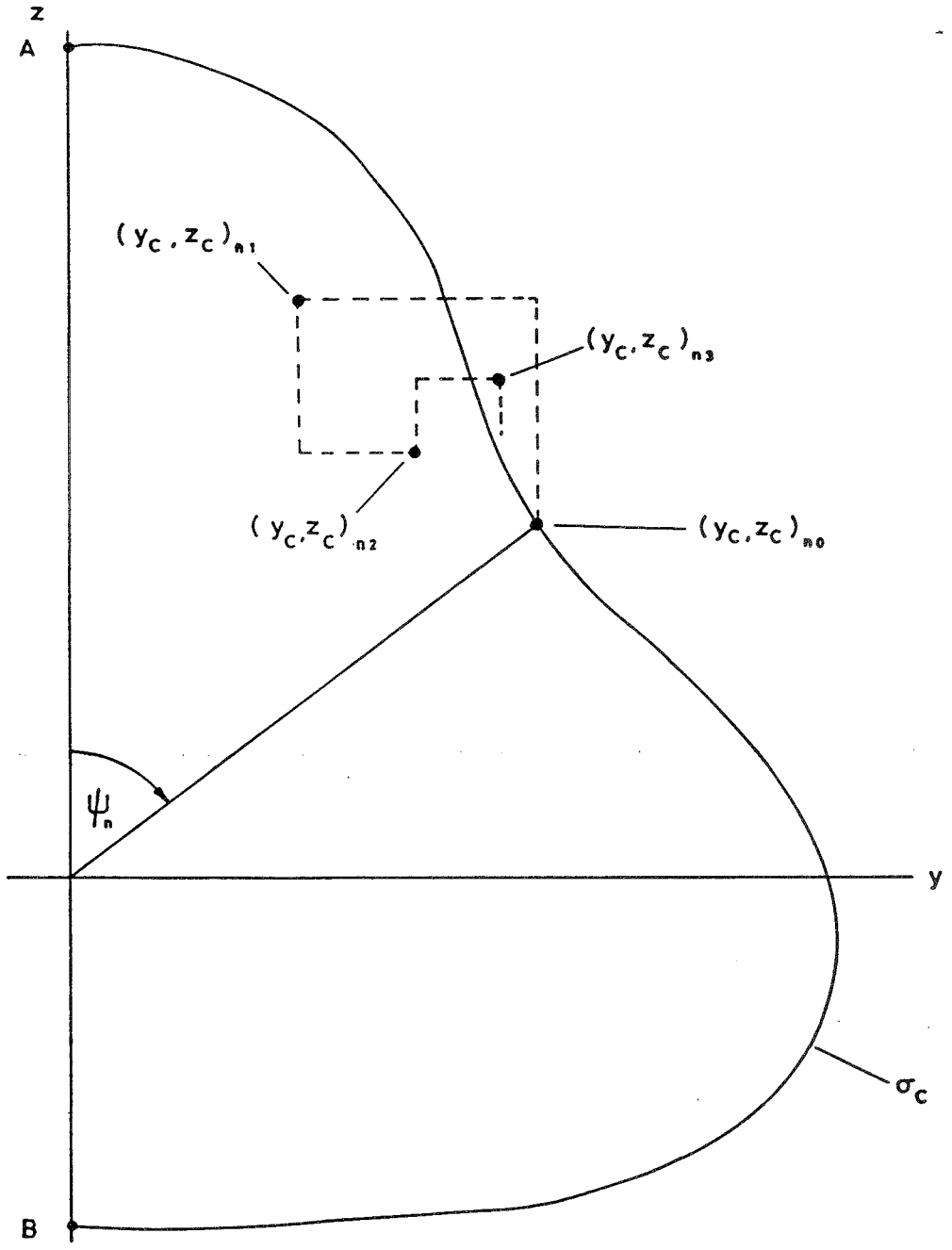

Fig. 18. Convergence of the Iteration Procedure.